REVIEWS OF GEOPHYSICS AND SPACE PHYSICS, VOL. 9, NO. 1, FEBRUARY 1971

Distribution of Stresses in the Descending Lithosphere from a Global Survey of Focal-Mechanism Solutions of Mantle Earthquakes

BRYAN ISACKS

Earth Sciences Laboratories
National Oceanographic and Atmospheric Administration
Lamont-Doherty Geological Observatory of Columbia University
Palisades, New York 10964

PETER MOLNAR

Lamont-Doherty Geological Observatory of Columbia University
Palisades, New York 10964

A region-by-region analysis of 204 reliable focal-mechanism solutions for deep and intermediate-depth earthquakes strongly supports the idea that portions of the lithosphere that descend into the mantle are slablike stress guides that align the earthquake-generating stresses parallel to the inclined seismic zones. At intermediate depths extensional stresses parallel to the dip of the zone are predominant in zones characterized either by gaps in the seismicity as a function of depth or by an absence of deep earthquakes. Compressional stresses parallel to the dip of the zone are prevalent everywhere the zone exists below about 300 km. These results indicate that the lithosphere sinks into the asthenosphere under its own weight but encounters resistance to its downward motion below about 300 km. Additional results indicate contortions and disruptions of the descending slabs; however, stresses attributable to simple bending of the plates do not seem to be important in the generation of subcrustal earthquakes. This summary, intended to be comprehensive, includes nearly all solutions obtainable from the World-Wide Standardized Seismograph Network (WWSSN) for the period 1962 through part of 1968 plus a selection of reliable solutions of pre-1962 events, and it includes data from nearly every region in the world where earthquakes occur in the mantle. The double-couple or shear dislocation model of the source mechanism is adequate for all the data.

INTRODUCTION

The idea that deep and intermediate-depth earthquakes mark the location of a descending tongue of lithosphere provides a simple explanation for the peculiar orientation of subcrustal earthquake mechanisms; the events are not part of a deep megathrust fault but instead occur inside the descending lithosphere in response to compressional or extensional stresses aligned parallel to the slablike geometry of the lithosphere. This explanation [*Oliver and Isacks*, 1967; *Elsasser*, 1967; *Isacks et al.*, 1968, 1969] suggests that focal-mechanism data may therefore yield information about the forces applied to the lithosphere

and about the contortions and disruptions of its descending parts. In our previous paper [*Isacks and Molnar*, 1969] we used focal-mechanism data to support the ideas that at intermediate depths the lithosphere sinks into the asthenosphere under its own weight and at great depths encounters stronger or denser material. Our evidence came from regions where the planar two-dimensional structure of the arc is clear and well defined. In this paper we compile and summarize reliable focal-mechanism solutions for deep and intermediate-depth earthquakes (Figure 1) in nearly every region in the world where subcrustal earthquakes are known to occur. We present further evidence for the gravitational sinking of the lithosphere and, in addition, show that even in regions where the distribution of hypocenters and inferred stresses is complex, the idea of a stressed slab of lithosphere still provides the simplest interpretation of the results.

The standard classifications of shallow, intermediate, and deep foci [*Gutenberg and Richter*, 1954] also correspond to the main types of focal-mechanism solutions in island arcs and thus appear to be of major tectonic significance. The boundary of 60–70 km between shallow and intermediate depths approximately divides the earthquakes that occur in the shallow zone of thrust faulting between the converging plates of lithosphere from the earthquakes that occur inside the underthrust and descending plates. An overlapping of both types, although limited to few events, shows that the boundary is somewhat diffuse and perhaps slightly variable in depth from region to region. The boundary of approximately 300 km between intermediate and deep foci marks the most outstanding feature of the distribution of the stress orientations inside the descending lithosphere; the stress parallel to the dip of the zone tends to be compressional below 300 km and extensional or variable above 300 km.

Our purpose is to place emphasis on individual solutions that are reliable and well determined rather than to extract average features from a larger number of poorly determined solutions. We therefore include only solutions whose quality we are able to determine clearly (Figure 1, Table 1, and appendix). One hundred seventy-nine are based on data from the World-Wide Standardized Seismograph Network (WWSSN) and include nearly all the deep or intermediate-depth earthquakes that occurred from 1962 through part of 1968 and that were large enough that a reliable solution could be obtained. The additional solutions for events that occurred prior to 1962 are relatively few in number (25) because of the scarcity of reliable data for that period [*Ritsema*, 1964; *Stevens and Hodgson*, 1968] and because in certain cases the data from which an assessment of quality could be made was not available to us.

Ninety-five of the solutions are new and have not been published previously. The solutions for the New Guinea-New Britain-Solomons, New Hebrides, and South Sandwich regions are the first to be reported that rely upon WWSSN data. We also report numerous new data for the Peru-Chile and the Kurile-Japan regions.

We summarize and discuss the main results of this study on a global basis in the first two sections, and in the final section present the data and its analysis in detail for each region. The region-by-region analyses, besides providing the basis for our generalizations and inferences, yield information about the extent

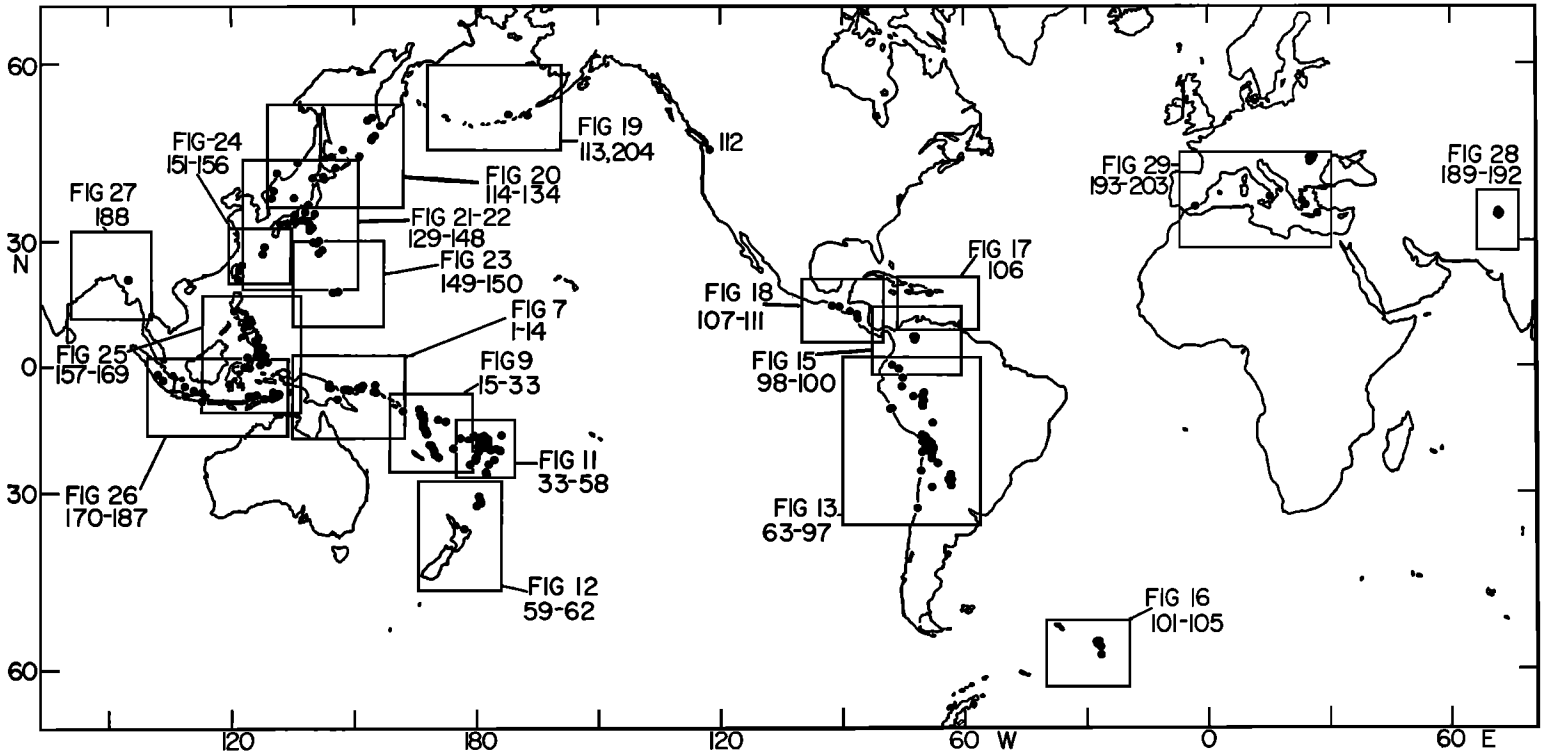

Fig. 1. Index map showing epicenters (small filled circles) of the deep and intermediate-depth earthquakes listed in Table 1. The focal-mechanism solutions for these 204 events are the basic data used in this paper. The rectangles show the areas and earthquakes included in Figures 7–29.

TABLE 1. FOCAL-MECHANISM SOLUTIONS OF DEEP AND INTERMEDIATE-DEPTH EARTHQUAKES

No.	Mo.	Day	Yr.	Epicenter Lat.	Epicenter Long.	Depth, km	Axis of Compression (P) Trend	Axis of Compression (P) Plunge	Axis of Tension (T) Trend	Axis of Tension (T) Plunge	Null Axis (B) Trend	Null Axis (B) Plunge	Pole of 1st Nodal Plane Trend	Pole of 1st Nodal Plane Plunge	Pole of 2nd Nodal Plane Trend	Pole of 2nd Nodal Plane Plunge	Down-dip Stress Type	Reference
SOLOMONS-NEW BRITAIN-NEW GUINEA (Figure 7)																		
1	Aug	5	1966	11.1S	162.6E	52	206	05	079	82	296	08	031	40	198	49	n. p.	N
2	Jan	7	1968	5.1S	153.9E	118	065	03	328	71	157	18	048	45	261	40	T	N
3	Aug	13	1964	5.5S	154.3E	392	282	76	056	10	149	10	044	54	244	34	P	N
4	July	6	1965	4.5S	155.1E	506	157	64	004	24	269	10	175	21	023	66	P	ISO-40
5	Dec	26	1965	5.4S	151.6E	74	174	40	308	40	060	25	330	00	240	65	T	N
6	Jan	14	1964	5.2S	150.8E	169	154	35	334	55	064	00	334	10	154	80	T	N
7	Jun	18	1962	5.0S	152.0E	103	169	05	349	85	079	00	349	40	169	50	X	N
8	Jun	13	1967	5.6S	148.1E	213	181	24	059	50	286	30	024	14	137	55	T	N
9	Sep	1	1967	5.6S	147.2E	182	357	01	090	68	267	22	018	42	157	40	T	N
10	Nov	14	1967	5.4S	147.1E	201	189	15	077	56	288	30	033	24	154	50	T	N
11	Feb	26	1963	7.6S	146.2E	182	105	41	249	41	355	20	085	00	175	70	n. p.	N
12	Apr	24	1964	5.1S	144.2E	98	083	55	264	35	172	01	093	10	269	80	n. p.	N
13	Sep	12	1964	4.4S	144.1E	107	215	43	035	47	125	00	035	02	215	88	n. p.	N
14	Dec	14	1966	4.9S	144.1E	80	032	15	212	75	122	00	212	30	032	60	n. p.	N
NEW HEBRIDES (Figure 9)																		
15	July	2	1962	10.6S	166.0E	114	Data fit solution for earthquake 17										T	N
16	Jan	19	1967	11.8S	166.4E	156	083	08	317	78	174	10	272	37	071	52	T	N
17	Jun	13	1966	12.2S	167.1E	259	130	01	038	62	220	28	334	38	104	40	T	N
18	May	22	1962	12.2S	166.7E	121	Data fit solution for earthquake 17										T	N
19	Aug	4	1965	13.2S	167.0E	209	Data fit solution for earthquake 17										T	N
20	Dec	1	1966	14.0S	167.1E	132	249	03	122	86	339	04	245	48	072	42	T	N
21	Nov	4	1963	15.1S	167.4E	123	275	05	095	85	005	00	275	50	095	40	T	N
22	Mar	31	1967	15.4S	167.5E	132	253	05	073	85	163	00	253	50	073	40	T	N
23	July	9	1964	15.5S	167.6E	121	263	09	083	81	174	00	263	54	083	36	T	N
24	Feb	4	1966	15.9S	167.9E	183	244	24	136	30	006	50	193	40	100	04	X	N
25	May	1	1963	19.0S	168.9E	142	250	20	138	46	355	38	206	48	097	16	X	N
26	Mar	30	1963	19.1S	169.0E	156	235	20	130	36	348	48	188	40	090	10	X	N
27	Dec	21	1966	20.0S	169.7E	249	338	32	246	02	152	58	027	21	287	24	X	N
28	Jan	20	1964	20.7S	169.9E	139	093	63	340	12	244	24	006	50	140	30	P	N

TABLE 1 (continued)

No.	Mo.	Day	Yr.	Epicenter Lat.	Epicenter Long.	Depth, km	Axis of Compression (P) Trend	Axis of Compression (P) Plunge	Axis of Tension (T) Trend	Axis of Tension (T) Plunge	Null Axis (B) Trend	Null Axis (B) Plunge	Pole of 1st Nodal Plane Trend	Pole of 1st Nodal Plane Plunge	Pole of 2nd Nodal Plane Trend	Pole of 2nd Nodal Plane Plunge	Down-dip Stress Type	Reference
				degrees														
29	Oct	7	1966	21.6S	170.6E	160	239	00	328	30	148	60	280	20	017	20	X	N
30	Apr	10	1965	13.4S	170.3E	644	283	22	190	07	083	68	328	09	234	20	X	N
31	Nov	4	1968	14.2S	172.0E	585	152	69	271	10	005	18	106	32	250	52	X	N
32	Oct	1	1965	19.9S	174.5E	544	026	39	147	30	262	36	357	05	094	53	X	ISO-38
TONGA (Figure 11)																		
33	Jan	28	1966	17.6S	177.0E	560	285	36	020	06	118	52	339	30	236	20	n. p.	ISO-24
34	Sep	12	1964	17.6S	179.7W	592	243	48	044	41	142	10	232	05	347	79	n. p.	ISO-25
35	Dec	25	1965	18.2S	179.1W	624	264	67	002	03	094	23	202	38	340	44	n. p.	ISO-26
36	Apr	10	1965	17.8S	178.8W	535	236	28	348	33	116	44	022	04	288	46	n. p.	ISO-27
37	Aug	25	1963	17.5S	178.7W	563	244	42	118	33	006	30	273	05	174	60	n. p.	ISO-28
38	July	21	1966	17.8S	178.6W	590	276	28	009	07	112	62	230	14	326	24	n. p.	ISO-29
39	Dec	9	1965	18.1S	178.1W	653	095	46	189	04	282	43	042	28	153	34	n. p	ISO-30
40	May	22	1965	21.1S	178.6W	540	347	71	208	14	116	12	018	30	224	58	P	ISO-32
41	Mar	17	1966	21.1S	179.2W	630	311	65	121	25	213	04	304	20	110	70	P	ISO-33
42	Sep	10	1962	21.3S	179.1W	618	341	60	087	10	182	28	057	46	291	30	P	N
43	Oct	2	1967	21.0S	178.8W	604	339	53	186	34	086	12	354	10	226	74	P	N
44	Oct	9	1967	21.1S	179.3W	654	330	48	138	40	234	06	324	04	087	82	P	N
45	Oct	12	1967	21.1S	179.2W	636	341	43	109	32	220	30	312	06	052	60	P	N
46	Dec	28	1964	22.2S	179.6W	579	305	38	162	46	051	19	143	04	243	70	P	ISO-34
47	Sep	8	1963	23.6S	180.0	559	278	27	075	62	183	07	090	18	307	70	P	ISO-36
48	Oct	7	1963	23.6S	180.0	548	284	33	073	51	183	16	090	08	333	72	P	ISO-37
49	Jan	17	1965	24.6S	178.4E	557	069	54	228	34	326	10	057	10	190	76	X	ISO-35
50	Mar	11	1968	16.2S	173.9W	112	339	48	234	12	137	39	025	23	272	42	X	N
51	Aug	10	1966	20.2S	175.3W	95	282	54	062	29	163	20	258	14	021	66	P	ISO-19
52	Mar	18	1965	19.9S	175.9W	219	266	38	133	43	018	25	109	03	202	64	P	ISO-18
53	May	21	1962	19.9S	177.2W	351	294	50	098	38	195	08	051	80	285	06	P	N
54	Nov	18	1965	18.8S	177.8W	424	327	45	147	45	057	00	147	00	147	90	P	ISO-31
55	Aug	20	1965	22.9S	176.1W	79	263	40	093	50	357	06	088	05	220	82	P	ISO-20
56	Aug	12	1967	24.7S	177.5W	134	350	27	193	61	085	10	177	18	324	70	X	N
57	July	21	1964	26.0S	177.9W	200	308	42	107	47	208	08	118	03	012	80	P	ISO-21
58	July	4	1963	26.3S	177.8W	190	339	39	071	01	164	51	288	25	031	28	P	ISO-22

TABLE 1 (continued)

No.	Mo.	Day	Yr.	Epicenter Lat.	Epicenter Long.	Depth, km	Axis of Compression (P) Trend	Axis of Compression (P) Plunge	Axis of Tension (T) Trend	Axis of Tension (T) Plunge	Null Axis (B) Trend	Null Axis (B) Plunge	Pole of 1st Nodal Plane Trend	Pole of 1st Nodal Plane Plunge	Pole of 2nd Nodal Plane Trend	Pole of 2nd Nodal Plane Plunge	Down-dip Stress Type	Reference
				degrees														
KERMADEC-NEW ZEALAND (Figure 12)																		
59	Jan	20	1968	29.9S	179.5W	349	330	62	071	07	164	26	044	45	273	33	P	N
60	Sep	4	1967	31.4S	179.4W	231	061	32	263	56	158	10	029	74	250	12	T	N
61	Aug	5	1964	32.2S	179.8E	216	074	32	254	58	344	00	254	13	074	77	T	ISO-23
62	Dec	8	1965	37.1S	177.5E	156	042	15	288	57	140	30	245	24	008	50	T	N
PERU-CHILE (Figure 13)																		
63	Mar	2	1967	0.3S	78.7W	121	040	49	181	34	286	20	129	68	018	08	n. p.	N
64	Sep	17	1965	1.5S	77.7W	191	242	52	038	36	137	12	229	08	352	76	n. p.	N
65	Nov	2	1964	4.1S	76.9W	91	290	85	059	02	150	04	243	42	056	48	T	N
66	Apr	13	1963	6.3S	76.6W	115	022	68	262	16	166	18	283	54	066	30	X	N
67	May	1	1966	8.4S	74.3W	154	263	60	118	25	021	15	286	19	148	66	X	N
68	Sep	17	1963	10.6S	78.2W	76	192	77	066	08	334	10	236	36	078	52	T	N
69	Sep	24	1963	10.7S	78.3W	60	220	63	040	27	130	00	220	18	040	72	T	N
70	Jan	26	1964	16.3S	71.7W	119	181	43	064	26	313	36	112	52	216	10	T	N
71	Dec	30	1965	16.6S	71.1W	112	257	51	070	38	163	03	252	06	045	83	T	N
72	July	30	1965	18.1S	70.8W	72	200	38	073	38	316	30	226	00	136	60	T	N
73	Dec	29	1963	18.3S	69.5W	125	271	53	070	34	165	09	259	10	034	76	T	N
74	Aug	20	1965	18.9S	69.0W	128	228	51	072	37	333	12	241	07	120	76	T	N
75	Feb	5	1966	19.1S	69.3W	142	135	05	037	54	229	35	343	31	102	40	X	N
76	May	11	1967	20.3S	68.5W	120	260	63	033	20	129	19	227	23	004	59	X	N
77	Jun	12	1965	20.5S	69.3W	102	240	55	060	35	150	00	240	10	060	80	T	N
78	Dec	27	1967	21.2S	68.3W	135	215	77	064	10	334	07	239	33	073	56	T	N
79	Dec	25	1967	21.5S	70.4W	53	238	60	088	27	352	13	257	16	118	69	T	N
80	May	7	1963	22.0S	68.5W	95	239	41	097	41	348	20	078	00	168	70	T	N
81	Aug	3	1965	23.2S	67.1W	140	256	69	076	21	166	00	076	66	256	24	T	N
82	Feb	23	1965	25.7S	70.5W	80	284	45	104	45	014	00	104	00	000	90	T	N
83	July	12	1965	28.4S	68.3W	118	298	74	054	07	146	14	246	36	038	50	T	N
84	Mar	28	1965	32.4S	71.3W	72	246	55	066	35	156	00	246	10	066	80	T	N
85	Nov	9	1963	8.8S	71.7W	576	017	84	258	03	168	04	263	48	074	42	P	BJ*
86	Nov	10	1963	9.0S	71.5W	596	011	74	257	07	165	14	266	50	064	37	P	BJ*

TABLE 1 (continued)

No.	Mo.	Day	Yr.	Epicenter Lat.	Epicenter Long.	Depth, km	Axis of Compression (P) Trend	Axis of Compression (P) Plunge	Axis of Tension (T) Trend	Axis of Tension (T) Plunge	Null Axis (B) Trend	Null Axis (B) Plunge	Pole of 1st Nodal Plane Trend	Pole of 1st Nodal Plane Plunge	Pole of 2nd Nodal Plane Trend	Pole of 2nd Nodal Plane Plunge	Down-dip Stress Type	Reference
				degrees														
87	Nov	28	1964	7.9S	71.3W	650	085	82	241	07	332	03	238	52	064	39	P	N
88	Nov	28	1964	7.9S	71.3W	651	All data fit solution for earthquake 87										P	N
89	Nov	3	1965	9.1S	71.4W	593	079	85	259	05	169	00	259	50	079	40	P	N
90	Feb	15	1967	9.0S	71.3W	597	102	85	256	04	348	02	254	50	078	38	P	N
91	Aug	15	1963	13.8S	69.3W	593	039	66	299	04	207	24	322	44	098	37	n. p.	Ch
92	Sep	29	1962	27.1S	63.2W	563	028	60	275	13	179	26	305	50	074	28	P	N
93	Dec	9	1964	27.5S	63.2W	578	081	57	261	33	171	00	261	78	081	12	P	N
94	Mar	5	1965	27.0S	63.3W	573	060	67	266	20	172	08	282	64	078	24	P	N
95	Dec	20	1966	26.1S	63.2W	586	092	60	243	26	340	12	216	68	073	18	P	N
96	Jan	17	1967	27.4S	63.3W	590	038	61	267	20	169	20	298	60	071	22	P	N
97 C	1936-1967,33 eqs.			24S-29S	62W-64W	545-625	097	54	256	35	353	10	265	80	039	12	P	Md
COLOMBIA, SOUTH AMERICA (Figure 15)																		
98	Feb	26	1965	6.9N	73.0W	147	240	39	126	26	012	39	276	08	177	50	n. p.	MS-125
99	Sep	11	1966	6.8N	73.0W	162	269	02	002	42	177	48	306	30	054	26	n. p.	MS-124
100	July	29	1967	6.8N	73.0W	161	254	32	127	44	004	29	098	08	200	60	n. p.	MS-126
SOUTH SANDWICH (Figure 16)																		
101	May	26	1965	56.1S	27.6W	120	052	00	146	50	322	39	085	35	202	30	X	N
102	May	27	1964	56.1S	27.6W	101	221	06	125	57	315	34	070	33	192	40	X	N
103	May	26	1964	56.4S	27.7W	114	041	14	156	38	298	45	083	40	188	19	X	N
104	Jan	16	1965	56.6S	27.4W	101	068	30	248	60	158	00	068	75	248	15	T	N
105	June	17	1967	58.3S	26.6W	140	272	64	073	24	167	08	056	68	259	20	P	N
WEST INDIES (Figure 17)																		
106	Dec	22	1964	18.4N	68.7W	117	203	00	113	68	293	20	183	40	041	40	n. p.	MS-112
MIDDLE AMERICA (Figure 18)																		
107	Aug	27	1967	12.3N	86.2W	183	238	31	062	59	328	02	059	14	230	76	T	N
108	Oct	15	1967	11.9N	86.0W	162	232	28	068	61	327	04	059	14	222	74	T	N
109	Apr	24	1964	13.7N	88.6W	150	228	24	033	64	135	06	044	20	235	69	T	MS-154
110	Feb	24	1963	14.6N	91.4W	133	236	35	056	55	326	00	056	10	236	80	T	MS-144
111	Mar	1	1965	15.4N	92.4W	85	204	46	061	39	313	19	223	04	121	70	T	MS-141

TABLE 1 (continued)

No.	Mo.	Day	Yr.	Epicenter Lat. degrees	Epicenter Long. degrees	Depth, km	Axis of Compression (P) Trend	Axis of Compression (P) Plunge	Axis of Tension (T) Trend	Axis of Tension (T) Plunge	Null Axis (B) Trend	Null Axis (B) Plunge	Pole of 1st Nodal Plane Trend	Pole of 1st Nodal Plane Plunge	Pole of 2nd Nodal Plane Trend	Pole of 2nd Nodal Plane Plunge	Down-dip Stress Type	Reference
NORTHWESTERN U.S.A.																		
112	Apr	29	1965	47.4N	122.3W	59	274	60	063	26	161	14	255	18	025	68	n.p.	N
ALEUTIANS (Figure 19)																		
113	Apr	2	1963	53.1N	171.7W	157	348	57	251	05	158	24	047	35	273	45	P	SB
204	July	2	1965	53.1N	167.6W	60	138	50	339	39	240	11	149	06	034	78	T	St
KURILE-KAMCHATKA-EASTERN HOKKAIDO (Figure 20)																		
114	Mar	18	1964	52.6N	153.7E	424	320	45	140	45	050	00	140	00	320	90	P	BJ
115	Oct	12	1967	52.2N	152.5E	476	331	46	093	20	199	36	049	50	300	15	P	N
116	Nov	22	1966	48.0N	146.8E	452	282	15	102	75	012	00	282	60	102	30	X	N
117	Dec	26	1964	51.9N	156.7E	145	300	45	120	45	030	00	300	00	120	90	P	N
118	Aug	4	1964	46.6N	151.4E	86	313	39	133	51	043	00	313	84	133	06	P	N
119	Feb	5	1966	50.0N	155.4E	121	141	28	280	54	040	21	305	14	182	65	T	N
120	Jan	29	1963	49.7N	155.0E	143	122	40	328	48	224	13	314	04	060	76	T	N
121	Dec	1	1967	49.5N	154.4E	136	117	36	325	51	218	14	310	08	069	74	T	N
122	Apr	5	1965	44.5N	150.9E	76	090	24	321	54	192	25	049	60	289	16	n.p.	N
123	Jun	30	1964	46.6N	144.6E	383	151	36	018	43	261	26	354	04	092	64	T	N
124	Oct	25	1965	44.2N	145.3E	181	139	36	346	50	237	14	091	74	330	08	T	N
125	Jun	23	1964	43.2N	146.2E	76	142	36	356	48	246	18	337	04	085	71	T	N
126	Sep	19	1967	43.0N	145.2E	84	148	35	006	50	252	20	345	08	096	69	T	N
127	July	4	1967	43.2N	142.5E	160	193	43	356	45	096	10	004	02	264	80	T	N
NORTH HONSHU-SEA OF JAPAN-MANCHURIA (Figures 20-21																		
128	Aug	20	1966	43.1N	140.6E	163	328	33	120	53	229	14	136	10	009	73	P	N
129	Feb	20	1931	44.9N	135.8E	350	311	27	207	27	079	50	259	40	349	00	P	H-D12
130	Mar	4	1959	37.6N	138.7E	219	350	23	246	07	141	67	291	20	026	10	X	I-96
131	May	31	1935	38.6N	134.2E	450	291	41	027	07	126	48	349	24	242	22	P	Hi
132	Jan	3	1957	43.8N	130.6E	593	287	33	086	55	190	10	099	10	322	75	P	Hi
133	Oct	8	1960	40.2N	130.0E	605	298	34	118	56	028	00	118	11	298	79	P	Hi
134	Jan	24	1964	38.8N	129.5E	557	294	26	157	56	034	20	256	64	130	17	P	N

TABLE 1 (continued)

No.	Mo.	Day	Yr.	Epicenter Lat. degrees	Epicenter Long. degrees	Depth, km	Axis of Compression (P) Trend	Axis of Compression (P) Plunge	Axis of Tension (T) Trend	Axis of Tension (T) Plunge	Null Axis (B) Trend	Null Axis (B) Plunge	Pole of 1st Nodal Plane Trend	Pole of 1st Nodal Plane Plunge	Pole of 2nd Nodal Plane Trend	Pole of 2nd Nodal Plane Plunge	Down-dip Stress Type	Reference
CENTRAL HONSHU - IZU-BONIN (Figures 21-22)																		
135	Combined solution, 1949-62, N of Tokyo					70-100	140	23	280	60	044	18	308	20	173	62	n. p.	I
136	May	14	1954	36.0N	137.4E	225	071	49	198	29	304	28	150	60	040	12	n. p.	R
137	Aug	13	1967	35.3N	135.3E	357	124	59	330	28	233	12	000	70	140	16	n. p.	N
138	May	5	1932	34.6N	135.3E	360	235	45	055	45	145	00	055	00	235	90	P	H-D19
139	Jun	2	1929	34.5N	137.2E	350	278	32	098	58	008	00	098	13	278	77	P	H-D9
140	Oct	26	1952	34.3N	137.5E	290	272	24	178	08	070	64	317	10	222	24	P	Hi
141	Apr	20	1942	33.0N	137.8E	350	280	45	100	45	010	00	280	90	100	00	P	H-D61
142	Jun	25	1936	32.4N	138.0E	300	282	43	076	43	179	14	359	76	089	00	P	H-D44
143	Mar	10	1966	32.2N	137.7E	390	255	33	101	53	354	13	086	10	212	74	P	KS-17
144	Apr	4	1932	30.6N	139.5E	445	263	43	053	43	158	16	338	74	068	00	P	H-D17
145	Apr	12	1965	30.2N	138.7E	428	263	32	048	51	161	19	067	10	313	69	P	KS-9
146	Feb	18	1956	30.2N	138.1E	475	246	35	338	04	075	55	298	27	197	20	P	R
147	July	11	1951	28.1N	139.9E	475	268	53	037	26	140	25	355	60	237	15	P	R
148	Jan	15	1964	29.2N	141.1E	80	154	12	034	66	249	20	131	52	351	31	X	KS-6
MARIANAS (Figure 23)																		
149	Jan	2	1965	19.1N	145.8E	136	043	60	177	22	276	20	013	20	144	61	X	KS-8
150	Mar	7	1962	19.1N	145.2E	683	049	90	049	00	139	00	049	45	229	45	P	KS-1
RYUKYUS - TAIWAN (Figure 24)																		
151	Sept	21	1965	29.0N	128.2E	201	329	52	090	22	193	30	050	55	292	18	P	KS-12
152	Jan	6	1964	27.3N	127.5E	115	321	48	100	35	206	20	045	69	298	07	P	KS-5
153	July	1	1966	24.6N	122.4E	119	214	18	034	72	124	00	034	27	214	63	n. p.	KS-21
154	Feb	13	1963	24.3N	122.1E	67	169	16	349	74	079	00	169	61	349	29	n. p.	KS-2
155	Oct	25	1967	24.4N	122.2E	70	274	10	018	60	180	28	071	31	304	46	n. p.	KS-26
156	May	17	1965	22.4N	121.2E	72	155	20	055	26	278	56	014	04	106	32	n. p.	KS-11
PHILIPPINES - CELEBES (Figure 25)																		
157	Jan	5	1967	13.8N	120.7E	166	243	06	139	66	336	24	082	34	218	46	n. p.	FM-26
158	Sep	16	1965	7.1N	126.6E	183	060	02	328	48	152	42	026	34	274	31	T	FM-21
159	Apr	2	1964	5.8N	125.7E	168	078	39	258	51	168	00	078	84	258	06	T	FM-20

TABLE 1 (continued)

No.	Mo.	Day	Yr.	Epicenter Lat.	Epicenter Long.	Depth, km	Axis of Compression (P) Trend	Axis of Compression (P) Plunge	Axis of Tension (T) Trend	Axis of Tension (T) Plunge	Null Axis (B) Trend	Null Axis (B) Plunge	Pole of 1st Nodal Plane Trend	Pole of 1st Nodal Plane Plunge	Pole of 2nd Nodal Plane Trend	Pole of 2nd Nodal Plane Plunge	Down-dip Stress Type	Reference
				degrees														
160	Oct	24	1965	4.2N	125.8E	151	064	29	244	61	154	00	064	74	244	16	T	FM-19
161	Jun	19	1963	4.7N	126.5E	183	084	35	264	55	174	00	264	10	084	80	T	F_b-34
162	Sep	7	1967	2.7N	124.3E	274	245	64	346	06	079	25	187	35	321	45	P	FM-24
163	Jun	10	1964	5.0N	127.4E	92	328	05	148	85	058	00	148	40	328	50	n. p.	FM-23
164	Nov	1	1964	3.1N	128.1E	77	182	08	281	49	085	40	128	39	241	26	n. p.	F_b-30
165	Sep	8	1966	2.4N	128.3E	71	231	04	002	83	140	04	046	39	237	50	n. p.	FM-25
166	Mar	10	1964	1.9N	127.5E	138	325	45	145	45	055	00	145	90	145	00	n. p.	FM-28
167	Feb	3	1966	0.1N	123.5E	165	130	14	019	62	228	26	104	51	333	29	n. p.	FM-18
168	Feb	19	1967	0.0	124.2E	101	118	21	249	60	020	22	151	61	281	21	n. p.	FM-22
169	Jan	8	1964	3.7S	119.5E	81	077	05	257	85	167	00	077	50	257	40	n. p.	FM-27
SUNDA (Figure 26)																		
170	May	21	1967	1.0S	101.5E	173	244	25	077	65	335	05	068	20	232	70	T	FM-2
171	Jun	30	1963	2.5S	102.5E	176	207	32	080	45	320	30	050	06	154	60	T	FM-3
172	Jan	17	1965	6.8S	109.1E	242	176	40	280	16	026	46	134	15	238	40	X	FM-4
173	Feb	29	1964	8.5S	112.7E	140	183	65	003	25	093	00	003	70	183	20	X	FM-1
174	Dec	15	1963	4.9S	108.1E	654	345	71	230	09	137	18	035	34	230	50	P	FM-5
175	Feb	3	1967	5.6S	110.5E	560	292	72	028	02	118	19	010	44	282	40	P	FM-6
176	Mar	24	1967	6.0S	112.3E	600	199	69	019	21	108	00	019	66	199	24	P	FM-7
177	Nov	9	1967	7.2S	123.6E	560	324	90	144	00	054	00	144	45	324	45	P	FM-8
178	Oct	18	1964	7.2S	123.9E	585	059	74	158	03	250	16	142	45	354	40	P	FM-9
179	Jun	22	1966	7.2S	124.7E	537	133	61	248	13	345	26	089	27	218	51	P	FM-10
180	Feb	14	1963	7.2S	127.8E	261	268	11	020	62	174	25	068	30	296	50	n. p.	FM-17
181	Nov	20	1963	7.3S	129.2E	140	110	22	241	59	010	22	142	60	272	20	n. p.	FM-16
182	Nov	21	1965	6.3S	130.3E	132	104	24	235	52	003	25	104	60	266	15	n. p.	FM-12
183	Aug	9	1967	6.4S	130.4E	89	023	04	284	64	114	25	226	36	358	44	n. p.	FM-13
184	May	12	1965	6.2S	130.3E	125	054	31	288	47	163	28	006	60	259	11	n. p.	FM-14
185	July	8	1964	5.5S	129.8E	189	225	31	357	49	119	25	024	10	274	63	n. p.	FM-15
186	Aug	20	1965	5.7S	128.6E	327	050	35	284	40	165	30	076	88	256	02	n. p.	FM-11
187	Mar	21	1964	6.4S	128.0E	373	033	35	144	24	258	43	088	48	355	04	n. p.	TB

TABLE 1 (continued)

No.	Mo.	Day	Yr.	Epicenter Lat.	Epicenter Long.	Depth, km	Axis of Compression (P) Trend	Axis of Compression (P) Plunge	Axis of Tension (T) Trend	Axis of Tension (T) Plunge	Null Axis (B) Trend	Null Axis (B) Plunge	Pole of 1st Nodal Plane Trend	Pole of 1st Nodal Plane Plunge	Pole of 2nd Nodal Plane Trend	Pole of 2nd Nodal Plane Plunge	Down-dip Stress Type	Reference
				degrees														
BURMA (Figure 27)																		
188	Feb	27	1964	21.7N	94.4E	91	208	30	090	40	322	34	056	04	153	54	T	F_a-8
HINDU KUSH (Figure 28)																		
189	July	6	1962	36.5N	70.3E	204	189	35	344	52	090	12	358	09	234	74	T	S
190	Jan	28	1964	36.5N	71.0E	197	124	25	280	63	029	09	296	19	147	69	T	HH
191	Mar	14	1965	36.3N	70.7E	219	215	15	035	75	125	00	035	30	215	60	T	R_b
192	1949-65, average solution			36-1/2N	70-1/2E	150-240	204	19	356	68	110	10	016	24	222	63	T	R_b
VRANCEA REGION OF THE EASTERN CARPATHIANS (Figure 29)																		
193	Jun	24	1940	45.7N	26.8E	115	302	10	163	74	037	07	132	35	297	54	T	VR
194	Oct	22	1940	45.7N	26.8E	120	303	10	162	75	036	06	130	34	295	55	T	CRE-6
195	Nov	10	1940	45.7N	26.8E	130	302	10	163	74	037	07	132	35	297	54	T	VR
196	May	1	1955	45.5N	26.5E	150	303	10	162	75	036	06	130	34	295	55	T	CE
197	Jan	26	1960	45.8N	26.3E	160	060	02	155	78	330	12	227	45	072	43	T	CE
AEGEAN (HELLENIC ARC) (Figure 29)																		
198	Nov	28	1965	36.3N	27.5E	89	244	25	348	28	118	52	294	38	028	06	n. p.	M
199	Mar	31	1965	38.6N	22.4E	78	235	17	029	60	140	10	262	70	046	14	T	M
200	July	17	1964	38.1N	23.6E	155	218	13	097	50	323	29	176	56	063	16	T	M
CALABRIAN ARC (Figure 29)																		
201	Feb	1	1956	39.1N	15.6E	215	324	62	118	25	213	10	306	17	093	70	P	CRE-48
202	1938-62, composite of 10 earthquakes			39 N	15 E	60-450	320	52	105	34	207	17	300	10	060	70	P	R_c
SPAIN (Figure 29)																		
203	Mar	29	1954	37.0N	3.5W	650	086	47	270	43	178	02	088	02	310	86	n. p.	HC

and configuration of the parts of lithospheric plates that have descended into the mantle during the past 10 m.y. or more.

DOUBLE-COUPLE MODEL OF THE SOURCE MECHANISM

The double-couple model [*Honda*, 1962] is adequate for all the solutions we obtained or examined. Alternate models, such as a sudden volume change, if present in combination with a double-couple component, would cause the nodal planes to be nonorthogonal and would affect the directions of first motions of shear waves. We find no evidence for such effects [see also *Ritsema*, 1964], although we cannot, in general, exclude minor contributions from such components [*Randall*, 1968].

We adhere to the following standard terminology for the parameters of the double-couple solutions: The two orthogonal axes that bisect the quadrants of dilatational and compressional first motions are the compressional, or P, axis and the tensional, or T, axis, respectively. A third axis, perpendicular to both the P and T axes and coincident with the intersection of the nodal planes, is the B, or null, axis. In the dislocation model equivalent to the double couple, one of the nodal planes is the fault plane, and the pole of the other nodal plane is parallel to the slip vector.

The correspondence of the P, B, and T axes and the principal axes of maximum, intermediate, and minimum compressive stress is an assumption, justified basically by the results (described in the next section), that for deep and intermediate-depth earthquakes the P, B, and T axes are the most closely grouped of the double-couple parameters and are most nearly parallel to the planar geometry of the seismic zones [*Isacks et al.*, 1968, 1969; *McKenzie*, 1969*a*; *Isacks and Molnar*, 1969]. Hence, the physical mechanisms of mantle earthquakes may be such that the shearing or faulting forms at an angle of about 45° to the axis of maximum compressive stress. If the angle between the P axis and the axis of maximum compressive stress were as much as 15°, however, detection of such an effect [*Isacks et al.*, 1969] would be difficult with the present resolution of our data. Thus, in terms of a Coulomb-Mohr-type process, we can only suggest that the effective coefficient of internal friction is probably less than 1 and may be 0.

STRESS WITHIN DESCENDING LITHOSPHERIC PLATES

Parallelism between Stress Axes and Inclined Seismic Zones

The parallelism between the axes of compression or tension of the double-couple solutions and the seismic zones is the primary evidence that the earthquakes in the mantle occur inside descending lithospheric plates in response to stresses within the plates. The nonparallelism between the nodal planes (one of which is the fault plane) and the seismic zones shows that the solutions cannot be interpreted as simple shearing parallel to the zones. We demonstrated these relationships in our previous paper (Figure 1 of *Isacks and Molnar* [1969]) by plotting the axes and poles of the solutions on a common projection oriented relative to the local strike and dip of the well-defined inclined seismic zones. We do

not use this method of presentation further in this paper because (1) the precision with which the orientation of a zone can be determined varies greatly from region to region, and (2) a major cause of variations among solutions for a region may be variations in the structure of the zone rather than some inherent feature of the mechanism. Thus, further quantitative study of the closeness of grouping of the axes requires detailed resolution of the distribution of hypocenters near the events with well-determined solutions. In this paper we seek instead a broad global survey of the outstanding features that can be discerned with presently available information.

The parallelism between the stress axes and the seismic zones is demonstrated individually for each region in Figures 7 through 29. In most cases either the P or the T axis is parallel to the zone. Often either the P or the T axis may group strongly about a common direction, while the other two axes interchange positions or form a girdle about the stably oriented axis. This feature suggests that the intermediate principal stress is nearly equal in magnitude to one of the other principal stresses [*Balakina*, 1962]. In some regions all three stress axes interchange positions. Although the cause of such a marked spatial variability in the distribution of stresses may be obscure, the idea of a stressed plate does offer a general explanation for this otherwise puzzling result.

Hypotheses for deep earthquakes of the type proposed by *Sugimura and Uyeda* [1967] and *Savage* [1969] do not account for the results of the preceding paragraph. In these hypotheses the shearing and faulting is constrained to be parallel to planes of pre-existing weakness in the material; thus the poles of the nodal planes, or at least one set of poles, rather than the P or T axes, should be the most closely grouped parameter of the solutions and have the most consistent relationship to the orientation of the seismic zone. Savage recognizes this problem and proposes that the interchanging of stress axes is characteristic only of more contorted parts of slabs. In our study, however, we can find little evidence to support this; the interchanging of axes occurs in zones such as those in parts of the Izu-Bonin, Tonga, and New Hebrides regions that are relatively uncontorted.

Ritsema [1964, 1966, 1970] reports that the poles of the nodal planes for earthquakes in the mantle tend to be horizontal or vertical and that the sense of shearing across the more horizontal nodal plane reverses from intermediate to great depths. To explain these results Ritsema proposes a predominantly horizontal motion of material through the gap of seismicity between deep and intermediate-depth earthquakes (see also *Harrington* [1963]). This reversal in orientation is in agreement with our findings except that we interpret this as a change from extension to compression inside an inclined slab of lithosphere. The main difference is that we find that the nodal planes or their poles do not tend to be horizontal or vertical. A histogram of the plunges of the poles listed in Table 1 shows a nearly uniform distribution of angles between 0° (horizontal) and 90° (vertical). The difference seems to be a result of *Ritsema's* [1970, p. 504] rejection of solutions in which the pattern of first motions is dominated by one polarity. His selection would thus be biased against solutions that do not have a nearly vertical nodal plane.

The lack of a strong tendency for the nodal planes to be vertical and hori-

zontal also argues against the hypothesis (e.g., *Lliboutry* [1969]) that the lithosphere breaks up and sinks vertically along en echelon vertical faults.

A few solutions for intermediate-depth earthquakes can be interpreted as a downward continuation of the thrust faulting characteristic of shallow portions of inclined seismic zones. The depths of these events are less than about 100 km. Although in some cases either or both the hypocentral depth and the dip of the seismic zone are uncertain, further results of this type may give some indication of the thickness of the overthrust plate of lithosphere.

Predominance and Variations of Down-Dip Stress Orientations

For brevity we refer to orientations of the stress axes in which the P or T axis is parallel to the local dip of the seismic zone as 'down-dip compression' or 'down-dip extension,' respectively. The prevalence of these orientations is demonstrated by the fact that two-thirds of the 204 solutions listed in Table 1 are of one type or the other. Included are solutions from nearly every region where mantle earthquakes occur, so that the generalization is global in scope. In regions where the structure of the zone is known best, the axes tend to scatter within 25° or less of the direction of dip; it is not certain how much of the scatter is due to complexities in the structure of the zones or small systematic differences between the P, T, and B axes and the principal axes of stress in the material. In other regions, where the orientations of the zones are not so well known, the available evidence is still sufficient in many cases to conclude that the parameter most nearly parallel to the dip of the zone is either the P or the T axis. The remaining third of the solutions are for events in markedly contorted parts of zones or in zones of undetermined structure, or are more or less well-established exceptions.

Figure 2 is a summary of the variations of down-dip stress type as a function of region and depth. Also shown are the approximate configurations of the deep seismic zones, the maximum depths, and the locations of marked gaps in seismic activity as a function of depth. The data and interpretations upon which this figure is based are described in detail in the regional sections and are summarized in the next-to-last column of Table 1. Not included in the figure are certain complex regions near prominent junctions or ends of zones (discussed in the next section) and a few regions where the structure is very poorly known. The figure illustrates the following major results of this study:

1. There are remarkable systematic differences between intermediate-depth and deep solutions:
   (a) The deep solutions are very strongly dominated by down-dip compression.
   (b) The intermediate-depth solutions are more variable and include down-dip compression and extension, as well as many solutions that are clearly neither (X's in Figure 2).

2. There is a correlation between the down-dip stress type at intermediate depths and the gross nature of the distribution of seismicity as a function of depth:

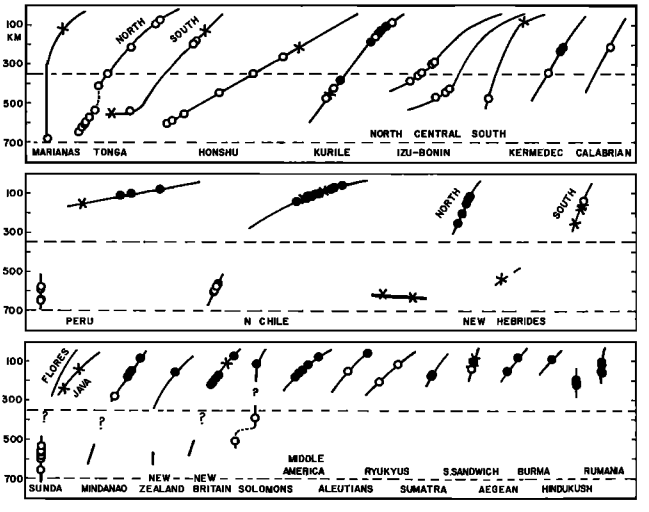

Fig. 2. Global summary of the distribution of down-dip stresses in inclined seismic zones. The stress axis that is approximately parallel to the dip of the zone is represented by an unfilled (open) circle for the compressional or P axis and a filled (solid) circle for the tensional or T axis; an X indicates that neither the P nor the T axis is approximately parallel to the dip. The data plotted are tabulated in the second-to-last column of Table 1. For each region the line represents the seismic zone in a vertical section aligned perpendicular to the strike of the zone. The lines show approximately the dips and lengths of the zone and gaps in the seismic activity as a function of depth.

(a) Down-dip extension is predominant in regions where either marked gaps in seismicity are present between deep and intermediate-depth events or where no deep earthquakes are present.

(b) Down-dip compression is predominant where the zone is continuous, but this correlation is tenuous.

3. There is no obvious correlation between the bends in the vertical sections shown in Figure 2 and the down-dip stress type. Down-dip compression is dominant below 300 km regardless of the configuration of the zone, whereas at intermediate depths the variations in down-dip stress type are not related in any obvious way to the structure of the zone.

Sinking of the Lithosphere

Sinking at intermediate depths. We claimed in our previous paper that generalizations 1 and especially 2 listed above constitute evidence for the models shown in Figure 3 in which lithospheric plates, more dense than the surrounding mantle, sink into the asthenosphere under their own weight and are thereby placed under extension. Thus the sections shown in the middle and lower parts of Figure 2 correspond to models *a*, *b*, or possibly *d* in Figure 3, whereas those in the upper part correspond to *c* (or possibly *b* in the Kurile-Kermadec sections). The idea that the suboceanic lithosphere is gravitationally unstable and can sink into the asthenosphere is physically plausible and supported by seismological and gravity data (e.g., *Elsasser* [1967], *Oliver and Isacks* [1967, 1968], *McKenzie*

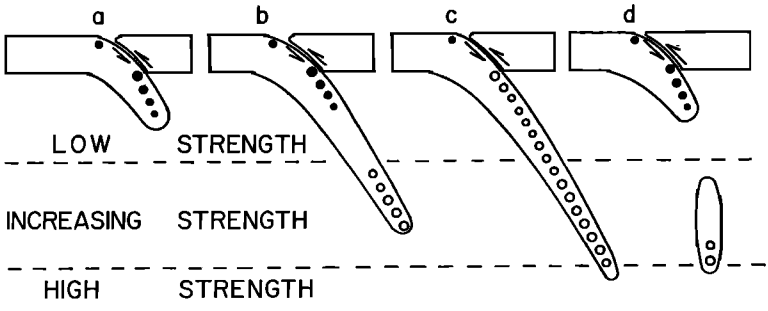

Fig. 3. A model showing plausible distributions of stresses within slabs where gravitational forces act on excess mass within the slabs. A filled circle represents down-dip extension, an unfilled circle represents down-dip compression, and the size of the circle qualitatively indicates the relative amount of seismic activity. In (a) the slab sinks into the asthenosphere, and the load of excess mass is mainly supported by forces applied to the slab above the sinking portion; in (b) the slab penetrates stronger material, and part of the load is supported from below, part from above; the stress changes from extension to compression as a function of depth. In (c) the entire load is supported from below, and the slab is under compression throughout. In (d) a piece has broken off. A gap in seismicity as a function of depth would be expected for (b) and (d), whereas no deep earthquakes occur beneath (a). The horizontal dashed lines in the figures indicate possible phase changes in the upper mantle near 350–400 km and 650–700 km [*Anderson*, 1967]. (Figure after *Isacks and Molnar*, 1969.)

[1969*b*], *Press* [1969], *Hatherton* [1969, 1970], *Jacoby* [1970], and *Griggs* [1971]).

Most of the seismic zones shown in Figure 2 appear to be in descending pieces of suboceanic lithosphere. Beneath several continental regions in the Alpide belt, such as Burma, the Hindu Kush, and Rumania, however, the subcrustal zones cannot be traced to any nearby piece of oceanic crust. Although there is no problem in having oceanic lithosphere sink into the mantle, continental lithosphere is probably buoyant and would tend to remain on the surface. Geological evidence indicates that much of the Alpide belt may be beneath or near the suture where an ocean has closed and where collision of continental plates has taken place [*Holmes*, 1965]. Thus the prevalence of nearly vertical extensional stresses in the mantle beneath these regions suggests that pieces of oceanic lithosphere, remnants of a consumed suboceanic plate, are now pulling away and downward from the continental piece to which it is attached.

The imperfection of the correlation between down-dip stress type at intermediate depths and the distribution of seismicity as a function of depth—notably, the variability of stresses within the Kurile arc and the southern New Hebrides, the down-dip compressions in the South Sandwich and Ryukyu arcs, and the complex orientations that are found in several other regions—suggest that at intermediate depths stresses other than the simple two-dimensional type implied in Figure 3 are present in certain regions. This is not surprising, since events at intermediate depths are nearest the region where the plate bends downward

into the mantle; thus in certain regions geometric adjustments to this major deformation may locally control the orientation of stress inside the plate. Other complications may include effects of seamounts and other topographic features on the forces applied to the descending slab in the underthrusting zone; effects of fault zones and other mechanical heterogeneities inherited from the formation and deformation of the slab on the surface prior to its descent; variations in the gravitational force due to a heterogeneous distribution of excess mass in the slab; and localized effects of chemical or phase transitions that are not distributed uniformly through the descending slab. Some of these effects could also explain the nests of intense activity or remarkable gaps in activity that characterize the distribution of earthquakes along the strike of many zones.

Down-dip compression between 300 and 700 km. The most consistent result of this investigation is the predominance of down-dip compression everywhere below about 300 km. One interpretation of this result is that the forces on the lower portions of the slab that resist its motion become relatively important below 300 km. The compressional stress inside the slab would be the result of the downward-directed forces applied to the upper portions of the slab and the upward-directed resisting forces applied to the lower parts of the slab. The cause of this resistance might be either an increase in strength in the surrounding mantle or a buoyant effect if the density of the slab were lower than that in the surrounding mantle.

The interval of depth in which down-dip compression is prevalent is bounded approximately by the depths of 350–400 and 650–700 km at which major phase changes are thought to occur in the normal mantle [*Anderson,* 1967]. If the shallower transition (near 350–400 km) occurs at shallower depths in the slab than in the adjacent mantle [*Griggs,* 1971], the additional load of dense material would further drive the lower portions of the slab downward and therefore accentuate the compressional stress inside the slab below 300 km. This effect is supported by both the focal-mechanism data and the estimated parameters of the phase change [*Anderson,* 1967; *Akimoto and Fujisawa,* 1968].

On the other hand, the parameters given by Anderson suggest that the deeper phase change (near 650–700 km) would occur at greater depth in the slab than in the surrounding mantle. This would provide an upward buoyant force that resists the sinking of the lithosphere. The critical parameters in this case are the slope of the pressure-temperature curve at the phase boundary and a possible increase in the iron-magnesium ratio with depth. Unfortunately, however, to our knowledge these parameters are not well determined. If the parameters of the phase change are such that buoyant resistance does not occur, the prevalence of down-dip compression provides strong evidence for an increase in strength in the mantle. Alternatively, if the strength does not increase enough to support the heavy slabs, then the focal-mechanism data support the idea that the buoyant resisting force is important.

In Figure 3 we suggest a zone of increasing strength below depths of about 350 km to account for the compressional stresses in seismic zones that reach depths of only 500 km. This is reasonable in view of the indications of a minimum of creep strength as a function of depth in the upper 300–400 km of the mantle

[*Gordon,* 1965; *Anderson,* 1966; *McConnell,* 1968; *Weertman,* 1970]. However, the strength of the material through which the slab penetrates must remain significantly smaller than the strength of the slab if the plate is to maintain its identity as such to the depths of the deepest earthquakes. 'Strength' as used here is creep strength as defined by *Weertman* [1970].

Gaps in the lithosphere. Figure 3 shows two possible explanations for the gaps in seismic activity as a function of depth; in Figure 3*b* the lithosphere is continuous, but the deviatoric stress goes to zero in changing from compression to extension. In Figure 3*d* the lithosphere is discontinuous, and the gap in seismicity corresponds to a gap in the lithosphere. In this model a piece of lithosphere has become detached and is sinking independently.

There is evidence that at least in some regions a piece of lithosphere may be detached as shown in Figure 3*d*. The remarkable configurations of the zones beneath Peru and western Brazil and the New Hebrides (Figures 10 and 14) suggest this. The deep earthquakes beneath the North Island of New Zealand [*Adams,* 1963] represent a significant discrepancy in the otherwise regular relationship between the length of the seismic zone and the rate of convergence along the Tonga-Kermadec-New Zealand island arc [*Isacks et al.,* 1968; *McKenzie,* 1969*b*] and therefore may be located in a detached piece of lithosphere. The solution for the Spanish deep earthquake, in comparison with results for nearly every other region of deep-focus activity in the world, is not explicable as down-dip compression in a lithospheric slab that is traceable to a presently active island arc on the surface; this earthquake may thus also be located in a piece of lithosphere that is detached from a surface plate.

Observations of the frequencies and amplitudes of seismic shear waves from deep earthquakes recorded at suitable locations might indicate the presence or absence of a gap in the lithosphere. In New Zealand [*Mooney,* 1970], the New Hebrides (Barazangi, personal communication, 1970), New Britain, the Solomons, and Chile [*Molnar and Oliver,* 1969; *Sacks,* 1969], regions where notable gaps in seismicity are present, high-frequency shear waves pass through the gap. In the case of the Peru-western Brazil region [*Molnar and Oliver,* 1969; *Sacks,* 1969], the results are as yet ambiguous. The clearly recorded high-frequency phases mean either that the lithosphere is continuous through these gaps or that the zone of large attentuation in the adacent normal mantle is confined primarily to the region above the gaps, i.e., above about 300 km. Since the last alternative cannot be excluded, the question remains open.

Contortions and Disruptions of the Descending Lithosphere

The two major world-encircling belts of island-arc or island-arc-like structures, the circum-Pacific and Alpide belts, are divided into more or less well-defined discrete segments. The junctions between these segments are characterized by abrupt changes or offsets in trend, marked changes in the dip of the seismic zones, gaps in the seismic activity, shallowing of the oceanic trench, and intersection of major transverse features. The curvature of the island arc on the surface, though generally convex toward the oceanic side, varies considerably among the segments of island arcs. In some cases the arc ends abruptly and the inclined

seismic zone has a well-defined lateral edge. These features imply that the descending edges of lithospheric plates are contorted and segmented. Thus, it would be surprising if the distribution of stresses inside the descending portions could be completely understood in terms of the two-dimensional models of Figure 3. In particular, the solutions excluded from Figure 2 are for events located near major junctions and contorted edges of seismic zones, and are discussed below. Moreover, some of the solutions shown in Figure 2 by an X (i.e., solutions interpretable as neither down-dip compression nor extension), as well as some of the anomalous down-dip types, can be attributed to deformations of the slabs that result from three-dimensional geometrical effects rather than the two-dimensional effects of Figure 3.

Bending of lateral edges of inclined seismic zones. The distribution of hypocenters at the northern end of the Tonga island arc (Figure 11) and beneath the Banda Sea at the eastern end of the Sunda island arc (Figure 26) show that the lateral edges of the seismic zones in these two regions are bent upward. A simplified picture of such a deformation is shown in Figure 4. Limited evidence suggests that bent edges are also located at the northeastern end of the seismic zone beneath Colombia, South America (near the Bucaramanga 'nest'), the northern ends of the West Indies and the South Sandwich arcs, the southern end of the New Hebrides arc, and the northern end of the Izu-Bonin arc.

Direct effects of the bending, i.e., a compression or an extension perpendicular to the axis of bending, are indicated clearly by only two solutions for deep events beneath the Banda Sea and by solutions for intermediate-depth events in Colombia. In the latter region the interpretation is very uncertain. In contrast, the solutions for events near the northern end of the Tonga arc appear to be merely rotated versions of the solutions in the unbent part, wherein the axis of rotation corresponds to the axis of bending. This relationship implies that the bending

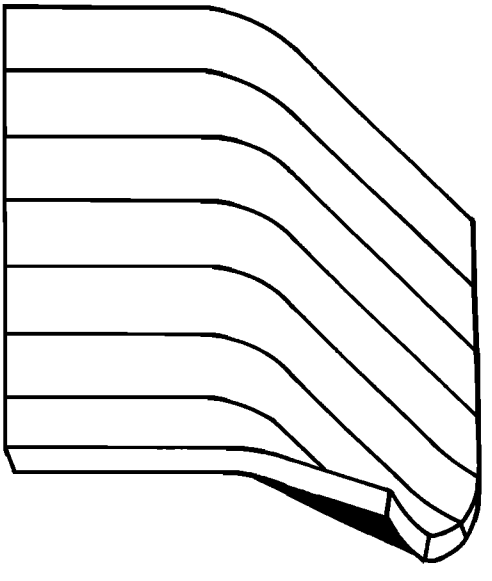

Fig. 4. Diagram showing a bent edge of a descending lithospheric plate. The surficial portion of the plate is to the left; on the right side the plate bends down and descends into the mantle. The lower corner of the descending part of the slab curls upward, as shown in the lower right-hand side of the model. Such a structure is postulated, for example, for the eastern, northern, and southern ends of the Sunda, Tonga, and New Hebrides arcs, respectively. (Figure after *Fitch and Molnar* [1969].)

does not produce the stress released by the earthquakes but merely changes the orientation of the stress guide.

Oblique-angled junctions. Three notable oblique-angle junctions, all concave toward the oceanic side, are located respectively at the junctions of the Kurile, North Honshu, and Izu-Bonin arcs and between the island-arc-like structures of Peru and Chile in western South America. Only near the junction between the North Honshu and Izu-Bonin segments do we find good evidence for localized effects on the focal-mechanism solutions. The data suggest that the lithosphere may be tearing beneath central Honshu and descending beneath the Sea of Japan and south of Honshu as separate slabs (Fig. 5*b*).

Wyss [1970] suggests that the low apparent stress calculated for intermediate-depth events near the Peru-Chile corner may be due to a tear in the slab. However, the solutions for intermediate-depth events exhibit no obvious effects of the corner, but seem to be related to stresses inside one of the segments rather than to stresses attributable to the presumed tearing.

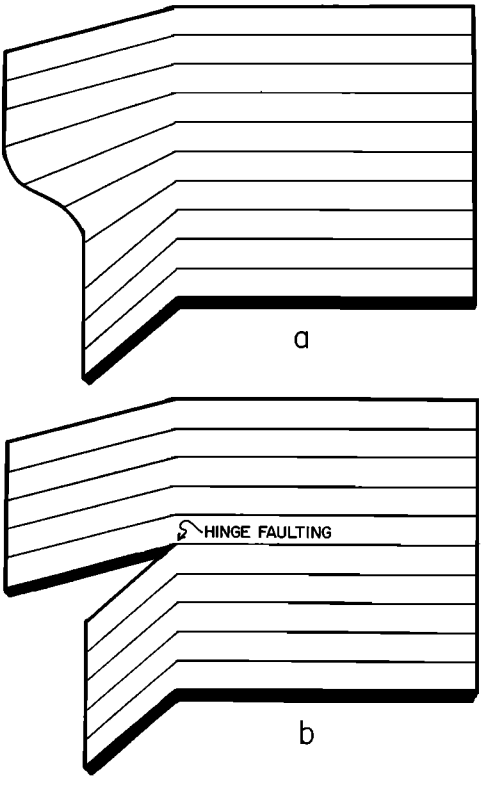

Fig. 5. Contortion (a) or disruption (b) between two segments of a slab with different dips. In (a) the portion between the two segments is bent and stretched. In (b) the two segments tear apart along a vertical hinge fault. In this type of faulting the motion would be nearly vertical and such that the more steeply dipping side moves down relative to the more gently dipping side. An example may be located beneath south-central Honshu (Figures 21 and 22).

This may also be the case for the junction between the Kurile and North Honshu segments, where the solutions seem more related to patterns on either side than to effects of the corner itself. However, the interpretation for this region is more complex because of the variability of stress orientations within the Kurile zone.

Junctions between the Tonga and Kermadec island arcs and the North Island of New Zealand, and between the Izu-Bonin and Marianas, are characterized by low seismic activity; and few solutions near these junctions were obtained. The distribution of hypocenters suggests that the Tonga-Kermadec zone is disrupted into two segments corresponding to a Tonga slab and a Kermadec slab.

Convex curvature. *Frank* [1968] points out that unless a simple geometrical relationship holds between the dip and the curvature of the surface trace of the seismic zone, surface area is not conserved, and the descending plate will be either laterally compressed or stretched. *Stauder* [1968*b*] suggests that such an effect could account for extension parallel to the strike of the seismic zone that he inferred from the solution of an intermediate-depth event in the Aleutians (Figure 19). Although Stauder's argument is based on a flat-earth model (as depicted in Figure 6), extension is still to be expected there because of the steep dip of the seismic zone [*Davies and McKenzie,* 1969; *Murdock,* 1969]. A similar effect may account for solutions of several events in the Sunda, Mindanao, and New Hebrides arcs.

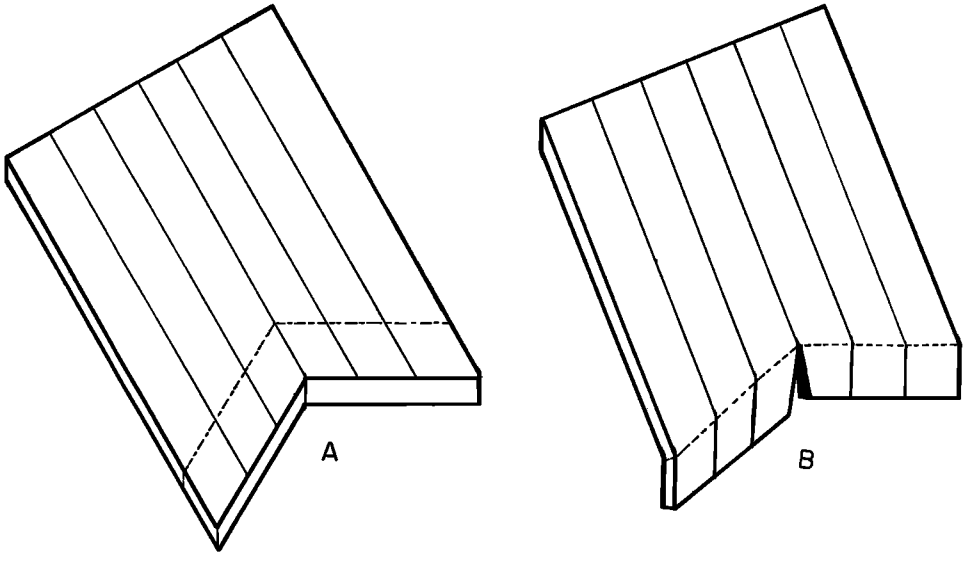

Fig. 6. Illustration of how lateral extension can be produced in the descending portion of a plate near a corner (or bend) that is concave toward the direction of dip of the slab. The dotted line represents the axis of the trench and the axis of bending. In 6A a horizontal, undeformed slab is shown. Bending of the underthrust edge of the slab along the trench axis produces lateral extension or separation near the corner; in 6B a separation is shown for clarity. An example of possible lateral extension is shown in Figure 19 for the Aleutian arc [*Stauder,* 1968*b*].

On the other hand, if the dip of the seismic zone is less than twice the radius of curvature (in degrees) of the surface trace of the arc, then lateral compression should result. One solution in agreement with this is found at intermediate depths in the nearly straight Izu-Bonin arc.

By the same reasoning, lateral compression should be present near the concave corners discussed in the last section. In those cases, however, the zones on either side differ appreciably in dip so that a contortion or disruption of the types depicted in Figure 5 may apply instead.

Bending as the source of earthquake-producing stresses. The evidence reviewed above, plus the lack of effect on the mechanism solutions of the bends in the seismic zones depicted in Figure 1, suggests that stresses due to bending of the lithospheric plates do not play an important role in the generation of earthquakes in the mantle. This conclusion is not surprising in view of the lack of any appreciable seismic activity that can be associated with the very pronounced bending of the lithosphere as it turns downward beneath the island arc. The only earthquakes that appear to be clearly associated with this bend are shallow earthquakes located beneath or slightly seaward of the axis of the trench and characterized by horizontal extension perpendicular to the trench. These are most prominent in the Aleutian arc [*Stauder,* 1968*b*], although a few examples are reported for other arcs [*Molnar and Sykes,* 1969; *Katsumata and Sykes,* 1969; *Fitch,* 1970*a*; *Isacks,* 1970]. An event at 80 km beneath the axis of the Kurile trench may also be associated with compressional stress at the bottom of the bending lithosphere, although in this case the interpretation is uncertain (Figure 20). The part of the underthrust lithosphere between the trench axis and the volcanoes, where the bending is presumably most severe, appears to be relatively aseismic. The relief of extensional stress near the upper part of the bent suboceanic lithosphere by earthquakes must therefore be suppressed when the upper surface of the plate moves beneath the arc.

The implication of these observations is that the generation of intermediate-depth and deep earthquakes is governed not only by the distribution of stress within the lithosphere but also by unusual physical properties or conditions within the downgoing part of the plate. This is further suggested by the fact that earthquakes inside the lithosphere are apparently rare except in the downgoing part. Of three general types of hypotheses that have been proposed to explain the process of shear fracturing in a deep earthquake—(1) an embrittlement or weakening [*Raleigh and Paterson,* 1965] or some other effect (e.g., *Griggs and Handin* [1960] and *Savage* [1969]) associated with a fluid phase; (2) a high-temperature instability in the creep rate (e.g., *Orowan* [1965], *Griggs and Baker* [1969]); and (3) a high-pressure, low-temperature mechanical instability [*Byerlee and Brace,* 1969]—the first might be expected to apply more to the sides than to the center of the descending slab. The lack of effects attributable to simple bending of the slabs suggests that the earthquakes are located nearer the center than the sides, and further suggests that the earthquakes occur in the coldest material. These inferences concur with (3), although both the theoretical and the experimental bases for that hypothesis with respect to deep earthquakes are uncertain.

Implications for Plate Tectonics and Mantle Convection

In adding further support to the concept of subcrustal earthquake zones as parts of coherent and strong plates of lithosphere, our results contribute to two major conditions that a convection theory should satisfy. The first is that lithospheric material can descend to depths of at least 650–700 km. Furthermore, the predominance of compressive stresses at great depths and the correspondence of the depth of the sharp cutoff in world seismicity as a function of depth with a major discontinuity or transition region in the mantle [*Engdahl and Flinn,* 1969] suggest but do not prove that the lithospheric material does not penetrate deeper than 700 km. The second condition is that, because the descending slabs would be impenetrable, the configuration of the inclined seismic zones places strong constraints on the movement of material in the asthenosphere; any flow of material must turn down near the zones and cannot pass through them. By the same reasoning, the contortions of the slabs contain information about the integrated history of the relative motions between the lithosphere, the asthenosphere, and, possibly, the mesosphere in the cases of the deepest zones. Although the contortions are not of sufficient magnitude to obscure the basic inclined-plane asymmetry of most zones, they do attest to relative motions between the upper and lower parts of slabs, including both translations and rotations.

The forces involved in the gravitational sinking at intermediate depths, if transmitted past the bending and underthrusting part of the lithosphere near the trench and island arc, could be an important contribution to the driving mechanism of sea-floor spreading and continental drift. Moreover, the increased resistance to the downward motion of the lithosphere at depths greater than 300 km might cause alterations in the pattern of movements of surficial plates of lithosphere. Our results for the Tonga region may have a direct bearing on these questions. The Tonga arc includes the clearest example of a continuous zone under compression through a range of depths between about 80 km and greater than 600 km; in this case the resisting forces applied to the lower part of the slab apparently support nearly the entire load of excess mass within the slab. Thus (1) the excess mass above 80 km is sufficient to drive the slab downward; (2) the slab is being pushed downward by forces applied mainly to the surface portions; or (3) the downward motions are essentially stopping. The high level of shallow seismicity [*Brune,* 1968; *Davies and Brune,* 1971], the lack of sediments in the Tonga trench, the depth of the trench, and other geophysical and geological observations argue against but do not disprove (3). The first is not likely because the lithosphere itself may be nearly 80 km. Thus the results for this region (and probably for North Honshu also) suggest that the gravitational sinking force and resistance at great depth, although probably important in the dynamics of the descending portions of the plates, cannot be the only important forces driving the horizontal motions of the lithosphere.

REGION-BY-REGION PRESENTATION OF DATA

A detailed region-by-region analysis of the relationships between the stress axes inferred from the focal-mechanism solutions and the local structures of the seismic zones is presented in this section. The critical information is the distri-

bution of hypocenters near the earthquakes for which focal-mechanism solutions are available. Three basic sources of data used for all the regions are *Gutenberg and Richter* [1954], the locations of the Coast and Geodetic Survey (ESSA) as compiled by *Barazangi and Dorman* [1969], and *Duda* [1964]. In particular, enlarged versions of Barazangi and Dorman's maps of epicenters within intervals of 100-km depth were very helpful. These data are supplemented by more detailed studies of particular regions if available.

In each region the solutions are divided into groups according to their similarity and the locations of the earthquakes involved. If the structure of the seismic zone is reasonably well determined, the orientation of the stress axes can then be compared with that of a plane that best represents the local structure of the zone. This provides the basic test of the hypothesis that deep and intermediate-depth earthquakes indicate stresses within thin lithospheric plates as well as of additional hypotheses discussed in the previous section. On the other hand, if the structure of the seismic zone is poorly known, the procedure can be reversed; the stress axes of the solutions determine planes whose orientations can then be compared with the available information on the distribution of hypocenters and with other regional trends. This comparison yields additional weak tests for the hypothesis of stressed plates as well as information on the detailed regional tectonics.

In addition, the features used in the construction of Figure 2 are described for each region; these include the maximum depth of hypocenters and the presence and range of depths of a gap in the distribution of hypocenters as a function of depth. The determination of gaps is subject to some uncertainties; it is not possible to discriminate between a truly aseismic gap and a gap that is actually a minimum in a continuous but insufficiently sampled distribution.

The presentation starts with the New Guinea region and proceeds counterclockwise around the Pacific and thence through Indonesia and the Himalayan-Alpide belt to the Mediterranean Sea. The numbers used in Table 1 and the figures refer to either the earthquake or its mechanism solution.

New Guinea-New Britain-Solomon Islands (Figures 7 and 8)

Deep sea trenches, belts of volcanoes, and inclined zones of shallow- and deep-focus hypocenters form island-arc structures parallel to the New Britain and Solomon Islands. These two structures meet and form a sharp corner east of the southeastern tip of New Ireland. Like the New Hebrides arc farther east and unlike all other circum-Pacific arcs, the New Britain and Solomon arcs are convex to the south and face away from the Pacific basin. Apparently, lithosphere beneath the Coral and Solomon Seas is being consumed in these arcs. Southwest and west of New Britain subcrustal earthquakes occur beneath New Guinea, but the distribution of hypocenters is not well defined. Several additional zones of shallow earthquakes are present in the region. The most striking is a well-defined linear alignment of shallow epicenters that crosses the Bismarck Sea north of New Britain. Another follows the Bismarck archipelago, while a third appears to cross the Solomon Sea from the southeastern end of New Guinea to the Solomon Islands. These zones suggest that in this region the boundary between

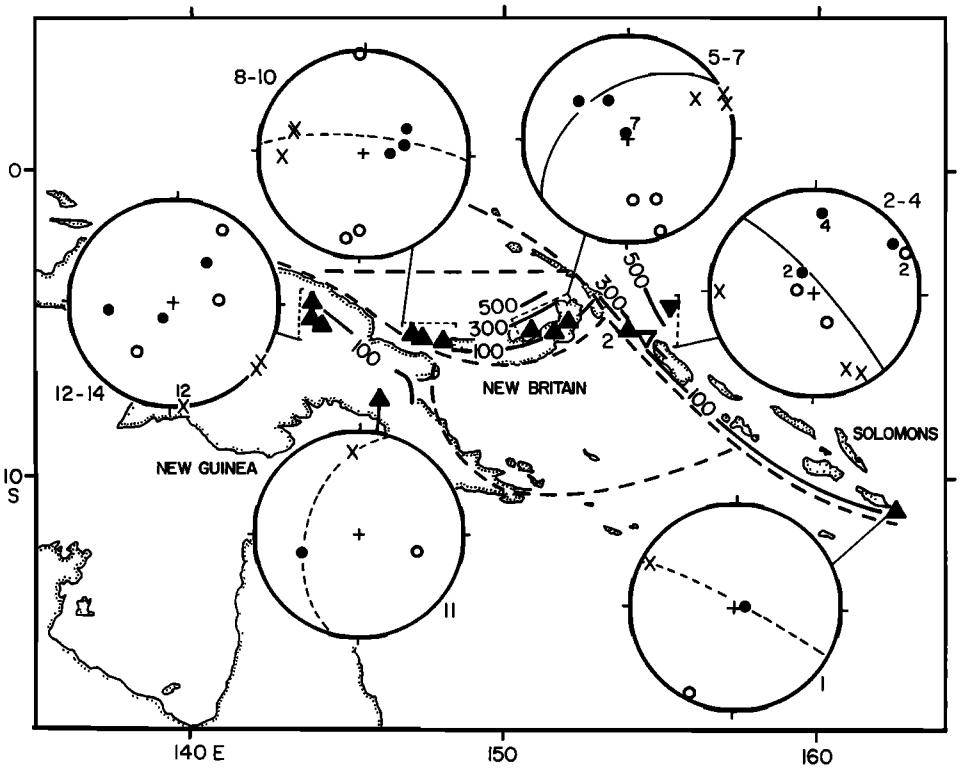

Fig. 7. The Solomons and the New Britain island arcs and the region of New Guinea. The following symbols apply to Figures 7–29: The large circles are equal-area projections of the lower hemisphere of a focal sphere and are oriented according to the directions of the map projection; in all cases the top and right-hand side correspond to north and east, respectively. A filled circle represents the axis of tension, T; an unfilled circle represents the axis of compression, P; and an X represents the null axis, B. A solid line in the projection is the trace of the plane that best fits the orientation of the seismic zone; a dashed line is the trace of a plane parallel to two of the stress axes (or the average positions of groups of axes) and perpendicular to the third axis. If earthquakes occur in thin, slablike stress guides, this plane should give the orientation of the slab. The numbers near the projections refer to the solutions plotted in the projection and listed in Table 1. On the map the contours of hypocentral depth (in kilometers) are shown by solid lines. The epicenters of the events are shown by filled, upward-pointing triangles for hypocentral depths of 70–229 km; unfilled, upward-pointing triangles for depths of 300–499 km; and filled, downward-pointing triangles for depths of 500–700 km. The landward side of coastlines are shown by dots. In this figure only, the dashed lines on the map represent zones of shallow earthquakes.

the large Australian and Pacific plates is complex and probably includes three or more additional small plates. An additional reference used for this region is *Denham* [1969].

Solomon arc. A zone of intermediate-depth earthquakes with depths mainly less than 150 km parallels the southeastern part of the Solomons. Deeper earthquakes appear to be confined to the westernmost part (west of about 155°E) and define a very steeply dipping zone that reaches depths of 500–600 km (Figure 8).

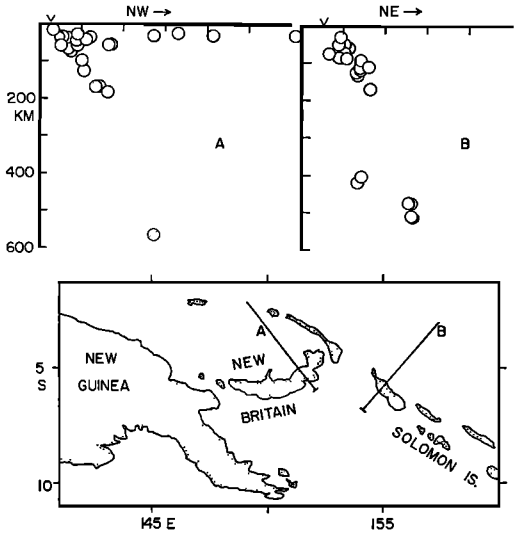

Fig. 8. Vertical sections through the New Britain arc (A) and the northwestern end of the Solomons arc (B). Sections include the most accurately located events based on data reported in the *Earthquake Data Reports* for 1961–1965. Events within 100 km of the sections A and B are plotted.

The deepest shocks are displaced northeast of the nearly vertical distribution of hypocenters above about 400 km. Denham's sections and Figure 8 suggest that a gap or a minimum in seismicity may be present between depths of about 200 and 350 km. Because earthquakes are few in number at all depths below 150 km, however, discrimination between the two possibilities is quite uncertain.

Earthquake 1 is located in the eastern part of the arc (Figure 7) where the inclined zone appears to dip steeply north. The T axis of 1 is nearly vertical and thus could indicate extension parallel to the dip of a nearly vertical zone. The B axis is approximately parallel to the trend of the arc. Although the depth given in the *Preliminary Determination of Epicenters* of the Coast and Geodetic Survey (ESSA) is 95 km, this depth is revised to 52 km in the Coast and Geodetic Survey's *Seismological Bulletin*. The shallower depth is in better accord with the character of the seismograms for this event. Moreover, the solution for 1 is consistent with solutions for other shallow earthquakes in the region (Molnar, unpublished data, 1969). Thus, the alternate and preferable interpretation is that 1 indicates underthrusting of the Coral Sea beneath the Solomons; i.e., slippage between two lithospheric plates.

Solutions 2–4 for earthquakes in the westernmost part of the zone exhibit a marked variation with depth. The solutions 3 and 4 for the events below 300-km depth have nearly vertical P axes, whereas the solution for the event at 118 km has a nearly vertical T axis. The zone above 400 km, including earthquakes 2 and 3, is nearly vertical and strikes approximately northwest; thus solutions 2 and 3 indicate, respectively, compression and extension parallel to the dip of the zone at depths of 118 and 392 km, respectively.

A plane parallel to the T and P axes and perpendicular to the B axis of 4 dips steeply but has a more northerly strike than that of the zone at intermediate depths. The distribution of hypocenters near 4, although not well defined, suggests

such a change in strike. The data may thus be consistent with an inference of down-dip compression near the bottom of the zone.

New Britain arc. Figure 8 and the sections given by Denham show an inclined seismic zone that dips north-northwesterly beneath the New Britain islands. These data plus recent locations not plotted in the figure show that this zone reaches depths greater than 500 km, although hypocenters deeper than about 200 km occur very infrequently. Toward the west the line of active volcanoes and the belt of shallow and intermediate-depth earthquakes bend around to a more westerly trend and intersect the northern coast of New Guinea. In this region the zone appears to steepen in dip.

Earthquakes 5–7 are located beneath eastern New Britain, where the seismic zone dips north-northeast at about 45°. The T axes of 5 and 6 are parallel to the dip of the zone, and the B axes are parallel to the strike of the zone. These results thus indicate down-dip extensional stress.

The T axis of 7, however, is nearly vertical, whereas one of the nodal planes is most nearly parallel to the seismic zone. This relationship is most simply accounted for as lithosphere beneath the Solomon Sea being thrust under New Britain. The depth of this earthquake (103 km) appears to be reliable. The solution for 7 may thus represent a downward continuation of the thrust faulting typical of shallow events in the region (Molnar, unpublished data, 1969).

The solutions for 8–10 for events located in the western part of the arc are similar to one another. A plane through the B and T axes strikes approximately parallel to the local alignment of earthquakes and volcanoes and dips very steeply north. This plane is also a reasonable representation of the distribution of hypocenters shown by Denham. These solutions, like those for 5 and 6, are thus consistent with down-dip extensional stress at intermediate depths.

New Guinea. The seismicity of New Guinea is very complex. A zone of subcrustal earthquakes with depths less than 200 km trends west-northwest beneath the northern and western parts of New Guinea and appears to dip south or southwest. This zone also appears to be nearly continuous with the steeply dipping zone of the New Britain arc. Near the intersection of these two zones, where the dip apparently reverses, the pattern is complicated by a third, very poorly defined zone that trends east-southeast. If the solution for 11 is indicative of down-dip extension, then this zone would have a westward dip. However, the solutions for three, closely grouped, intermediate-depth shocks (12–14) are quite different from one another, although one of these (12) is similar to 11. The data plotted in the appendix show that these differences are real. The variability in orientations exhibited by 11–14 and the unresolved complexities in the configuration of the seismic zone make further interpretation pointless.

New Hebrides (Figures 9 and 10)

Near the Santa Cruz Islands the seismic belt of the Solomons bends abruptly and continues as the linear south-southeasterly trending seismic zone of the New Hebrides island arc. The inclined seismic zone is very active at intermediate depths. Figure 10 shows that it has a slablike structure with a dip of about 65–70°. The zone is remarkably linear in strike and is parallel to the line of active volca-

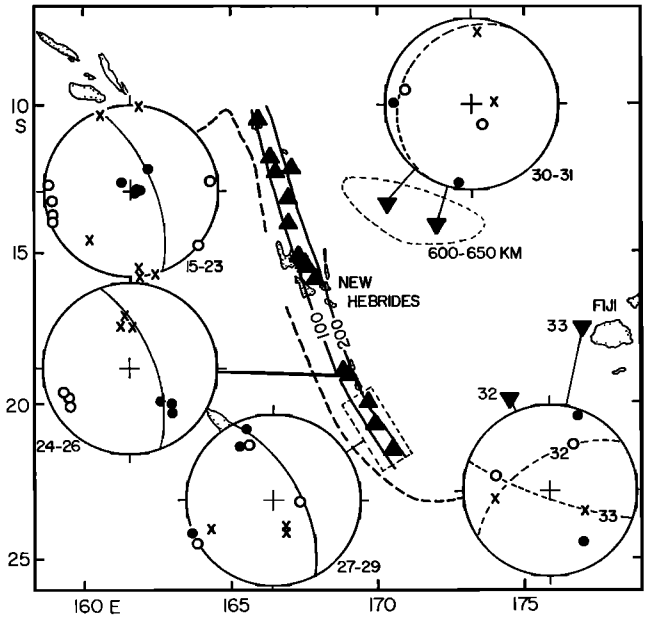

Fig. 9. The New Hebrides island arc. In this figure and in others, except where noted, the heavy dashed line on the map represents the axis of the oceanic trench associated with the arc. The light dashed line encloses the epicenters of deep earthquakes with depths between about 600 and 650 km.

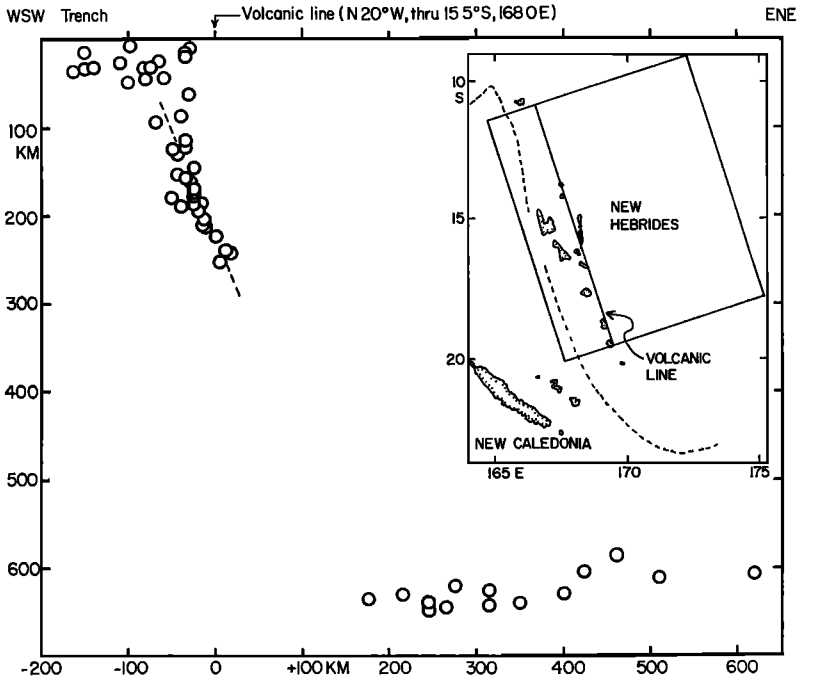

Fig. 10. Vertical section through the New Hebrides arc, including the most accurately located events that occurred between 1963 and 1967, selected from the same sources used in Figure 8 plus *Sykes* [1964]. The section includes events within the rectangular area shown on the map inset.

noes on the surface. Near its southern end the zone appears to bend slightly east and then terminates abruptly; many features of the seismicity and bathymetry [*Sykes et al.*, 1969] suggest that the arc is terminated by a transform fault trending east-northeast.

The evidence for a gap in activity between depths of about 300 to 500 km is good. At greater depths the distribution of hypocenters is quite remarkable (Figure 10). Figure 10 shows that hypocenters with depths predominantly between about 600 and 650 km occur in a nearly horizontal planar zone that in map view (Figure 9) is elliptical and has its longest dimension trending west-northwest. Only one deep earthquake (32) is known to have occurred south of this zone.

Intermediate-depth earthquakes. Solutions 15–23 for earthquakes in the northern half of the linear belt of intermediate-depth earthquakes all have very steeply dipping T axes that are more nearly parallel to the dip of the zone than are the poles of the nodal planes. These solutions are therefore in agreement with an inference of extensional stress parallel to the dip of the steeply dipping slab. Although four of these solutions have B and P axes approximately parallel, respectively, to the strike and normal directions of the inclined zone, the B and P axes of 17 and three others are distinctly nonparallel to those directions.

The solutions 24–29 for earthquakes in the southern part of the zone differ appreciably from those in the northern part. Solution 24 is nearly identical to 25 and 26, even though earthquake 24 is located closest to earthquakes of the northern group and separated by more than 300 km from earthquakes 25 and 26. Solutions 24–26 are similar to 15–25 in that the T and B axes are parallel to the inclined zone, but differ in that the T and B axes are distinctly not parallel to the dip and strike directions.

Earthquakes 28 and 29 are located nearest the southern end of the intermediate-depth zone, where the arc curves eastward. Although the B and P axes interchange positions from one solution to the other, both indicate extensional stress parallel to the strike of the zone, and may thus indicate the type of deformation shown in Figure 6.

Solution 27 is different from the others in that the T axis is perpendicular rather than parallel to the inclined zone. The solution indicates that the zone is under compression parallel to its strike. The depth of the shock, 249 km, is about 100 km greater than the depths of the others in the intermediate-depth groups except 17. Both 27 and 17 are near the lower part of the intermediate-depth zone, i.e., near the gap in seismic activity.

Although the solutions for 24–29 differ remarkably, the stress axes remain closely grouped and oriented parallel or perpendicular to the over-all planar geometry of the inclined zone. This result offers strong support to the idea that the earthquakes result from stresses in a thin plate. The causes of the spatial variations of the stress orientations, however, are not known.

Deep earthquakes. Solutions 30–31 for two earthquakes located in the nearly horizontal zone of deep earthquakes also exhibit a remarkable variation in orientation. Although all of the stress axes interchange positions from one solution to the other, the axes remain approximately parallel or perpendicular to the planar geometry of the zone. A plane through the more nearly horizontal axes

(the dashed line in the projection in Figure 9) actually dips about 10° west and is consistent with the distribution of hypocenters shown in Figure 10. These results support the concept of a stressed plate and suggest a nearly horizontal, possibly isolated, piece of lithosphere. The causes of the spatial variations in stress are not known.

The solution for the single deep event (32) in the southern part of the region is shown in Figure 9 together with the solution for 33, the westernmost deep event of the Tonga zone. Earthquake 33 appears to be located in a belt of deep earthquakes (34–38) that trends westward from the northern end of the Tonga deep zone, and its solution is similar to those (34–38) in that zone (see Figure 11). The orientation of solution 32 with respect to the southern end of the New Hebrides arc is similar to that of 33 (and 34–38) with respect to the northern end of the Tonga arc. These relationships may thus indicate a bend in the lower southern edge of a New Hebrides deep zone similar to that at the northern end of the Tonga zone.

In summary, the data for the northern part of the New Hebrides arc clearly indicate down-dip extension at intermediate depths. In the southern end of the zone and at great depths below a marked gap in seismic activity, the orientation of stress, although highly variable, is still parallel or perpendicular to the planar geometry of the zone, as would be expected for stresses in a thin plate.

Tonga-Kermadec-New Zealand Region

The nearly linear island-arc system that extends from Samoa through the North Island of New Zealand can be divided into three distinct segments on the basis of seismicity and other tectonic features: the Tonga arc, the Kermadec arc, and the North Island of New Zealand [*Sykes*, 1966; *Hamilton and Gale*, 1968].

Tonga arc (*Figure 11*). Figure 11 summarizes the results of *Isacks et al.* [1969] plus eight new solutions not reported in that paper. The contours in the figure summarize the locations of *Sykes* [1966] and *Sykes et al.* [1969] and show that the zone can be represented by an inclined plane that has contortions along its lower and lateral edges. Between depths of 450 and 650 km the northern part of the zone bends sharply toward the northwest. At depths less than 450 km the northwesterly bending is probably present but considerably attenuated. The distribution of seismicity is continuous at depths less than about 680 km. Partly as a result of the contortions along the lower edge of the zone, hypocentral depths decrease southward to less than 600 km and then abruptly increase to greater than 600 km near 26°S.

The main consistency among the solutions of both deep and intermediate-depth shocks is the parallelism between the P axes and the local dip of the seismic zone. This is shown clearly by solutions 40–48 and 51–55 for the earthquakes located away from the northern and southern lateral boundaries of the zone.

The solutions for earthquakes near the lateral boundaries are more complex. The orientations of solutions 33–39 can be explained, however, by a simple geometric effect. The structure of the zone near earthquakes 33–39, though complex in detail, can be represented approximately as a bend of the lower northern

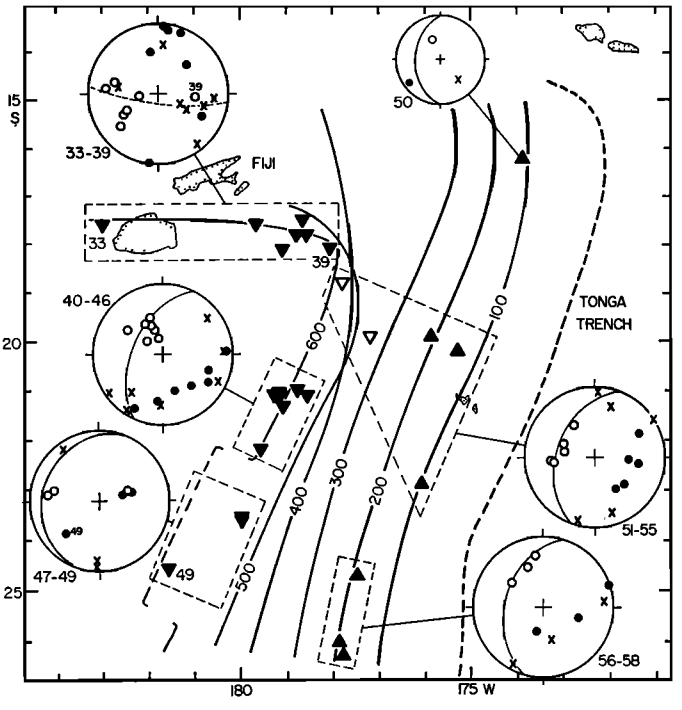

Fig. 11. Tonga island arc.

corner of the inclined zone (as in Figure 4). The plane shown by the dashed line in the equal-area projection of 33–39 (Figure 11) is approximately parallel to the groupings of P and B axes and perpendicular to the grouping of T axes. This plane is a reasonable representation of the part of the inclined zone bent around to the west. Thus, the main differences between the solutions for 33–39 and those for 40–48 in the unbent part can be accounted for by a rotation about the axis of bending and not by stresses caused by the bending.

Solution 37, in the dense cluster of hypocenters that includes 36 and 38, is different in respect to an interchange of the B and T axes. This relative instability of the orientation of the B and T axes is also characteristic of the shocks in the main part of the arc. However, 39, located nearest the bend and deeper than the others, differs from the solutions for nearby events in that the B and P axes have interchanged. This one solution may be related to the deformation near the end.

The solution for 33 is similar to others in the group 34–38, although the location of 33 is more than 400 km to the west of 34–38. Several deep earthquakes reliably located between 33 and 34–39 indicate that the zone is continuous to 33; this is shown by the 600-km contour in Figure 11. If this bend were straightened out, the deep zone would extend considerably north of the edge of the zone as defined by the distribution of hypocenters above 450 km. It is interesting that if the whole inclined zone were unbent and moved to the surface, the part of the zone corresponding to the 600-km contour would then extend considerably north of the presently active transform fault located along the 15°S latitude line. That part corresponding to the zone at depths less than

450 km would, however, nearly coincide with the transform fault. These relationships, as well as the discrepancy between the location of the presently active transform fault and the expected location for this feature farther north along the border of the Fiji plateau, can be explained by a change in the direction of relative motion between the Pacific and Australian plates from a west-northwesterly direction perpendicular to the Tonga trench to a westerly direction parallel to the seismic zone along 15°S. The slip vectors inferred from mechanism solutions of shallow earthquakes [*Isacks et al.*, 1969] do not clearly discriminate between these two directions. The appropriate length along the northern edge of the Tonga slab is about 750 km, which, if divided by *LePichon's* [1968] rate for the northern end of the arc, yields a time of approximately 8 m.y. ago for the change in direction. Instead of a change in direction, C. Chase suggested to the authors that the hinge-transform fault system that terminates the northern end of the Tonga arc migrated southward and thereby shortened the lateral dimension of the descending slab.

Earthquake 50 is located at intermediate depth near the northern edge of the zone, where the westward curvature is present but not pronounced. Although the stress axes of this solution do not appear to be closely parallel or perpendicular to the seismic zone, their orientations with respect to the northern end of the Tonga arc are similar to those of 28 (Figure 9) with respect to the southern end of the New Hebrides arc.

Solution 49 is anomalous in that the T axis, rather than the P axis, appears to be parallel to the seismic zone (but not to its dip). This solution may indicate a localized reorientation of stress near the lower edge of the zone.

Solutions 56–58 for intermediate-depth events located nearest the junction between the Kermadec and Tonga arcs resemble others in the region and indicate no profound effect of the junction, although the northerly deflection of the P axes of 56 and 58 from the dip of the zone may indicate a minor effect.

In summary, the contortions of the seismic zone do not seem to have large effects on the focal-mechanism solutions; instead, the stress axes tend to follow the local structure as if embedded in the zone and suggest a compressional stress transmitted through nearly all parts of the slab. This is contrary to what would be expected if the mechanisms were related primarily to a localized stress near a contortion of the slab.

Kermadec arc (Figure 12). The inclined zone in this region dips more steeply than that of the Tonga arc and does not appear to extend to depths greater than 500–550 km [*Sykes*, 1966]. A plane striking N 20°E and dipping 60° west is a good representation of this zone.

Solutions 60–61 for earthquakes at depths near 230 km both have T axes parallel to the dip of the seismic zone, whereas 59, for an earthquake located north and 120 km deeper than 60–61, shows down-dip compression. Although the data are limited, these results suggest a change from down-dip extension to down-dip compression somewhere between 230 and 350 km.

An unusual feature is that the other stress axes, although closely grouped, are not parallel to the strike and normal directions of the seismic zone.

North Island, New Zealand (Figure 12). Hamilton and Gale [1968, 1969]

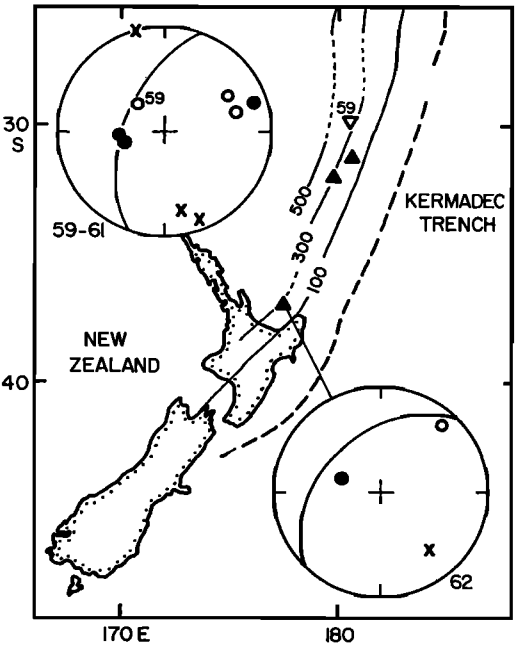

Fig. 12. Kermadec island arc and New Zealand.

showed that the seismic activity at intermediate depths beneath the North Island of New Zealand has a slablike structure. Below depths of about 350 km only three earthquakes are known [*Adams*, 1963]. These three, near a depth of 600 km, are located almost vertically beneath the southern part of the intermediate-depth zone.

Near 62 the zone can be approximately represented by a plane striking about N 45°E and dipping northwest. Both the T and the P axes of 62 appear to parallel the zone; the T axis is approximately parallel to the dip, and the P axis is parallel to the strike.

Adams [1963] reported a solution different from 62 for an event located in the southern part of the intermediate-depth zone. Adams found that first motions recorded at New Zealand stations from the three deep shocks are generally the opposite in polarity of those from the intermediate-depth shocks. This result may indicate a variation in mechanisms with depth similar to that in the Kermadec region. The predominantly dilatational readings reported by Adams for the deep shocks are consistent with a P axis oriented more nearly vertical than horizontal, i.e., a P axis parallel to a steeply dipping deep zone.

South America

The distribution of earthquakes and other island-arc-like tectonic features indicates that the coast region of western South America north of the Chile rise is a major zone of convergence between an oceanic and a continental lithospheric plate. Mechanisms of shallow earthquakes [*Isacks*, 1970] indicate that between Ecuador and the Chile rise the oceanic Nazca plate underthrusts the continent of South America in an east-northeasterly direction. North of Ecuador an

island-arc-like structure continues through Colombia, but the plate tectonics of this region are complex and have yet to be fully worked out [*Molnar and Sykes*, 1969]. In the following, South America is considered in two parts, one north and one south of Ecuador. South of the Chile rise the seismicity decreases markedly and provides little evidence of the nature of the connection between the South Sandwich arc and the main seismically active structures of Chile.

Region of the Peru-Chile trench (Figures 13 and 14). Additional sources of information on the distribution of earthquakes in this region are *Ocala* [1966] and *Santo* [1969*a*]. At intermediate depths the seismic zone is slablike and dips gently beneath the continent. The section in Figure 13 shows this for the inclined zone beneath Peru; the slablike zone of intermediate-depth hypocenters, separated from a zone of shallow, probably crustal earthquakes that lies above it, has a dip of only 10° to 15° and reaches depths of about 200 km. *Santo* [1969*a*] shows that the zone beneath northern Chile dips more steeply at about 25–30° and reaches depths of about 300 to 350 km. Between latitudes of about 16°S and 25°S the zone of earthquakes with depths between about 70–150 km is extremely active; this is illustrated by the large number of earthquakes in this region for which focal-mechanism solutions were obtained. Near the border between Chile and Peru the seismic zone, topographic features, and the line of active volcanoes all appear to curve around toward the northwest. Just north of this bend, near 16°S in southern Peru, the seismic activity at intermediate depths decreases markedly and the zone of historically active volcanoes terminates.

Beneath depths of about 200 km in Peru and about 300 km in Chile the seismic activity decreases remarkably. Santo's plot of the frequency of earth-

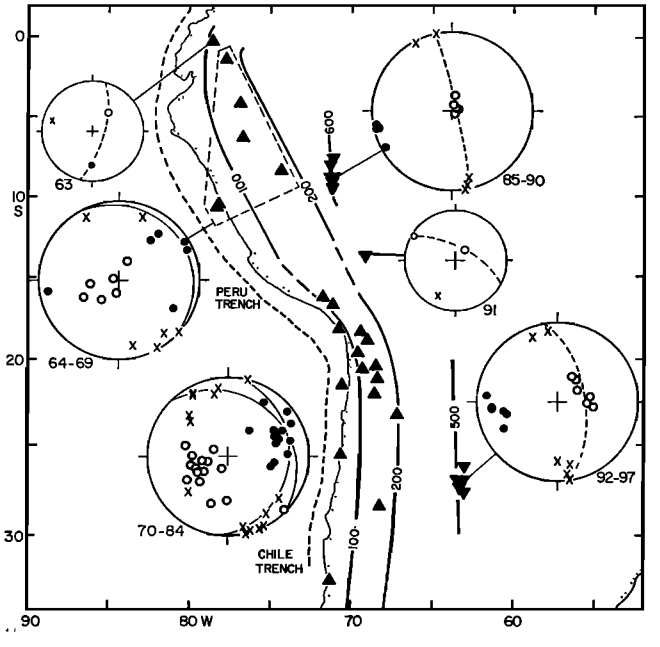

Fig. 13. The Peru-Chile trench and the adjacent region of western South America. Coastline shown extends from Ecuador to central Chile. The northern deep zone (600-km contour) is beneath western Brazil, and the southern deep zone (500-km contour) is beneath western Argentina.

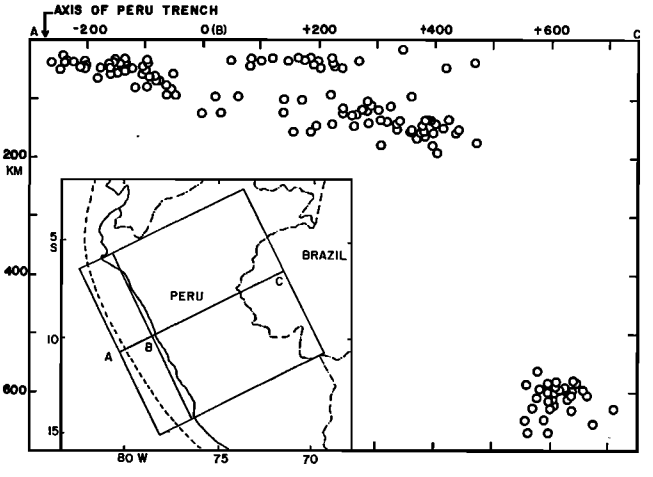

Fig. 14. Vertical section through Peru including events within the area shown in the inset. The events are those with magnitudes greater than about 5 reported in the *Preliminary Determination of Epicenters* [1961–1967].

quakes as a function of depth shows a pronounced gap between about 350 and 500 km. This gap is especially prominent because the seismic-energy release at great depths in this region is so high; Santo estimates that during the past 50 years it is larger in South America than that at great depths in any other single region. Santo tabulates only six small earthquakes located by the Coast and Geodetic Survey (ESSA) with depths between 300 and 500 km. These locations, however, are determined by few and poorly distributed data and could probably be moved either above or below the gap in seismicity. These six are all in the Chile-Argentina region; none have been reported for the gap in the Peru-western Brazil zone.

At depths of 500–650 km, beneath the gap in seismic activity, the hypocenters are confined to two remarkably linear belts, one beneath western Argentina and one beneath western Brazil. These belts are parallel and trend slightly west of north, but the one beneath western Brazil is offset about 500 km west of that beneath western Argentina. Between these zones two large earthquakes occurred in 1958 and 1963 (no. 91) at nearly the same location beneath the Peru-Bolivia border. These events are closest to the deep earthquakes beneath western Brazil and may thus be on a southeastward extension of that zone.

Recent studies of focal-mechanism solutions reported by *Stauder* [1969] and *Ritsema* [1970] appear to be in good agreement with our analysis, although Ritsema places a different interpretation on the results.

The zone of intense intermediate-depth activity beneath northern Chile and southern Peru, including earthquakes 70–84, is represented on the equal-area plot in Figure 13 by two planes. One has the N 7°E strike of the linear coast of Chile, and the second has the northwest strike of southeast Peru; both have a dip of 28°. The orientation of the zone in the bend between Chile and Peru probably varies between these two extremes. Although the stress axes scatter somewhat, partially as a result of the inclusion of solutions of varying quality (see appendix), the T and P axes of 70–84 show a distinct grouping. The plunges of the T axes vary between 7° and 54° but have an average of 31°, which is

very close to Santo's estimate of 28° for the dip of the zone. The trends of the T and B axes, although somewhat scattered, do not vary systematically with respect to the location of the event and thus do not follow the major bend of the coastline and other tectonic features in the region of the Peru-Chile border. Instead, the axes trend approximately parallel or perpendicular to a direction between the strikes of the coastlines of southern Peru and northern Chile. The east-northeasterly trend of the T axes is approximately parallel to the direction of underthrusting inferred from the solutions of shallow earthquakes [*Isacks*, 1970] and approximately perpendicular to the alignment of active volcanoes in northern Chile. These results are in good agreement with down-dip extension in the zone but do not reveal any marked effect of the bend in the coastline between Chile and Peru.

Although less closely grouped than 70–84, the T axes of 64–69 also tend to parallel the dip of the intermediate-depth zone beneath Peru. From the epicentral locations alone it is not clear whether earthquakes 63 and 64 (beneath Ecuador) are at the northern end of the Peruvian zone, at the southern end of the northeastward-trending zone in Colombia, or in a bend between two zones. The similarity between 64 and those for other events in Peru suggests that this earthquake may be in the northern part of a coherent slab beneath Peru. The solution for 63 is quite different in orientation. This event could be related to deformation near a junction between the inclined zones of Peru and Colombia.

The solution for 67 is also different from others beneath Peru, although the earthquake is located in the central part of Peru. Nevertheless, the B and T axes, although not parallel to the dip and strike directions, remain approximately parallel to the inclined seismic zone.

Included in this analysis are mechanisms of several earthquakes (68, 69, 72, 79, 82, 84) whose depths vary ±20 km around the 70-km borderline between intermediate and shallow depths. In some cases the depths are controlled fairly well by pP readings, but in other cases they are uncertain. In all cases, however, some evidence of a depth greater than normal was found. The additional basis for inclusion in the analysis is the similarity between the solutions for these earthquakes and those for the well-located events at greater depths. Because of the gentle dip of the seismic zones, these solutions have a distinctly different orientation from that characteristic of the underthrust type of shallow earthquakes in the region.

Solutions 85–90 for the deep earthquakes located beneath western Brazil are nearly identical to one another. The P axes are all nearly vertical, whereas the B and P axes are approximately parallel and perpendicular to the linear trend of the deep seismic zone. A plane through the B and P axes is more nearly parallel to the N 10°W trend of the belt of deep earthquakes than to the northwest trend of the Peru trench and coastline. This relationship suggests that the plane through the B and P axes represents the local structure of the deep zone and is thus consistent with an inference of down-dip compression within a nearly vertical zone. The location of the deep events nearly vertically beneath the lower part of the intermediate-depth zone further supports this interpretation.

Solutions 92–97 for deep earthquakes beneath western Argentina have B and

T axes that are also more nearly parallel to the belt of deep hypocenters than to the Chile trench and coastline, but the difference in this case is small. A plane through the B and P axes dips about 70° east and is approximately parallel to a plane joining the deep and intermediate-depth earthquakes through the gap in seismicity. These results are in agreement with an inference of down-dip compression within a steeply dipping deep slab.

Solution 91 for the large multiple event beneath the Peru-Bolivia border [*Chandra*, 1970*b*] appears to indicate down-dip compression in a steeply dipping zone. The B and T axes, however, have significantly different trends than those in the deep zones beneath either western Brazil or western Argentina. The simplest interpretation is that the seismic zone near 91 strikes northwest, and the T rather than the B axis is parallel to the zone. A straightforward connection between 91 and the zone beneath western Brazil would require this strike. The parallelism of the T axis and the inferred strike of the zone may be related to a stretching or some other contortion in this region.

In summary, the most outstanding result for the Peru-Chile region is the change from down-dip extension at intermediate depths to down-dip compression at great depths.

Colombia: the Bucaramanga nest (Figure 15). The island-arc-like features of the Peru-Chile region bend around in Ecuador and trend east-northeast in western Colombia. Earthquakes 98–100 are located in the zone of intense activity at depths near 150 km beneath Bucaramanga. This zone may be at the northern end of a continuous inclined zone that trends parallel to the island-arc-like features of Ecuador and Colombia. *Molnar and Sykes* [1969], for example, show

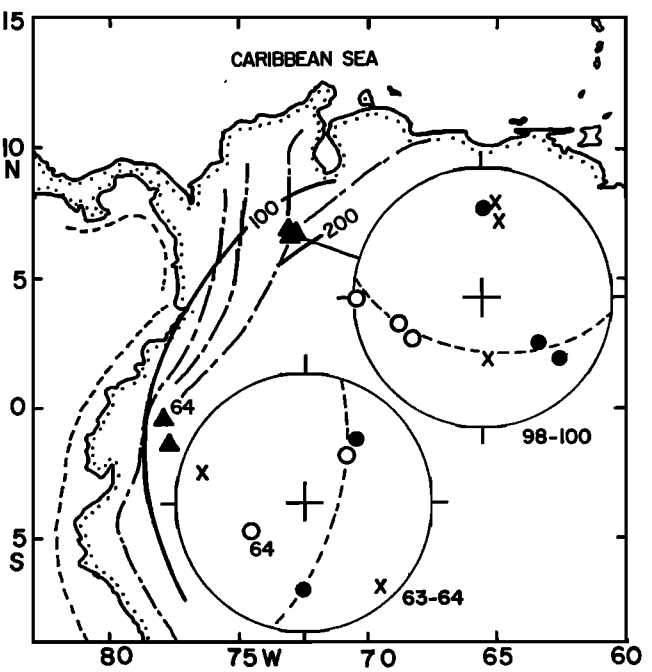

Fig. 15. Region of northwestern South America showing the zone of intermediate-depth earthquakes in Ecuador and Colombia. Earthquakes 98–100 are located in the Bucaramanga nest. The lines of alternating long and short dashes represent major mountain ranges and structural trends.

a zone dipping eastward beneath the coast of Colombia near 5°S. Although large numbers of earthquakes are very concentrated spatially near earthquakes 98–100 [*Tryggvason and Lawson,* 1970], shallower but subcrustal earthquakes are reliably located northwest to north-northeast of the Bucaramanga region, and deeper earthquakes (depths near 200 km) are located slightly southeast of the region [*Sykes and Ewing,* 1965]. A vertical section aligned northwest-southeast through the Bucaramanga 'nest' [*Santo,* 1969*a*] also shows a zone dipping southeast. These locations suggest that near Bucaramanga the zone may bend around to a more easterly strike than in Ecuador and southern Colombia.

Solutions 98 and 100 are nearly the same; the *T* axes could be parallel to a zone dipping southeast. The third solution (99), however, is not in agreement with that interpretation. Alternatively, a plane perpendicular to the close grouping of northward-plunging axes (represented by the dashed line in Figure 15) is parallel to all the other axes. The orientation of this plane is consistent with the other evidence cited above for a zone near Bucaramanga that dips more toward the south than toward the east. If this is the case, then the data indicate compressional stress oriented more nearly parallel to the strike than to the dip of the zone. Moreover, the approximate interchange of the positions of the *B* and *T* axes of 99 with respect to 98 and 100 suggests that compressional stress is dominant. One interpretation of these relationships is that the lateral compression results from a bending of the northern end of the slab.

Atlantic Island Arcs

South Sandwich arc (Figure 16). The seismicity of this region is poorly known, partly because of the lack of nearby seismograph stations. As in other arcs, most of the shallow earthquakes appear to occur beneath the landward wall of the trench; and in general, the intermediate-depth events are located west of the main zone of shallow activity. Earthquakes appear to be restricted to

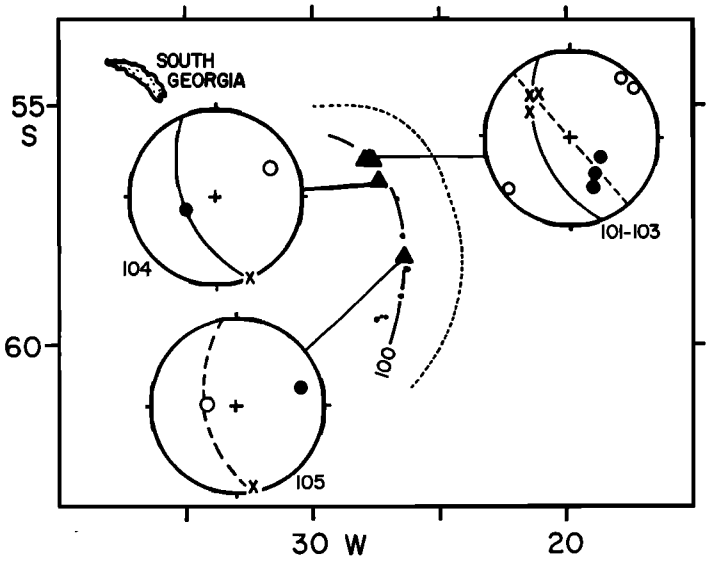

Fig. 16. South Sandwich island arc.

depths less than about 200 km. At the northern part of the arc, where the features bend toward the west, an intense concentration of hypocenters is located at a depth of about 100 km (near earthquakes 101–103). A vertical section through this part of the arc, oriented about N 60°E, shows an inclined zone dipping very steeply southwest [*Engdahl et al.*, 1969, and E. R. Engdahl, personal communication, 1970]. The data are not adequate to define the dip of the zone farther south along the arc.

Solution 104 indicates down-dip extension. Solutions 101–103 for the earthquakes located closest to the westward bend also indicate extensional stress parallel to the zone, but the axes are not parallel to the dip. This could be an effect of the westward bend, i.e., an effect of a contortion at the northern end of the zone.

In contrast, solution 105 for an earthquake located in the middle of the arc exhibits simple down-dip compression and is nearly the opposite of 104. Solution 105, plus two others (148–149) for earthquakes in the Ryukyu arc, are the only cases in which down-dip compression with the B axis parallel to the strike of the zone occurs in a seismic zone that does not reach depths greater than 300 km.

West Indian arc (Figure 17). The distribution of hypocenters [*Sykes and Ewing*, 1965] and the focal mechanisms of shallow earthquakes [*Molnar and Sykes*, 1969] demonstrate an eastward rigid-body motion of the Caribbean with respect to North America, South America, and the western Atlantic. In the Lesser Antilles the Atlantic sea floor underthrusts the Caribbean toward the west. Near the Puerto Rico trench, the Atlantic sea floor is also underthrusting the Caribbean, but the motion is nearly parallel to the strike of the trench. The seismicity of the Lesser Antilles portion of the arc clearly shows a westward-dipping zone of activity, but at the northern end of the arc the activity changes orientation abruptly and trends east-west, parallel to the Puerto Rico trench. This east-west belt has a more complex structure. No earthquakes in either portion of the arc have been located deeper than 250 km.

An intense source of intermediate-depth earthquakes is located beneath the eastern tip of Hispaniola. Although the distribution of hypocenters is not simple, Sykes and Ewing's section suggests a nearly vertical distribution of hypocenters near that source. Molnar and Sykes report solutions for three intermediate-depth

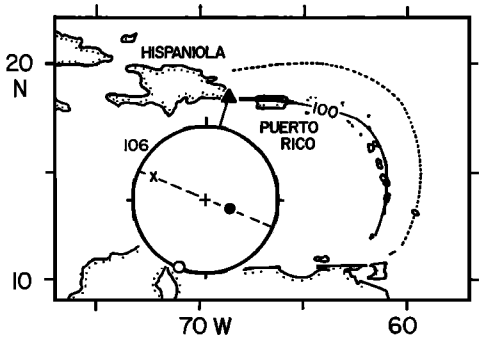

Fig. 17. West Indies island arc.

earthquakes in this region, but only one (106) is well determined. A plane through the B and T axes of 106 has a strike that is slightly north of the westerly trend of the Puerto Rico trench but is approximately parallel to the belt of seismic activity along the northern coast of Hispaniola. The vertical dip of this plane is consistent with the distribution of hypocenters. A nearly vertical slab under extension approximately parallel to its dip may thus be located beneath the eastern end of Hispaniola. It is interesting that both the locations and the solutions of 106 and 101–103 (Figure 16) have approximately similar relationships to the West Indian and the South Sandwich arcs, respectively.

Molnar and Sykes' two other solutions, though not well determined, are different from one another and from that of 106. This variability plus the complexity in the distribution of hypocenters in the region may also indicate a contortion or disruption of the slab.

Sykes and Ewing reported events with reliably determined depths between 70 and 120 km located at the southern end of the Antilles arc near Trinidad. Molnar and Sykes found evidence that some of the events in this region may be related to hinge faulting, whereby the portion of the western Atlantic-South American plate that underthrusts and descends beneath the Antilles arc tears away from the portion remaining on the surface. It is not clear, however, whether the intermediate-depth events are involved in this type of faulting. The hinge faulting at the northern end of the Tonga arc occurs at shallow depths [*Isacks et al.*, 1969].

Middle America Arc (Figure 18)

Molnar and Sykes [1969] show that the oceanic lithosphere is underthrusting Mexico and Central America in a northeast direction. Between about 86°W and 96°W the structure of the arc is particularly simple. The surface features are nearly straight, and the slablike zone of subcrustal earthquakes is relatively planar and free of major contortions. This region provides a particularly good

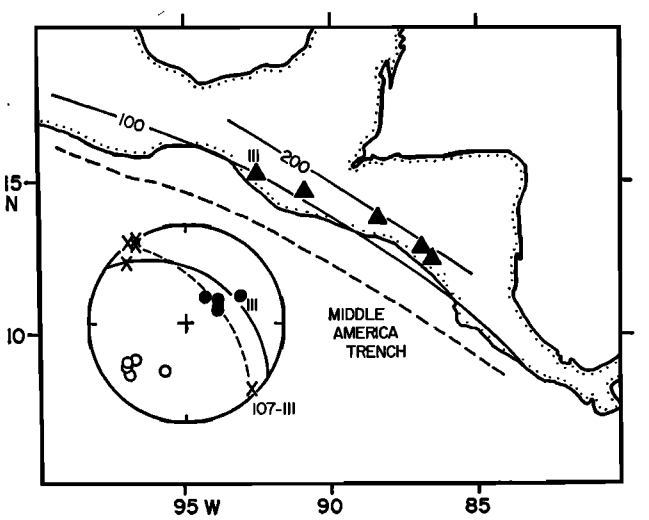

Fig. 18. Middle America trench and adjacent region of Central America.

test of the idea that, as a result of gravitational body forces on excess mass in the sinking lithosphere, extensional stress predominates in the slabs that are relatively uncontorted and that do not reach great depths (Figure 3*a*).

The plane that fits the close groupings of T and B axes of 107–110 strikes N 40°W and dips about 60°NE. The 20–25° difference between the trends of the B axes and the strike of the trench and seismic zone appears to be significant. The T axis of 111 has a plunge of about 40°. The difference between the plunges of 111 and 107–110 is determined by numerous readings in the central parts of the focal spheres and is probably real. Earthquake 111, at 85-km depth, is shallower than the other four. These results are consistent with down-dip extension in a zone that increases in dip from about 40° to 60° at depths greater than 85 km. Although such a change cannot be resolved by the data of Molnar and Sykes, their results do not exclude it. The data are thus in agreement with the model shown in Figure 3*a*, where the slab is sinking but has not descended beneath the asthenosphere.

Cascades

In the northwestern United States an island-arc-like structure trends parallel to the coasts of Oregon and Washington and is defined approximately by the volcanoes of the Cascade range. Subcrustal earthquakes may occur in this region [*Tobin and Sykes,* 1968], but the data are inadequate to define an inclined seismic zone. Several studies of the motions of the lithospheric plates in this region indicate that lithosphere has been consumed in the past and that the downgoing slab will dip east [*Morgan,* 1968; *McKenzie and Morgan,* 1969; *Silver,* 1969]. Although the depth of earthquake 112 (59 km) [*Algermissen and Harding,* 1965] is shallower than other events in this study, it is significantly deeper than others in the western United States. Moreover, its solution has an eastward-dipping T axis and therefore could indicate extensional stress parallel to an eastward-dipping zone.

Aleutian Arc (Figure 19)

The underthrusting of the Pacific plate northwestward beneath the Aleutians and Alaska is described by *McKenzie and Parker* [1967] and *Stauder* [1968*a*, *b*]. Focal depths are generally less than 200 km. At the western end of the zone of active volcanism and subcrustal seismicity (near 178°E) the dip of the zone, although not too well determined, appears to be about 60° [*Davies and McKenzie,* 1969; *Murdock,* 1969]. A plane through the P and T axes of 113 is approximately parallel to the seismic zone, and the solution indicates compression parallel to the dip or extension parallel to the strike of the zone. Since this earthquake is located where the curvature of the arc increases, *Stauder* [1968*b*] suggested that the extensional stress parallel to the strike results from the type of deformation of the descending slab shown in Figure 6. Solutions of this type are found in other regions where convex curvature is pronounced.

Solution 204 is similar to those for shallow events in the region and is interpreted by Stauder [1968*b*] as underthrusting on a nearly horizontal fault plane. Although the depth of 60 km for 204 is not quite intermediate, its loca-

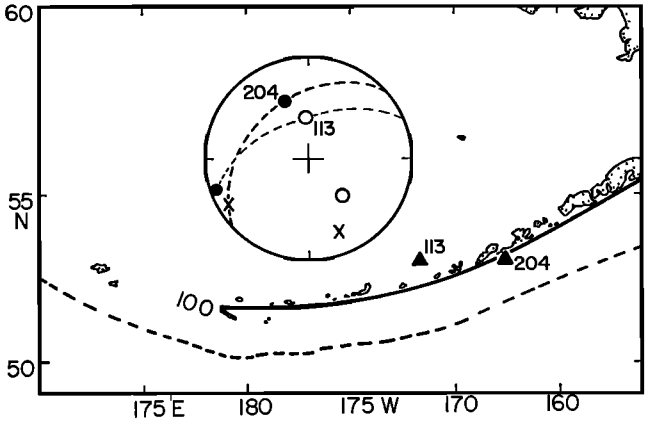

Fig. 19. Aleutian island arc.

tion is well determined; and the event is probably located in the part of the seismic zone that has a dip considerably greater than that required for the underthrusting interpretation. The solution is therefore more consistent with an inference of down-dip extension inside a northward-dipping slab. The dip of the zone inferred from the plunge of the T axis is about 40°. Down-dip extension is also a reasonable interpretation of the solution of the January 1, 1963, earthquake [Stauder, 1968*b*] located east of 204. The intermediate depth of 75 km for this event is determined by numerous pP readings and is preferable to the depth of 51 km listed by the *International Seismological Summary*. Thus, down-dip extension may be prevalent in the part of the descending lithosphere east of earthquake 113 that has a more nearly linear strike.

Northwest Pacific: Kamchatka-Japan-Marianas

A nearly continuous zone of deep and intermediate-depth earthquakes can be traced from Kamchatka through Japan and thence to the Marianas. This vast descending edge of the northwest Pacific lithosphere can be divided into four segments, each characterized by distinct trends of the oceanic trench, of the line of active volcanoes, and of the inclined zones of earthquakes. The Kurile-Kamchatka, North Honshu, and Izu-Bonin segments, trending northeastward, north-northeastward, and north-northwestward, respectively, form two oblique-angled corners near Hokkaido and east central Honshu. The fourth segment, the Marianas arc, continues the trend of the Izu-Bonin arc but is offset to the east and is separated from the Izu-Bonin segment by a gap in seismicity and by a shoaling of the oceanic trench. The dips of the inclined seismic zones differ notably among the four segments. The structure of the zone between the segments, whether continuous (and bent) or disrupted, cannot be clearly determined by the available data on locations alone. Additional sources used in determining the contours shown in Figures 20, 21, and 22 include *Fedotov* [1965, 1968] and *Sykes* [1966] for the Kurile-Kamchatka region; *Katsumata* [1966, 1967*a*, *b*] and *Ichikawa* [1961] for North Honshu and the Sea of Japan; and *Katsumata and Sykes* [1969] for the Izu-Bonin and Marianas regions.

As a result of the pioneering research of H. Honda and his colleagues, reliable solutions of many earthquakes that occurred during the last 40 years are available for the Japanese region. Although only solutions based on the most numerous and consistent data are listed in Table 1, other data, summarized by *Balakina* [1962] for the Kurile-Kamchatka region and by *Honda et al.* [1956, 1967], *Ichikawa* [1966], and *Aki* [1966] for the Japanese region, are in substantial agreement with the results selected for Table 1.

The Kurile-Kamchatka arc (Figure 20). Between Kamchatka and the Hokkaido-Sakhalin region the inclined seismic zone appears to be relatively simple in structure and can be represented by a plane with a dip of 45° and a strike varying from about N 35°E near Kamchatka to N 60°E near Hokkaido. Nearly all the large, well-located deep events northeast of the Hokkaido-Sakhalin region have depths between 400 and 500 km. Examination of reported locations suggests that the maximum depth of this zone is probably less than 600 km and may be near 500 km. A minimum in activity as a function of depth occurs between about 200 and 400 km, but apparently reliable locations of events with depths in this range (e.g., *Savarensky and Golubeva* [1969]) indicate that this minimum is not an aseismic gap in activity.

In nearly all the solutions for this region either the P or the T axes tend to

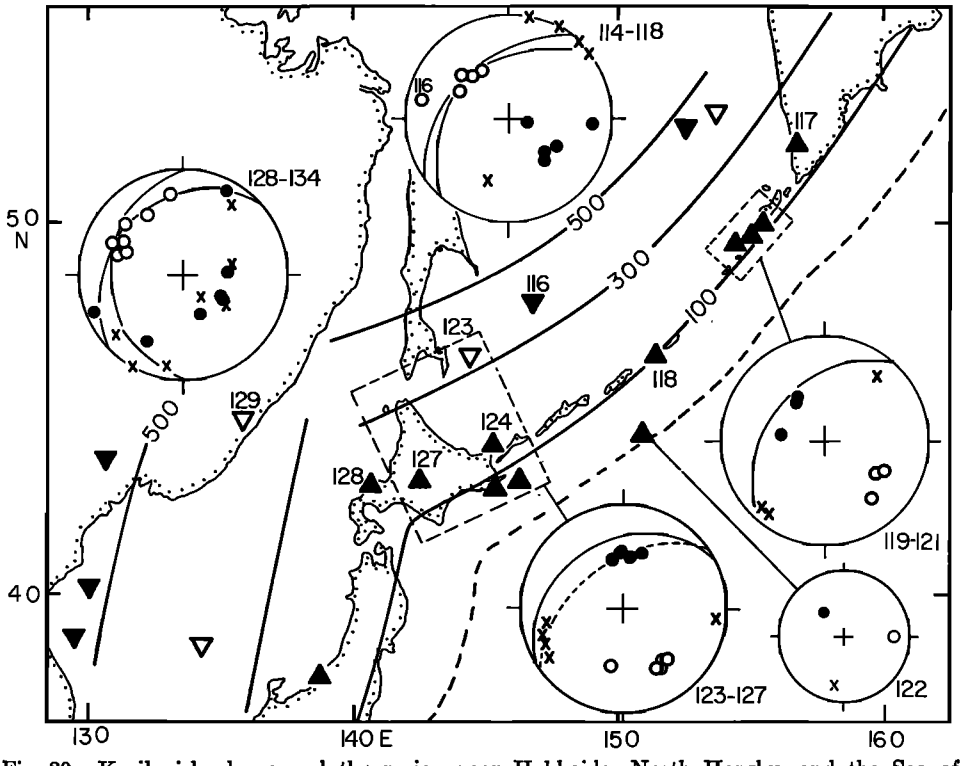

Fig. 20. Kurile island arc and the region near Hokkaido, North Honshu, and the Sea of Japan. The discontinuity in the contours of hypocentral depths represents a possible disruption between the Kurile and North Honshu seismic zones.

be parallel to the dip of the zone, while the B axes are approximately parallel to its strike. However, the pattern of down-dip stress in the region is complex and not just a function of depth. Solutions 123–127 for events near the junction between the Kurile and North Honshu zones all indicate down-dip extension, as do 119–121 for three intermediate-depth events located south of Kamchatka. In contrast, solutions 117–118 for intermediate-depth events located north and south of 119–121 and two solutions (114–115) for deep events all show down-dip compression.

Solution 116 for a deep earthquake has a different orientation from the others in the region and does not appear to be closely parallel to the over-all planar geometry of the zone. However, the parameter of the solution that is most nearly parallel to the dip of the zone is still the P axis.

The peculiar location of 122 at 80 km beneath the axis of the Kurile trench does not appear to be an error in the location. Shallow events characterized by solutions of the normal faulting type are found near the axis of trenches in other arcs, notably the Aleutians [*Stauder,* 1968*b*], and can be interpreted as extension near the upper part of the oceanic plate as it bends beneath the island arc. By the same reasoning, compression would be expected near the lower part of the plate. Although the trend of the P axis of 204 is not perpendicular to the axis of the trench, the P axis is more nearly horizontal than the T axis and could indicate compression of the lower part of the plate as it bends downward near the trench.

The Hokkaido corner (Figure 20). Solutions 123–129 for the events located in the region between the gently dipping North Honshu zone and the more steeply dipping Kurile zone are of two types. Solutions 123–127 for events located on the Kurile side of the corner all indicate down-dip extension and are thus similar to 119–121 for events in the northern Kuriles. Solutions 128 and 129 for events located on the North Honshu side of the corner are similar to 130–134 and are thus apparently related to the down-dip compression in the North Honshu zone. The solutions, therefore, appear to be related more to patterns on either side of the corner than to any special effect of the corner itself.

Honda et al. [1956] and *Ichikawa* [1966] report other solutions (not included in Table 1) for earthquakes near the corner, some of which can be interpreted to support the lateral stretching or tearing of a slab as shown in Figure 5. For example, three of their solutions for earthquakes near 123 have T axes that plunge between the dip direction and the strike direction of the zone; these solutions could be taken to indicate the oblique stretching of a slab as shown in Figure 5*a*. Also, one of the solutions has a vertical nodal plane striking north-northwest that, if taken as the fault plane, indicates that the Kurile slab moves down with respect to the North Honshu slab. This is in agreement with the hinge faulting shown in Figure 5*b*, and, if correct, it could indicate a disruption of the zone. However, examination of the solutions of Honda et al. and Ichikawa in these cases suggests to us that the differences between their solutions and those for 123–127 may not be real. In fact, it seems possible to fit most of the data given by Honda et al. and Ichikawa, with minor modifications, to the solutions for 123–127.

The distribution of earthquakes plus the remarkable difference between solutions 127 and 128 suggest that the main junction between the North Honshu and the Kurile zones is located beneath western Hokkaido (between 127 and 128) and beneath the northern Sea of Japan east of 129. Whether the zone is continuous or disrupted in this region is not clear from the distribution of hypocenters. The reorientation of stress between 127 and 128, however, may be easier to understand if the events result from stresses in separate slabs.

Although 125 and 126 are near the zone of shallow underthrusting, their depths near 80 km are reliably determined, and their solutions are quite similar to those for the deeper events. Solutions 125 and 126 thus appear to indicate stress within the descending plate rather than slip between plates. Moreover, the directions of slip inferred from the solutions, were the earthquakes shallower, indicate motion of the Pacific plate relative to the Asian plate that is significantly more northerly than the northwesterly direction indicated by *McKenzie and Parker* [1967]; *Isacks et al.* [1968]; *Le Pichon* [1968]; and *Stauder* [1968*b*]. Inclusion of such events probably accounts for the discrepant directions near Hokkaido shown in the worldwide plot of slip directions (Figure 3 of *Isacks et al.* [1968]).

North Honshu (Figures 20 and 21). The deep and intermediate-depth earthquakes that occur beneath the Sea of Japan are part of an inclined zone related to the active volcanoes and offshore trench that parallel the northeast coast of Honshu. *Ichikawa* [1961] and *Katsumata* [1967*a*] show that the zone has a dip of about 30°. Although seismic activity between depths of 200 and 500

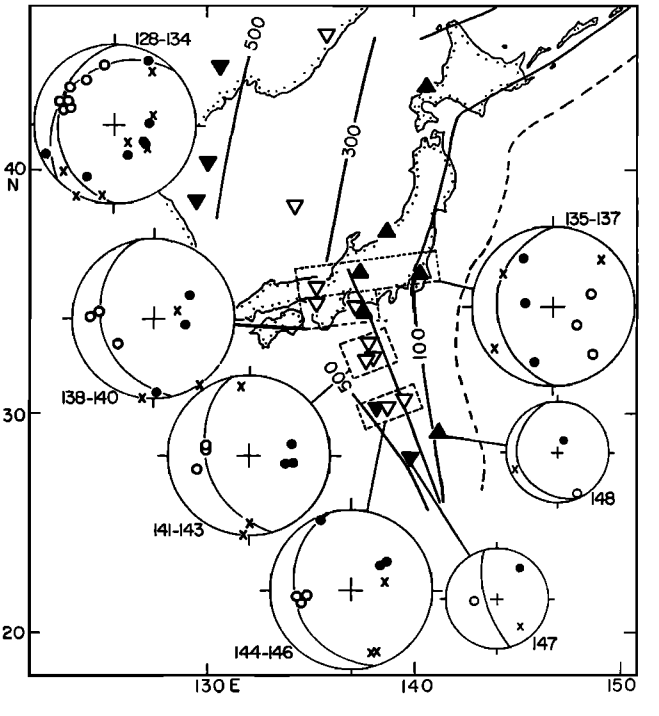

Fig. 21. Izu-Bonin island arc and the region of Honshu and the Sea of Japan. The area near earthquakes 135–137 is shown in more detail in Figure 22.

km is sparse, the zone appears to be continuous. It does not appear to reach depths much greater than about 600 km.

Nearly all of the P axes of 128–134 are approximately parallel to the dip of the North Honshu zone. Three solutions show an interchange of B and T axes with respect to the others. The consistency among the solutions is further evidence for the coherency of a single inclined zone dipping beneath the Sea of Japan. Other solutions reported by Honda et al. and Ichikawa agree with the results shown in Figures 20–21. In addition, their results suggest that down-dip compression may also be present at depths of 100–200 km beneath the northern coast of Honshu, but the data are limited. Thus the North Honshu slab may be under compression at all depths below 100 km.

The junction between the Izu-Bonin and the North Honshu segments (Figures 21 and 22). Both the distribution of hypocenters and the focal-mechanism solutions suggest that the junction between the Izu-Bonin and the North Honshu zones is located near 135–137 (Figures 21–22). The distribution of earthquakes shallower than 200 km, the oceanic trench, and the volcanic front [*Sugimura*, 1965] form a well-defined corner in the region of Tokyo and central Honshu. Subcrustal activity is especially intense at depths of 50–100 km near 135 and at depths of 200–300 km near 136. Earthquake 137, located at a depth of 360 km, appears to be at the northern end of the Izu-Bonin zone; to the north the activity decreases and appears to be part of the gently dipping North Honshu zone. As shown in Figure 21 and described in the next section, solutions for deep earthquakes in the Izu-Bonin zone located south of 136 and 137 are characterized by down-dip compression and are similar in this respect to those in the North Honshu arc. Solutions 135–137 for the events located between the two zones, however, have a distinctly different orientation and therefore probably reflect localized effects near the junction.

The solutions for 135–137 are in each case representative of solutions for other shocks in the vicinity of each hypocenter. Honda et al. and Ichikawa report two other solutions that agree with 137 and five solutions that agree (or for which

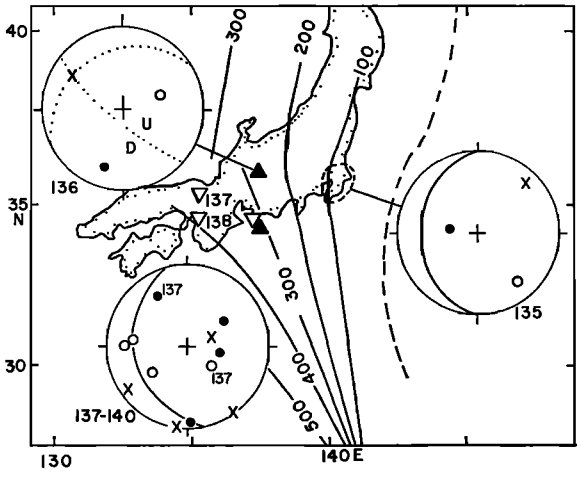

Fig. 22. The corner between the Izu-Bonin and the North Honshu zones. The dotted lines in the projection of solution 136 represent the nodal planes of the solution. U (up) and D (down) show the sense of motion on the more nearly vertical nodal plane taken as the fault plane. The solution is consistent with hinge faulting.

the data are not inconsistent) with 136. Solution 135 is an average of a group of solutions reported by *Ichikawa* [1966]. The individual solutions combined in 135 are quite similar to one another and agree with independent results of *Aki* [1966] for small earthquakes located in the region.

Solution 136 is consistent with the hinge faulting depicted in Figure 5*b*; in this case the steeply dipping Izu-Bonin slab tears away and moves downward with respect to the more gently dipping North Honshu slab. This type of deformation, however, does not account for the orientation of 135 or 137. If the tearing and hinge faulting are located in the zone of intense subcrustal seismic activity near earthquake 136, then at greater depths the two slabs will be separated. Hence, earthquake 137 may be in the northern edge of a separate Izu-Bonin slab. The difference between 137 and 138–146 may be attributable to a rotation of the axes due to a bend at the edge similar to that at the northern end of the Tonga arc (Figures 4 and 11). Further study of the detailed distribution of hypocenters in the region beneath central Honshu is required to test this interpretation.

The earthquakes comprising 135 may result from stresses in the portion of the slab above the tearing and disruption near 136. The orientation of 135, however, is most simply interpreted as a faulting parallel to the inclined seismic zone, i.e., thrust faulting between the converging Pacific and Asian plates. If this is correct, then the earthquakes comprising 135 would be an anomalously deep extension of the shallow thrust zone characteristic of the inner margins of the trenches. Most of the earthquakes comprising 135 have depths greater than 60 km, and many have depths between 80 and 100 km. In most cases these depths are accurately determined by numerous arrival times from stations within a degree of the epicenter.

Izu-Bonin arc (Figure 21). *Katsumata and Sykes* [1969] show that the inclined seismic zone south of Honshu, though slablike in structure, varies as a function of depth and location along the strike. The zone appears to be continuous to depths of about 550 km. In the separate equal-area plots of Figure 21, the data are shown relative to the local orientation of the zone. The P axes for the deep earthquakes 138–147 all appear to parallel the local dip of the seismic zones; i.e., the P axes tend to follow the local variations in dip. The T axes tend to be perpendicular to the zone except in two cases in which the B and the T axes interchange.

The data are sparse for intermediate depths. Ichikawa reports two solutions for earthquakes at depths of 150 and 130 km located southwest of Tokyo, just south of the junction described in the preceding section; both indicate down-dip compression. Solution 148 for an event at 80-km depth, however, indicates compression parallel to the strike of the zone. Mechanisms of this type are rare; the only other clear example is solution 27 for an intermediate-depth event located at the southern end of the New Hebrides arc (Figure 9).

Marianas arc (Figure 23). *Katsumata and Sykes* [1969] show that the inclined zone beneath the northern part of the Marianas arc has a remarkable structure. From shallow depths near the trench the slablike zone curves downward and below 250 km has a nearly vertical dip. The zone is continuous to a

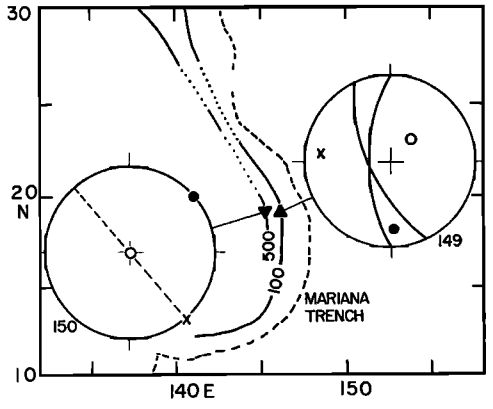

Fig. 23. Marianas island arc.

depth of 680 km. Most of the hypocenters below 500 km are confined to a narrow range along strike between about 19° and 20°N; few deep events occur between this zone and the southern end of the Izu-Bonin zone near 27°N. There is evidence [*Gutenberg and Richter,* 1954], however, for the location of earthquakes at depths of 500–600 km near about 24°N; a short solid segment of the 500-km contour in Figure 23 indicates the location of these events. A continuous and nearly straight 500-km contour that trends north-northwest and connects the Izu-Bonin and Marianas deep zones passes through the deep hypocenters near 24°N. The distribution of the deepest events does not therefore appear to reflect the offset that is prominent in the surface features of the Marianas arc.

The *P* axis of 150 plunges vertically and is thus parallel to the local dip of the Marianas deep zone. The *B* and *T* axes are horizontal and trend parallel and perpendicular to the north-northwesterly trend inferred above for the regional distribution of deep hypocenters. This relationship is evidence that the deep seismic zone is continuous between the Izu-Bonin and the Marianas arcs.

Solution 149 for an event at intermediate depth indicates extensional stress approximately parallel to the strike of the zone. Note that although the *P* and the *B* axes are not parallel to the zone, neither are the nodal planes. The solution is similar to others for earthquakes in regions where the surface features are curved, and can be explained by the lateral stretching effect shown in Figure 6.

Ryukyu Arc (Figure 24)

Katsumata and Sykes [1969] show that an inclined zone dips beneath the Ryukyu Islands at an angle of about 45° and reaches depths less than 300 km. Their solutions for shallow earthquakes indicate underthrusting of the Philippine Sea plate beneath the Ryukyus. In Taiwan the seismicity changes trend abruptly and trends south along the eastern coast. Subcrustal earthquakes are also found beneath Taiwan and may be part of an inclined zone that dips steeply eastward.

Earthquakes 151–152 are located away from either end of the arc. The solutions are similar to one another and indicate down-dip compression. In our previous paper [*Isacks and Molnar,* 1969] we suggested that these solutions are similar to 113 in the Aleutians in respect to indicating extensional stress

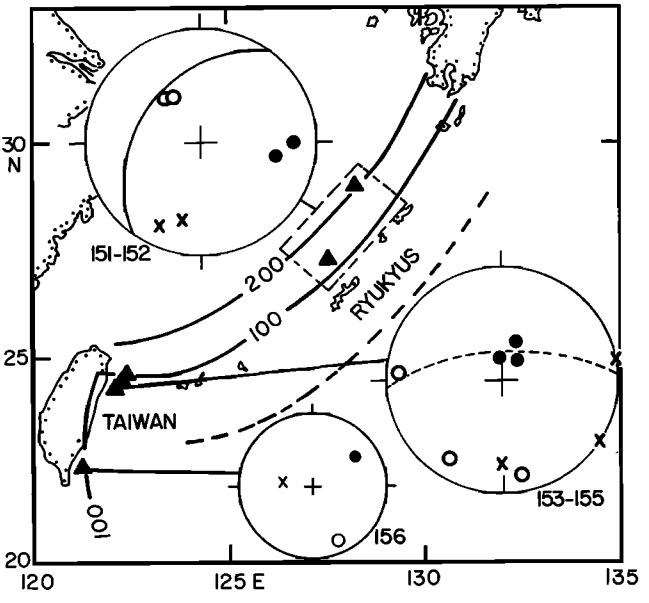

Fig. 24. The Ryukyus island arc and the region near Taiwan.

parallel to the strike. However, as shown in Figure 23, the T axes for the Ryukyu solutions are more nearly perpendicular to the zone and the B axes more nearly parallel to its strike. Thus, we cannot interpret these solutions by the lateral stretching effect shown in Figure 6.

Earthquakes 153–155 are located near the intersection of zones in Taiwan. Two of these have depths of 67 and 70 km and so are near the borderline between shallow and intermediate depths; the third (153) has a depth of 119 km. The T axes of all three plunge steeply northward, and the B and P axes tend to be nearly horizontal. The B and P axes of 154 and 155 approximately interchange positions. The data for the three solutions can thus be taken to suggest extension parallel to the dip of a nearly vertical and possibly contorted slab near the Taiwan corner.

Earthquake 156 is located at a depth of 72 km in the eastward-dipping zone south of the Taiwan intersection. The structure of the zone is not well enough known to interpret this solution.

Philippines-Celebes-Halmahera (Figure 25)

The tectonics of this region are especially complex and are not well understood. *Fitch* [1970*a*] summarizes evidence for a subdivision of the region into three distinct island-arc-like structures: the Luzon arc, the Mindanao arc, and the Talaud-Halmahera arc. Although all three have zones of subcrustal earthquakes, only the Mindanao arc has a fairly well-defined inclined zone that reaches great depths. The solutions for subcrustal earthquakes are also most simply grouped according to these divisions.

Luzon arc. A northward-striking trench [*Hayes and Ludwig*, 1967; *Ludwig et al.*, 1967] and the presence of volcanoes and shallow and intermediate-depth earthquakes indicate that an island-arc structure exists on the western side of

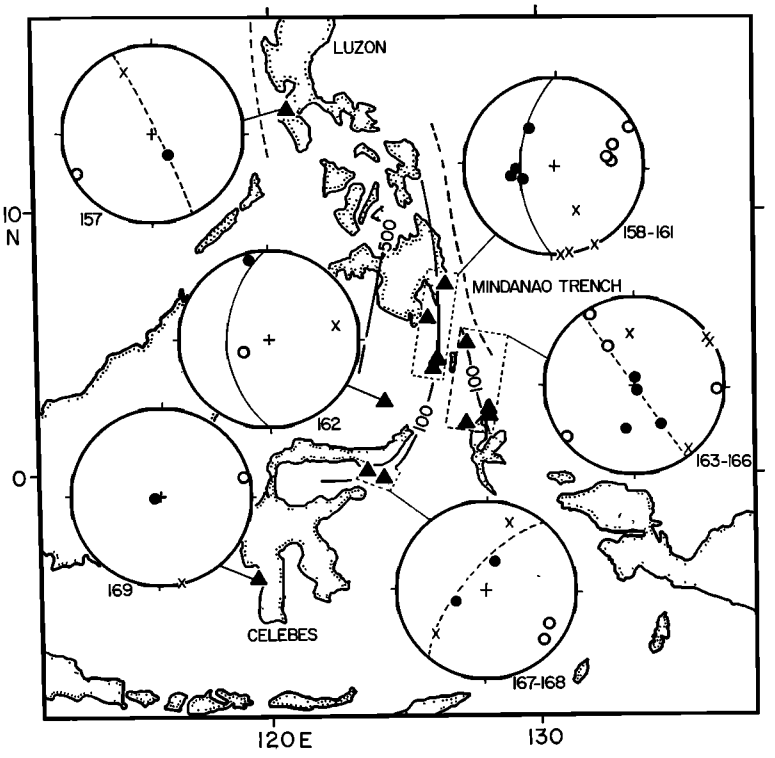

Fig. 25. Region of deep and intermediate-depth earthquakes near the Philippines, Halmahera, and Celebes islands. Talaud Island is located between the dashed rectangles that enclose earthquakes 158–161 and 163–166.

Luzon. An inclined seismic zone appears to dip east, but the data are inadequate to determine its dip. The only solution (157) for this zone can be interpreted as extension parallel to a steeply dipping zone or thrust faulting along a zone dipping about 45°. Because of the depth of the event (166 km), the former interpretation is more consistent with the data for other regions.

Mindanao arc. The inclined seismic zone associated with the Mindanao trench dips westward and reaches depths greater than 650 km (M. Katsumata, personal communication). A gap in activity appears to occur between depths of about 300 and 500 km. Shallow earthquake mechanisms in the region indicate a westward underthrusting of the Philippine Sea plate beneath Mindanao [*Fitch*, 1970*a*]. In the southern part of the structure the zones of earthquakes and active volcanoes appear to bend westward and parallel the east-west-trending peninsula of northern Celebes. *Fitch and Molnar* [1970] show that the zone may dip northward near Celebes.

Earthquakes 158–161 are located in the westward-dipping zone, and 167–168 are located where the arc bends and has a more northerly dip. Earthquake 163, though located close to 160 and 161, appears to be part of the eastward-dipping zone beneath Talaud and Halmahera; it is considered in the next section. The

T axes of 158–161 all dip westward and are consistent with down-dip extensional stress. Note that 161 is interpreted by Fitch as indicative of motion between plates, i.e., underthrusting of the Philippine Sea plate beneath the Celebes Sea plate. The depth reported in the *Preliminary Determination of Epicenters* of the Coast and Geodetic Survey [1963] is 64 km, but it is revised to 83 km in the *Seismological Bulletin* of the Coast and Geodetic Survey [1963] and 122 km in the *International Seismological Summary* [1963]. The data controlling depth for this event are poor, but examination of the seismograms suggests that the depth is greater than normal but probably not as great as that listed by the ISS. If the solutions for thrust faults in the shallow portion of the seismic zone have the same orientation as ones indicating extensional stress parallel to the zone at intermediate depths, the seismic zone must decrease in dip near the thrust zone. Although such a change in dip is difficult to resolve in the distribution of hypocenters, *Mitronovas et al.* [1969] demonstrate it for the Tonga arc.

The solution of 162 indicates compression parallel to the dip and extension parallel to the strike of the zone. This result may thus indicate an effect of the convex curvature of the arc near Celebes (Figure 6). The solutions for 167 and 168 for events located where the arc bends westward are consistent with extensional stress parallel to a zone dipping steeply northwestward.

In summary, solutions 158–161 and 167–168 are consistent with an inference of down-dip extension at intermediate depths, whereas 162 can be interpreted as an effect of the bend near Celebes. The results for great depths are uncertain; *Ritsema's* solutions [1964] for two deep events in the Mindanao zone are not clearly interpretable in terms of stress parallel to the deep zone.

Talaud-Halmahera arc. The distributions of volcanoes and earthquakes with depths between 70 and 200 km suggest an island-arc-like structure striking south-southeast between the islands of Talaud and Halmahera [*Hatherton and Dickinson,* 1969; *Fitch and Molnar,* 1970]. The apparent eastward dip of the zone is opposite to that of the adjacent Mindanao zone.

The *T* axes of 163–166 tend to be more nearly vertical, whereas the *P* and *B* axes tend to be more nearly horizontal. A nearly vertical plane approximately parallel to the island-arc-like surface features can be fitted through the stress axes of three of the solutions. This result suggests the presence of down-dip extension in a steeply dipping slab.

Celebes. Earthquake 169, located beneath southern Celebes, is isolated from the seismically active island-arc structures or from other zones of shallow earthquakes in the region. The plane through the *B* and *T* axes dips nearly vertically and strikes slightly west of north. This would be consistent with extension in a vertically sinking slab. Alternatively, the solution could indicate horizontal compression within a thick lithospheric plate on the surface. Examination of the seismograms and the location data for this event indicates that the depth of 81 km is reliable.

Sunda Arc (Figure 26)

Sumatra-Flores Sea. The Sunda arc is a nearly continuous structure extending from Burma to the Banda Sea. The portion shown in Figure 26 includes the

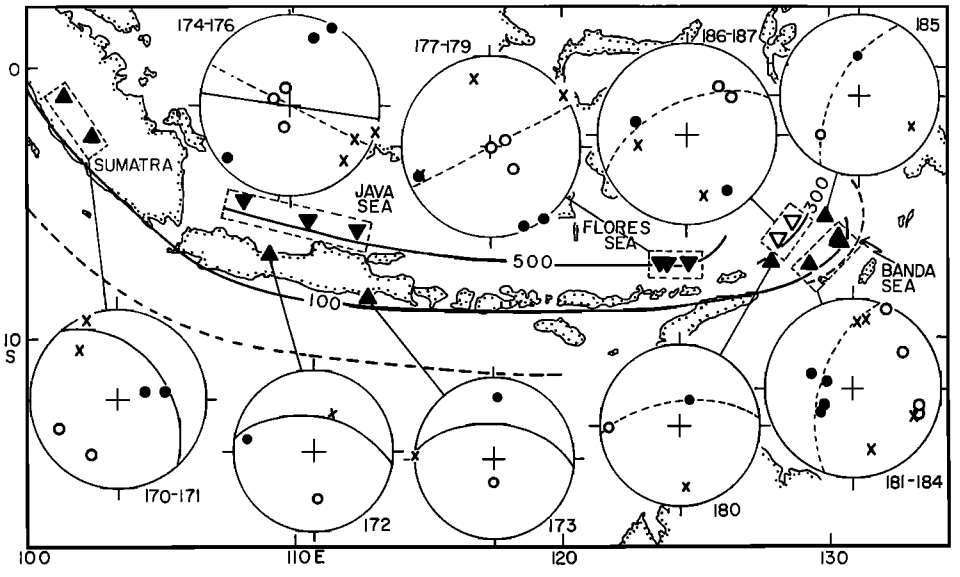

Fig. 26. Sunda island arc.

main belt of deep and intermediate-depth earthquakes. The distribution of earthquakes with depth appears to vary abruptly along the arc; near the Sunda Strait depths increase from less than 200 km beneath Sumatra to greater than 600 km beneath the Java Sea [*Fitch and Molnar*, 1970]. Between about 105°E and 126°E the zone reaches depths greater than 650 km and possibly greater than 700 km [*Gutenberg and Richter*, 1954]. Beneath the Flores and Java Seas a pronounced minimum in activity is present between depths of about 300 to 500 km.

The T axes of 170–171 plunge beneath Sumatra and can be interpreted as down-dip extension. Moreover, *Fitch* [1970*a*] reports a solution (his number 1) for an event at the northern end of Sumatra which, though not well determined, is also in agreement with extension parallel to the seismic zone; the solution is not in agreement with underthrust faulting. The intermediate depth of that event (70 km) appears to be reliable.

The T axis of 173 plunges gently north, whereas the dip of the zone near 173 appears to be steeper. The structure of the seismic zone, however, is not sufficiently well resolved to exclude the possibility that the zone dips more gently near 173 and steepens in dip at greater depth [*Fitch and Molnar*, 1970; *Engdahl et al.*, 1969; E. R. Engdahl, personal communication, 1970].

The solution of 172 indicates extension parallel to the strike of the zone. This earthquake is near the change of strike of the arc, where the distribution of hypocentral depths abruptly changes. Fitch and Molnar suggested that the convex curvature of the arc in this region may be responsible for the anomalous orientation of 169 and can be explained by the model of Figure 6.

The solutions 174–176 for three deep shocks beneath the Java Sea are in good agreement with an inference of simple down-dip compression. The vertical orien-

tation of the seismic zone shown in Figure 26 is based on sections [*Engdahl et al.*, 1969; *Fitch and Molnar*, 1970] that show a well-defined narrow zone that dips nearly vertically between depths of about 500 and 650 km.

The three solutions 177–179 for deep events beneath the Flores Sea also indicate down-dip compression parallel to a nearly vertical zone, but the trends of the B and T axes suggest that the zone may have a more nearly east-northeasterly strike rather than the easterly strike of the surface features and of the alignment of deep hypocenters farther west. This relationship plus reliable locations of deep events northeast of 177–179 suggest that the deep zone bends around in a fashion similar to the shallower zone beneath the Banda Sea (see next section). Solutions for three deep earthquakes reported by *Ritsema* [1964] are in approximate agreement with the solutions of 174–179.

Banda Sea. *Fitch and Molnar* [1970] argue that both the spatial distribution and the focal mechanisms of earthquakes located beneath the Banda Sea can be explained by the upward bending of the western edge of a lithospheric slab dipping beneath the Sunda arc (Figure 4). The earthquakes are not as deep beneath the Banda Sea as those farther west; furthermore, as a result of the bending, the activity at intermediate depths and at depths of 300 to 500 km is especially intense. This explanation implies that the gap in activity west of the bend corresponds to a minimum in stress within a continuous slab rather than an actual gap in the slab, i.e., implies model b rather than model d in Figure 3.

Solutions 180–187 indicate two predominant stress orientations in the zone: 180–185 indicate down-dip extension and an interchange of the positions of the B and P axes, whereas 186–187 have compressional axes oriented between the strike and dip of the zone and an interchange of the T and B axes. Solutions 186–187, for the two events located at depths greater than 300 km, could indicate a compressive stress in the upper part of a bent slab; this might also explain the parallelism of the P axes and the strike directions in the solutions of some of the events at intermediate depths. The predominance of down-dip extension, however, suggests that at intermediate depths the stress results mainly from a stretching rather than a bending of the slab.

In summary, the down-dip extension at intermediate depths and down-dip compression at great depths predominate in the Sunda arc. The solutions for the two deep events in the bent edge of the zone beneath the Banda Sea are among the few cases we have found in which the effects of bending may be important.

Alpide Belt: Asia

The most active zones of subcrustal seismic activity in the Alpide belt between Sumatra and the Mediterranean region are located beneath Burma and the Hindu Kush Mountains. Although subcrustal hypocenters have also been reported for the region of North Sumatra and the Andaman Islands, the Himalayan Front between Burma and the Hindu Kush, the Zagros belt of Iran, and the region of the Caspian Sea, focal-mechanism data for the regions are lacking.

Burma (Figure 27). The zone of intermediate-depth earthquakes located near the arcuate range of mountains between Assam and Burma appears to dip eastward and strikes parallel to the north-northeasterly trend of the mountain

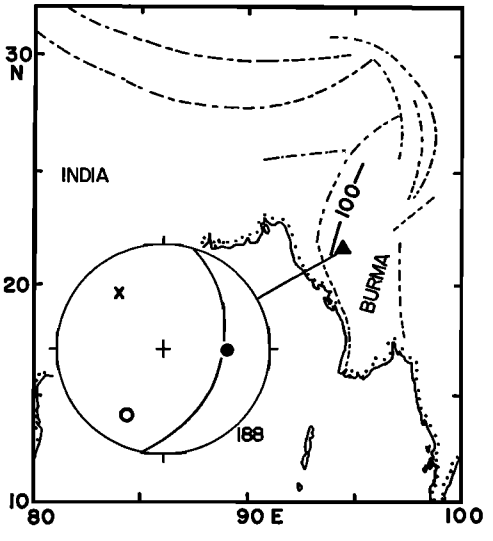

Fig. 27. Zone of intermediate-depth earthquakes in Burma. The lines of long and short dashes represent major mountain ranges.

belt. As *Santo* [1969*b*] notes, the level of shallow activity is low relative to that at intermediate depths. Focal depths probably do not exceed 200 km.

Fitch [1970*b*] reports solutions for two intermediate-depth events in this region. Although only one (188) is fairly well determined, the data for the other are in agreement with it. The T axis plunges eastward and is thus probably parallel to the dip of the inclined seismic zone. Although limited, the data are thus consistent with down-dip extensional stress within the eastward-dipping seismic zone. Note that the P axis, not the B axis, is more nearly parallel to the strike of the zone. This orientation, plus the depths of the events, argues against an interpretation of the data as thrust faulting along the inclined seismic zone.

Hindu Kush (Figure 28). The remarkable concentration of intermediate-depth hypocenters beneath the Hindu Kush is located near a complex junction of tectonic belts, and no simple island-arc-like structures are apparent. Near the Hindu Kush the seismicity is greatest at intermediate depths, whereas the most active nearby zone of shallow earthquakes is associated with the east-northeast-trending block-faulted structures of the Tien Shan located farther north. Beneath the Hindu Kush the largest earthquakes appear to be remarkably concentrated in space. Gutenberg and Richter's most accurately located events, including most of the largest shocks that occurred between 1907 and 1950, all have depths between 210 and 240 km and occur within a degree or less of 36¼°N and 70½°E. This spatial concentration of the largest shocks has continued during the period from 1954 to the present. Locations of earthquakes of smaller magnitude show that the zone has a discernible extent and structure and is not a pointlike source of earthquakes. The *Atlas Zemletryasenii SSSR* [1962] and *Nowroozi* [1971] show that earthquake hypocenters are distributed throughout the range of depths less than 300 km. Nowroozi, in particular, clearly delineates two thin, slablike zones; one is located between depths of about 70 and 175 km and trends northeast, and the second is located at depths between about

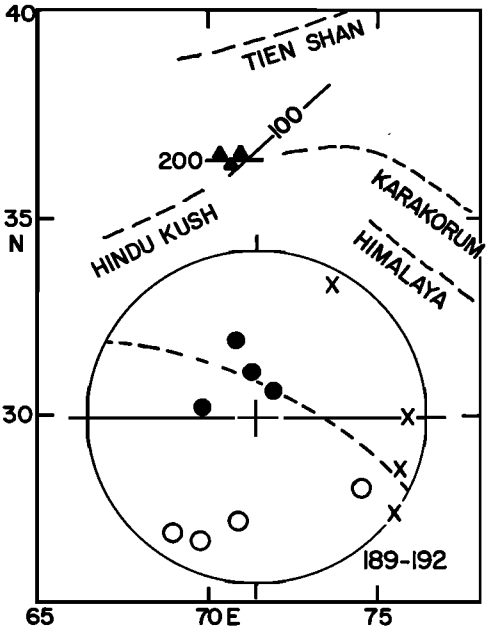

Fig. 28. Zone of intermediate-depth earthquakes beneath the Hindu Kush. The names refer to the major mountain belts in the region.

175 and 250 km and trends east-west. In Figure 28 these two zones are indicated by the 100-km and 200-km contours of hypocentral depths, respectively.

Focal-mechanism solutions for the region are summarized by *Ritsema* [1966], *Stevens* [1966], *Shirokova* [1967], and *Soboleva* [1967, 1968]. Stevens shows that solution 189 is representative of most of the data, if not all of the solutions, reported by other workers. Ritsema derives a common solution (192) for earthquakes that occurred during the period 1949–1965. Both are plotted in Figure 28 together with well-determined solutions for two other earthquakes (190 and 191). The results of Soboleva and Shirokova are in general agreement with the pattern exhibited by these data.

Earthquakes 189–191, as well as most of the events comprising 192, are probably located in the lower east-west-striking zone. The T axes dip steeply north, but the poles of one set of nodal planes dip as steeply south. From this relationship alone we could equally well infer either (*a*) shearing or slip parallel to the zone or (*b*) stress inside a thin slab. However, the interchange of the B and P axes of 190 relative to the other solutions, although difficult to explain in terms of vertical shearing or slip, is consistent with extensional stress inside a slab that dips steeply north. Nowroozi's data do not exclude a northward dip of the zone as small as, say, 75°. Thus, although further investigation is required, down-dip extension in this zone is the preferred interpretation of the data.

Alpide Belt: Mediterranean Region (Figure 29)

Known subcrustal earthquakes are confined to four separate areas in the region of the Mediterranean Sea: the Vrancea region of Rumania, the southern Aegean Sea, the Tyrrhenian Sea northwest of Calabria and Sicily, and southern

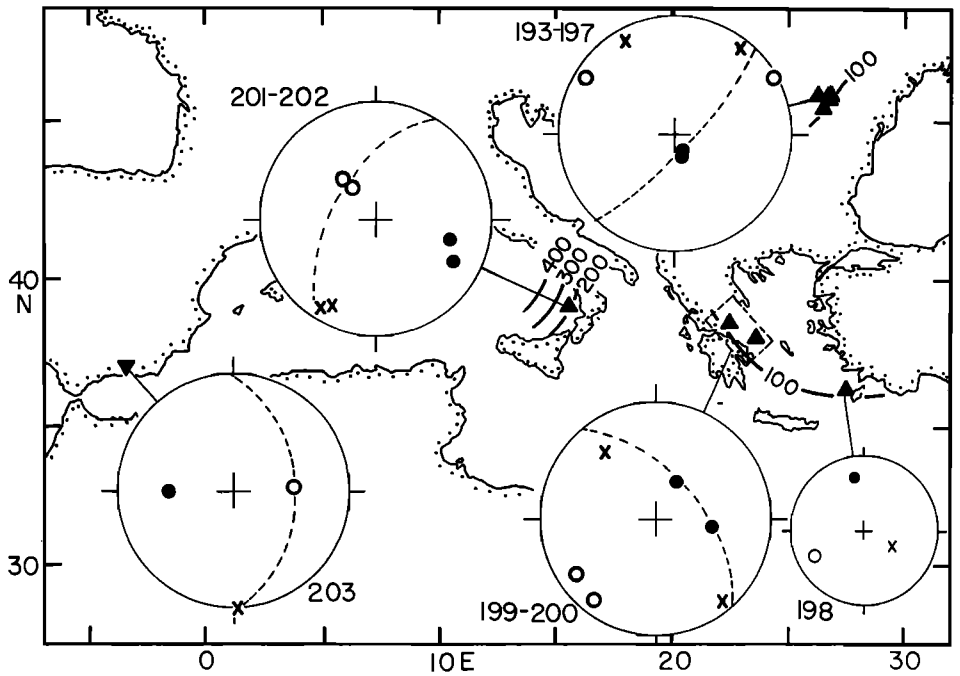

Fig. 29. The Alpide belt in and near the Mediterranean Sea, including the Vrancea region of Rumania (193–197), the Hellenic island arc (198–200), the Calabrian island arc (201–202), and the Spanish deep earthquake (203).

Spain. Solutions based on WWSSN data are available only for the Aegean area. Because of the numerous stations that have long been in operation in Europe, however, reliable solutions are also available for previous earthquakes.

Vrancea region of the eastern Carpathians. A concentrated source of earthquakes with depths between about 100 and 150 km is located just east of the sharp bend of the Carpathian Mountains. Although the detailed structure of this zone is not well determined, *Karnik* [1969], in a summary of Rumanian work, suggests that it reaches depths of about 200 km and dips steeply. *Radu* [1965] shows an inclined zone striking northeast and dipping northwest.

The five solutions 193–197 plotted in Figure 29 were selected from the literature as the most reliable that we were able to find. The solutions 193–196 are nearly identical; 197 differs in that the P and B axes approximately interchange positions with respect to others. The T axes of all five dip nearly vertically, and the nearly horizontal B and P axes are either parallel or perpendicular to the apparent strike of the subcrustal zone. The results thus suggest down-dip extensional stress within a nearly vertical slab. This inference is similar to that obtained for the concentrated source region beneath the Hindu Kush.

Hellenic arc. The distributions of shallow and intermediate-depth earthquakes and volcanoes, focal mechanisms of shallow earthquakes [*McKenzie*, 1970], and the data from marine geology [*Ryan et al.*, 1970] indicate an island-

arc structure bounding the southern and southwestern Aegean Sea. Solutions for shallow earthquakes along the arc indicate northeasterly underthrusting of the Mediterranean sea floor beneath the Aegean [*McKenzie*, 1970]. Because the seismicity is rather low for an island arc, the distribution of hypocenters is poorly known; the available data suggest a zone dipping north to northeast beneath the Aegean. *Karnik* [1969] finds that hypocentral depths do not exceed 200 km.

Solutions 199 and 200 are consistent with down-dip extension within a zone dipping about 60 degrees northeast. The T axis of 198 dips gently north and thus may indicate extension within a gently dipping zone, although the P and B axes are not parallel or perpendicular to the east-west strike of the western end of the arc.

Southern Italy: Calabrian arc. *Gutenberg and Richter* [1954] and *Peterschmitt* [1956] show that intermediate- and deep-focus earthquakes beneath the Tyrrhenian Sea are associated with an island-arc-like structure near Calabria and Sicily (see also *Ryan et al.*, 1970). The inclined seismic zone dips northwest and reaches depths of 450 km. Peterschmitt finds evidence that seismic-wave velocities near this zone are anomalously high, a result now thought to be characteristic of the island arcs of the Pacific [*Oliver and Isacks*, 1967; *Utsu*, 1967; *Davies and McKenzie*, 1969; *Mitronovas*, 1969].

Solution 202 is an average solution for subcrustal earthquakes derived by *Ritsema* [1969]. Both solutions 201 and 202 have P axes that plunge northeast and B axes that are nearly horizontal and parallel to the strike of the Calabrian arc. The data are thus in good agreement with down-dip compressional stress within the northwest-dipping zone.

Southern Spain. A large deep-focus earthquake occurred beneath the Sierra Nevada of southern Spain in 1954 at a depth of 650 km. No other deep seismic activity is known to be located in this region, and the event does not appear to be related to an obvious island arc or island-arc-like structure.

Solution 203 is well determined by numerous first motions reported by nearby European stations. In Figure 28 two planes are drawn through the stress axes of this solution. Extrapolation of results from other regions suggests that the plane through the P and B axes, a plane that strikes north and dips 45° east, would be the most likely orientation of a seismic zone near 203. In this case an east-dipping slab of lithosphere is under compression parallel to its dip. The surface trace of the inferred slab would be located near or west of Portugal and Gibraltar and would strike north-south. Tectonic trends of southern Spain are sometimes shown to be curved around through Gibraltar to join the riff structures of northern Africa; near Gibraltar such a belt would have a north-south strike and could thus be related to the surface trace of the postulated seismic zone. Alternatively, a vertical plane through the P and T axes is parallel to the predominantly east-west alignment of the belt of shallow earthquakes in the western Mediterranean and along the Azores-Gibraltar ridge. *McKenzie* [1970] claims that this belt marks the boundary between the converging African and Eurasian plates. Thus 203 may be related to lithospheric consumption along that zone, although the isolation of the event as well as the orientation of stress are anomalous. Until the complex tectonic history of the western Mediterranean is

better known, the relationship of the Spanish deep earthquake to the near-surface structure remains a puzzle.

APPENDIX

Table 1

Table 1 lists the locations and focal-mechanism solutions for the earthquakes plotted in Figures 1, 2, and 7 through 29. The location listed in each case is the most reliable one reported in the literature. If a relocation is not available from a special investigation of seismicity, or from the *International Seismological Summary* and the *Bulletins of the International Seismological Center,* the location is taken from the *Seismological Bulletin* of the Coast and Geodetic Survey (ESSA); if none of these is available (mainly for the more recent earthquakes), the location is taken from the *Preliminary Determination of Epicenters* of the Coast and Geodetic Survey.

The trends and plunges listed for the focal-mechanism solutions are measured in degrees clockwise from north and downward from the horzontal, respectively. The second to last column lists the data plotted in Figure 2. 'P' and 'T' indicate down-dip compression and tension, respectively; 'X' indicates that *neither* the *P* nor the *T* axis is approximately parallel to the dip of the zone; and 'n.p.' indicates that the solution is not plotted in Figure 3. The data not plotted are for earthquakes in regions where the structure of the zone is poorly known or very complex and no clear determination of down-dip stress type can be made.

In the last column on the right, the reference from which the solution is taken is tabulated as follows:

BJ	*Berckhemer and Jacob* [1968]	M	D. P. McKenzie, personal communication
CE	*Constantinescu and Enescu* [1962]		
Ch	*Chandra* [1970*b*]	Md	*Mendiguren* [1969]
CRE	*Constantinescu et al.* [1966]	MS	*Molnar and Sykes* [1969]
Fa	*Fitch* [1970*a*]	N	New solution obtained by us for this paper
Fb	*Fitch* [1970*b*]	Ra	*Ritsema* [1965]
FM	*Fitch and Molnar* [1970]	Rb	*Ritsema* [1966]
H	*Honda and Masatsuka* [1962] and *Honda et al.* [1956]	Rc	*Ritsema* [1969]
		S	*Stevens* [1966]
HC	*Hodgson and Cock* [1956]	St	*Stauder* [1968*b*]
Hi	*Hirasawa* [1966]	SB	*Stauder and Bollinger* [1965]
HH	*Hedayati and Hirasawa* [1966]	TB	*Teng and Ben-Menahem* [1965]
I	*Ichikawa* [1966]	VR	*Vvedenskaya and Ruprechtova* [1961]
ISO	*Isacks et al.* [1969]		
KS	*Katsumata and Sykes* [1969]		

The numbers following these abbreviations in the last column are those employed by the authors in each case to identify the particular earthquake.

New Focal-Mechanism Solutions

The new solutions ('N' in Table 1) are illustrated in appendix plates 1–4 on equal-area projections of the lower hemisphere of the focal sphere. In all cases the upper and right-hand side of the projections correspond to north and east, respectively. Filled or solid circles and triangles indicate compressional first motions, and unfilled or open circles and triangles indicate dilatational first motions. Triangles are for data on the upper hemisphere (pP or P at small distances) projected through the center onto the lower hemisphere; circles are for data on the lower hemisphere. X indicates compressional-wave data judged to be near a nodal plane. The direction of first motion of S is shown by an arrow. A small circle, triangle, or x and a dashed arrow indicate uncertain determinations.

Solutions for some of the events listed in Table 1 as new have also been reported by other investigators [e.g., *Stauder and Bollinger,* 1964, 1965; *Chandra,* 1970*a*; and *Mikumo,*

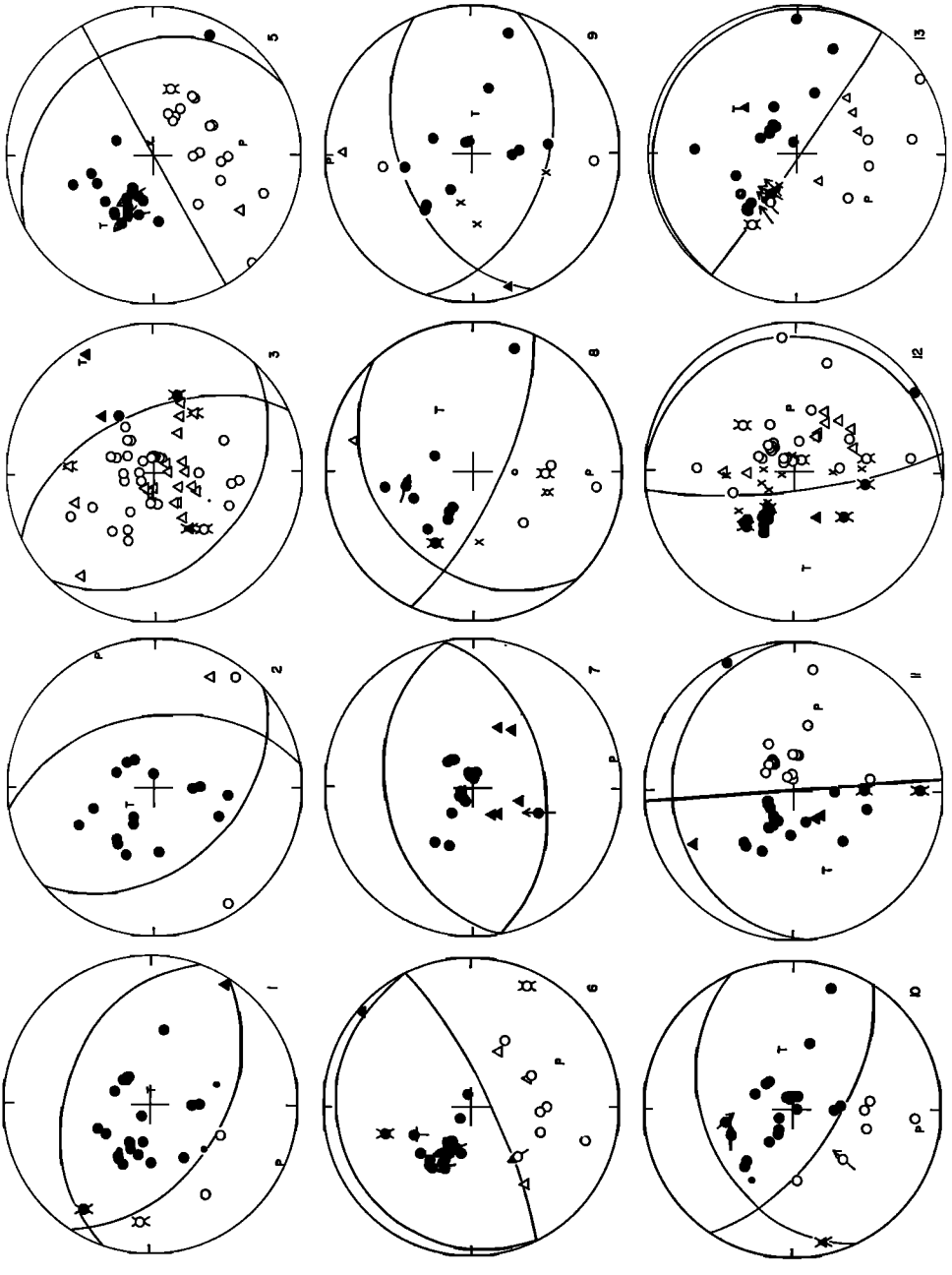

PLATE 1

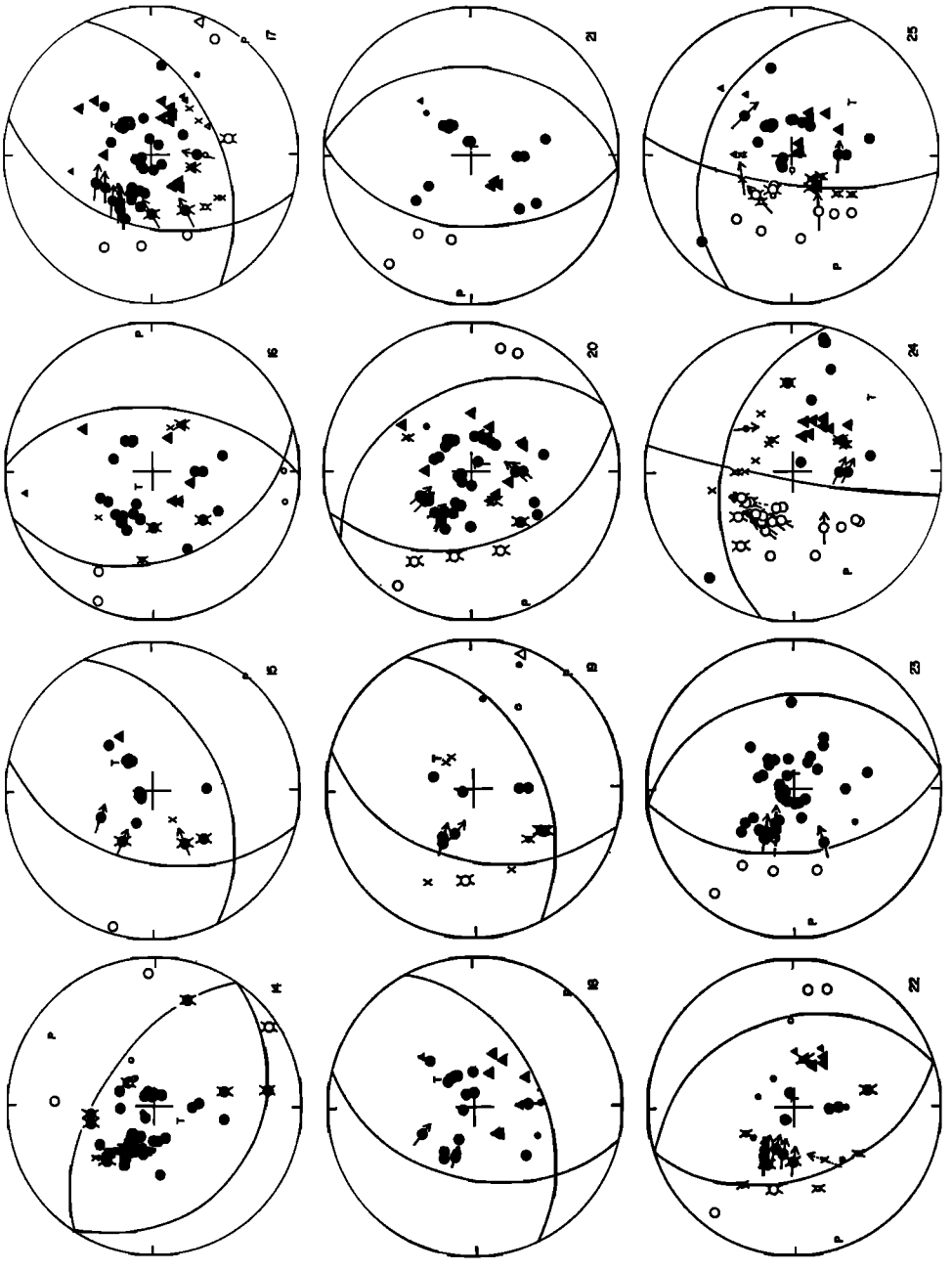

PLATE 1

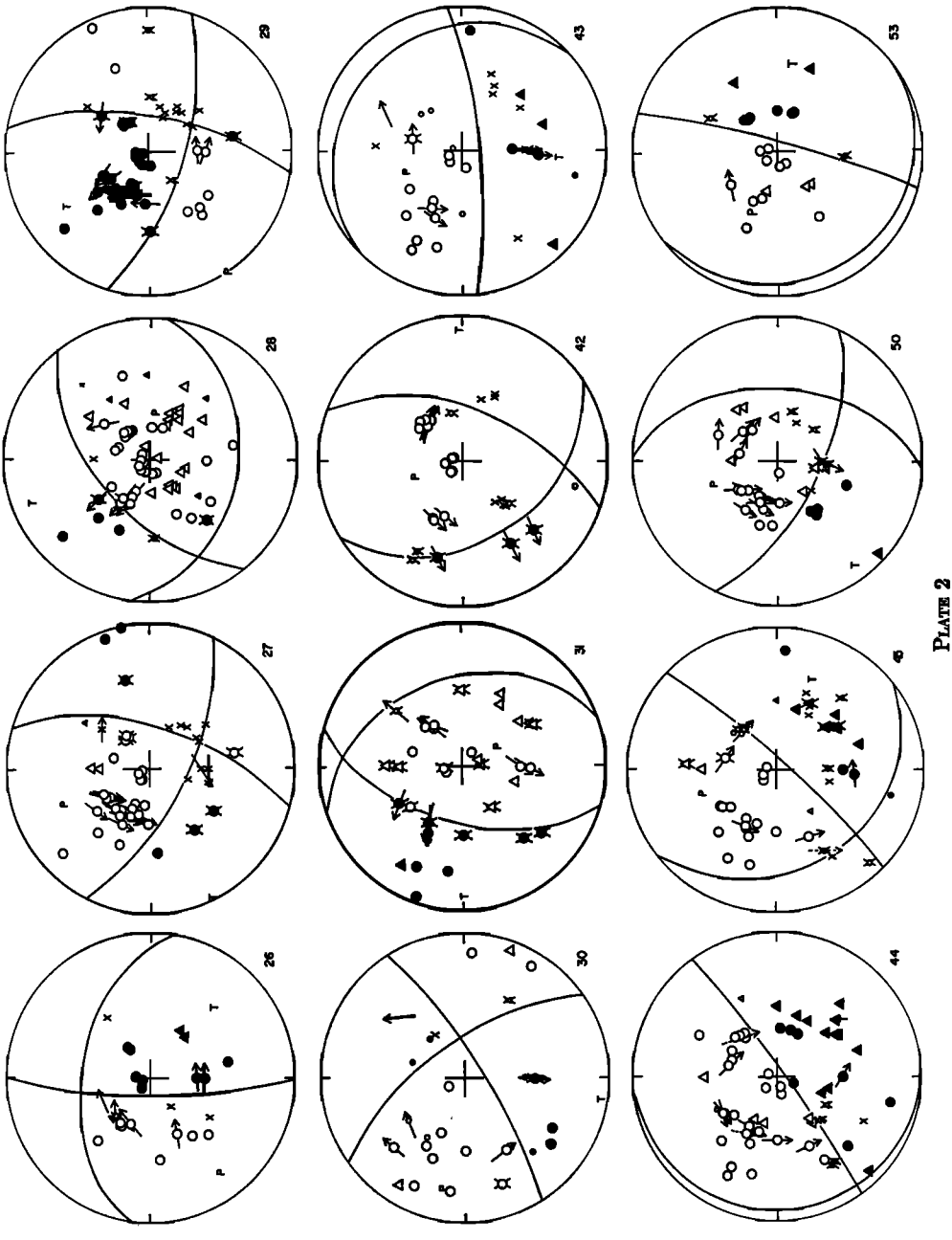

PLATE 2

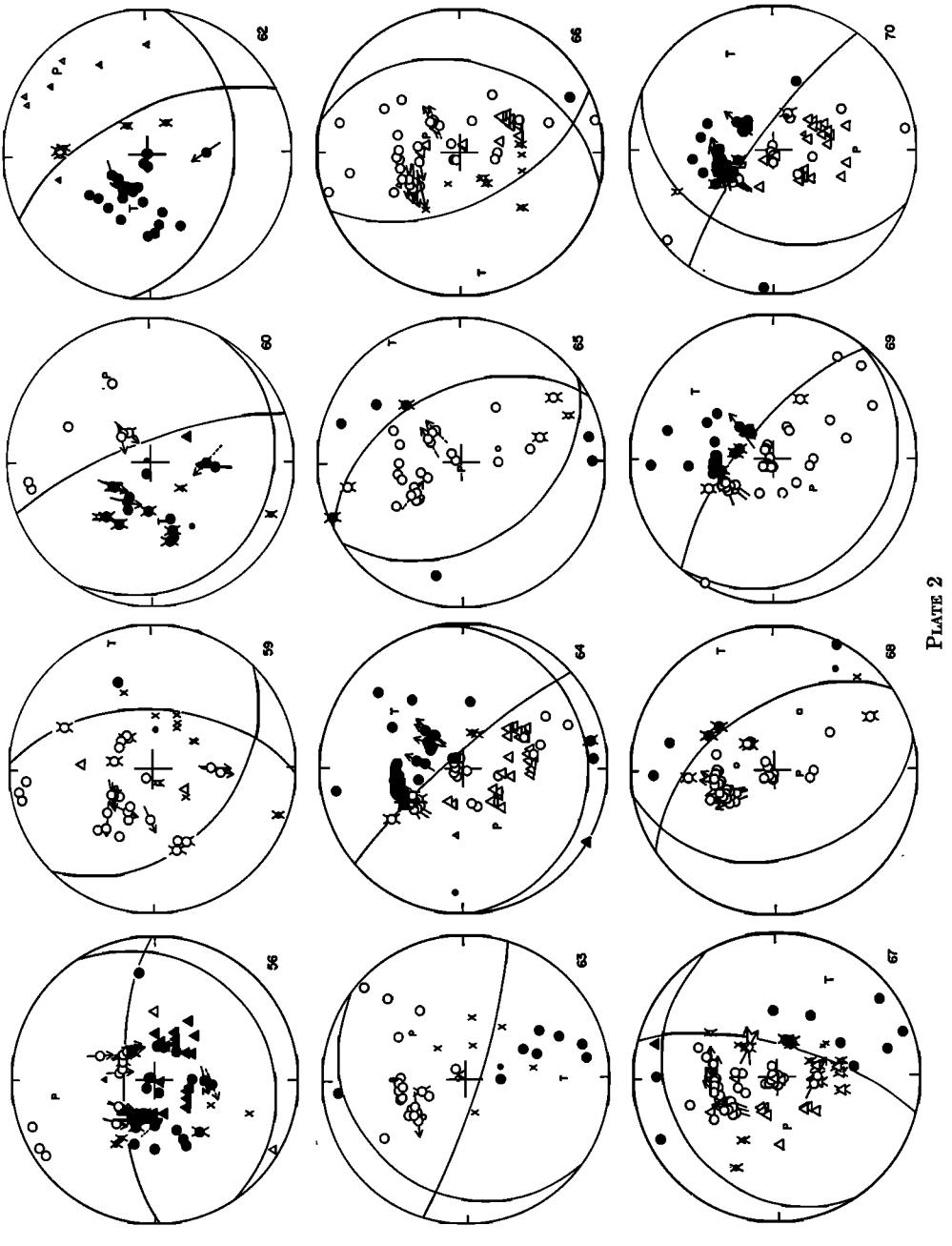

PLATE 2

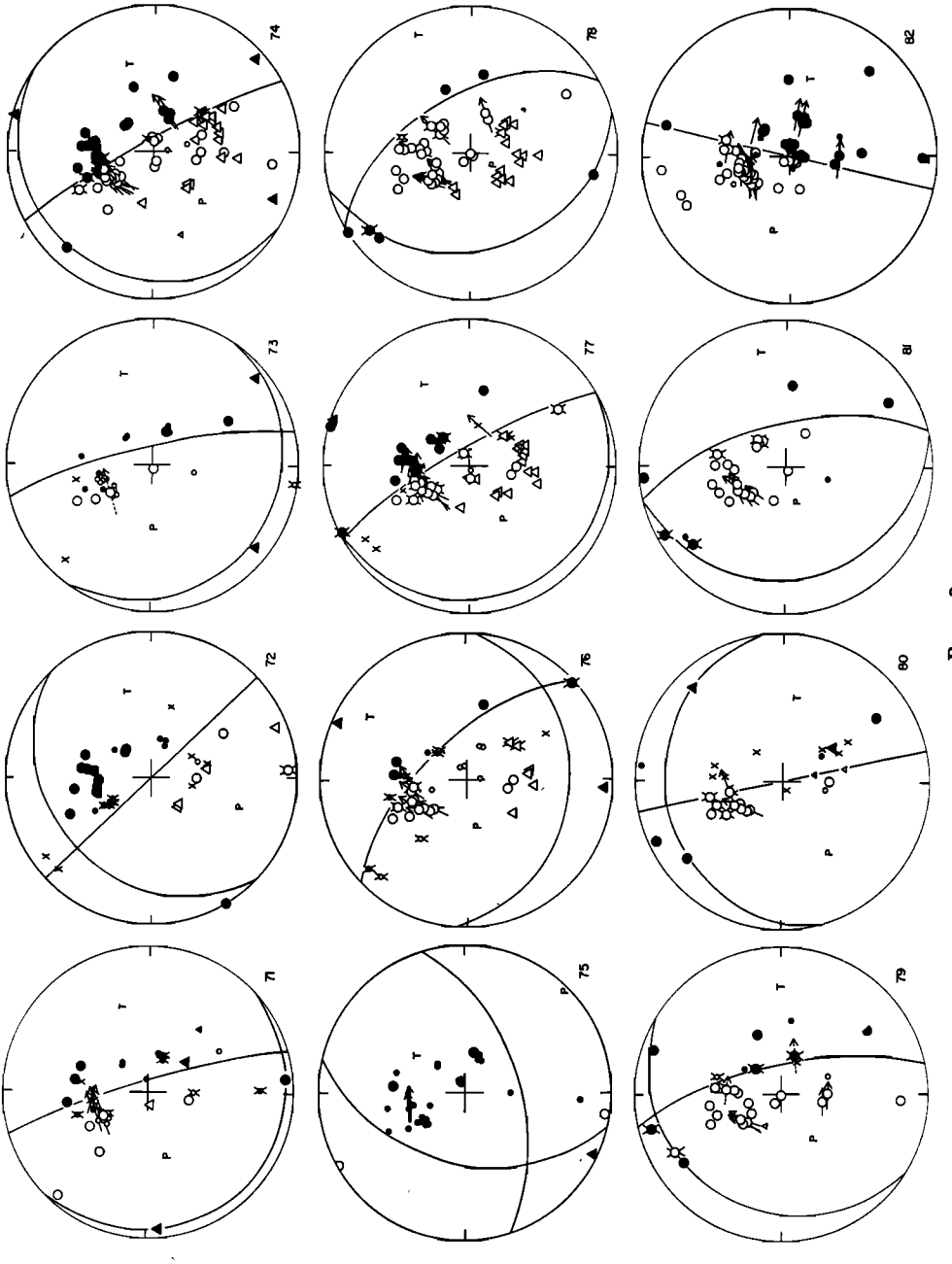

PLATE 3

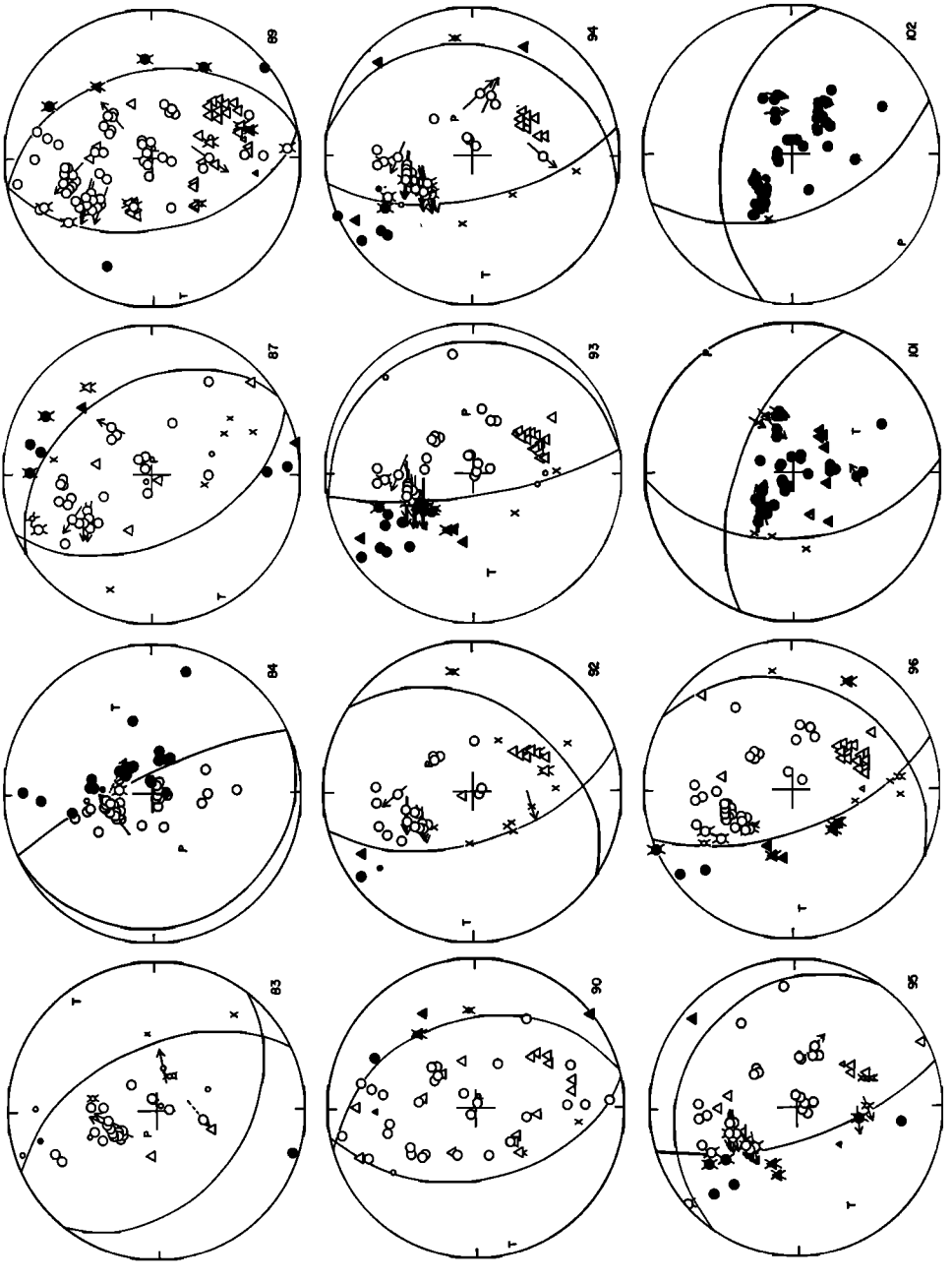

PLATE 3

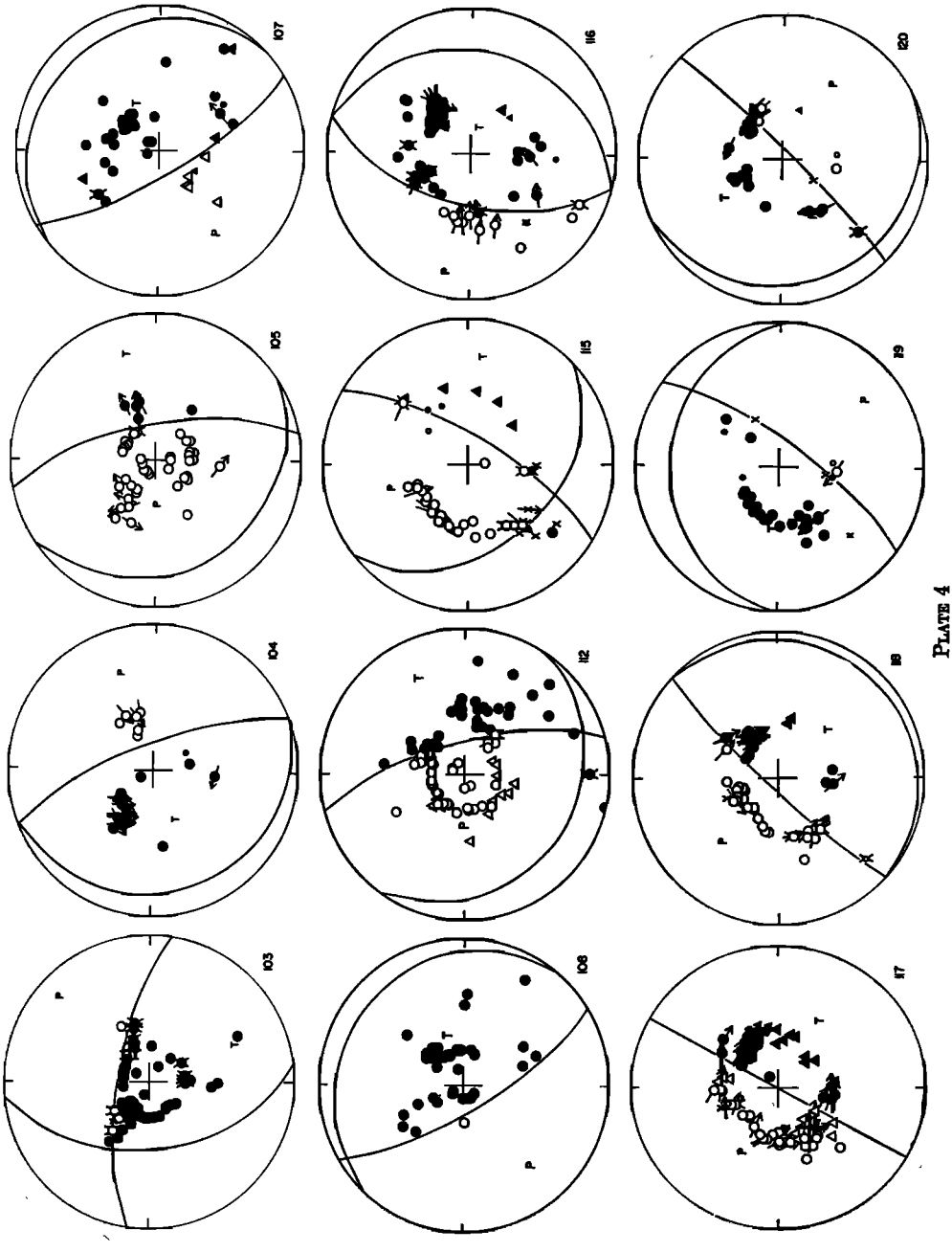

PLATE 4

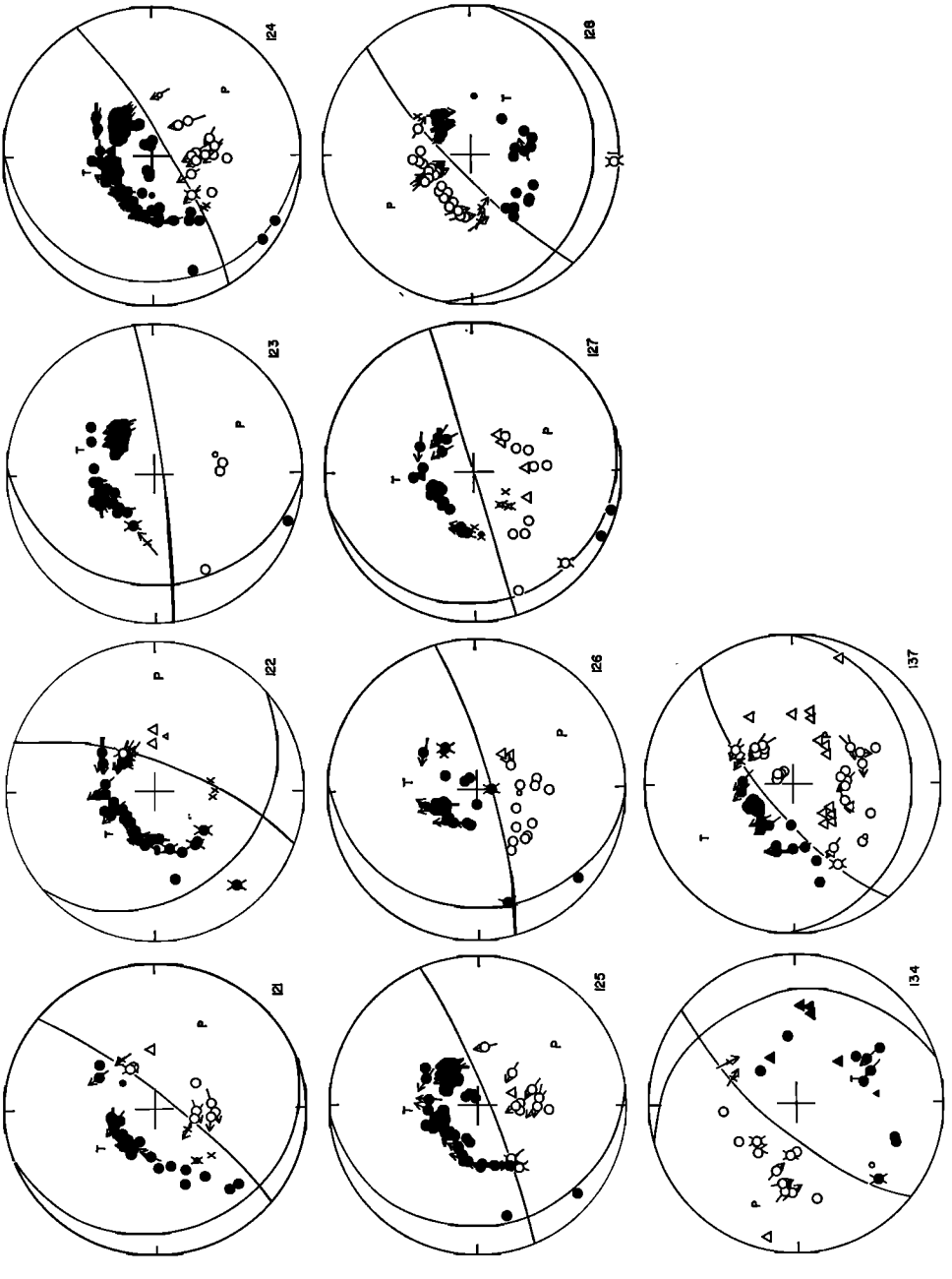

PLATE 4

1969]. In most cases the agreement of their solutions and ours is excellent and attests to the reliability of solutions based on WWSSN data. The largest discrepancies are associated with certain of Stauder and Bollinger's solutions for earthquakes in the Peru-Chile region. We attribute these discrepancies to their use of first-motion data for P waves that are reported in bulletins (and are often inconsistent) and their primary (nearly exclusive in some cases) reliance upon the polarization of shear waves.

Acknowledgments. Discussions with E. R. Engdahl, T. Fitch, D. T. Griggs, T. Hanks, V. Karnik, D. P. McKenzie, J. Oliver, A. R. Ritsema, C. Scholz, and L. R. Sykes were especially helpful. E. R. Engdahl, D. P. McKenzie, and A. Nowroozi kindly supplied data prior to publication of their work. We thank J. Oliver and L. R. Sykes for critically reading the manuscript.

This research was supported by NOAA, Department of Commerce, Grants E22-53-69G and E22-73-70G, and by National Science Foundation Grants NSF GA-11152 and NSF GA-1537. Contribution 1615 from Lamont-Doherty Geological Observatory.

REFERENCES

Adams, R. D., Source characteristics of some deep New Zealand earthquakes, *N. Z. J. Geol. Geophys., 6,* 209–220, 1963.

Aki, K., Earthquake generating stress in Japan for the years 1961 to 1963 obtained by smoothing the first motion radiation patterns, *Bull. Earthquake Res. Inst. Tokyo Univ., 44,* 447–471, 1966.

Akimoto, S., and H. Fujisawa, Olivine-spinel solid solution equilibria in the system Mg_2SiO_4-Fe_2SiO_4, *J. Geophys. Res., 73,* 1467–1479, 1968.

Algermissen, S. T., and S. T. Harding, *The Puget Sound, Washington Earthquake of April 29, 1965. Preliminary Seismological Report,* 26 pp., U. S. Dept. of Commerce, Coast and Geodetic Survey, Rockville, Md., 1965.

Anderson, D. L., Earth's viscosity, *Science, 151,* 321–322, 1966.

Anderson, D. L., Phase changes in the upper mantle, *Science, 157,* 1165–1173, 1967.

Atlas Zemletryasenii SSSR, Soviet Po Seismologii, 338 pp., Akad. Nauk SSSR, Moscow, 1962.

Balakina, L. F., General regularities in the directions of the principal stresses effective in the earthquake foci of the seismic belt of the Pacific Ocean, *Izv. Acad. Sci. USSR, Geophys. Ser.,* English transl., 918–926, 1962.

Barazangi, M., and J. Dorman, World seismicity maps compiled from ESSA, Coast and Geodetic Survey, epicenter data, 1961–1967, *Bull. Seismol. Soc. Amer., 59,* 369–380, 1969.

Berckhemer, H., and K. H. Jacob, Investigation of the dynamical process in earthquake foci by analyzing the pulse shape of body waves, 85 pp., *Final Rep., Contract AF61(052)-801,* Inst. of Meteorology and Geophysics, Univ. of Frankfurt, 1968.

Brune, J. N., Seismic moment, seismicity, and rate of slip along major fault zones, *J. Geophys. Res., 73,* 777–784, 1968.

Byerlee, J. D., and W. F. Brace, High-pressure mechanical instability in rocks, *Science, 164,* 713–715, 1969.

Chandra, U., Analysis of body-wave spectra for earthquake energy determination, *Bull. Seismol. Soc. Amer., 60,* 539–563, 1970*a*.

Chandra, U., The Peru-Bolivia border earthquake of August 15, 1963, *Bull. Seismol. Soc. Amer., 60,* 639–646, 1970*b*.

Constantinescu, L., and D. Enescu, Nature of faulting and stress pattern at the foci of some carpathian-arc-bend earthquakes, *Rev. Géol. Géogr., Acad. République Populaire Roumaine, Tirage à Part, VI* (1), 143–183, 1962.

Constantinescu, L., L. Ruprechtova, and D. Enescu, Mediterranean-Alpine earthquake mechanisms and their seismotectonic implications, *Geophys. J. Roy. Astron. Soc., 10,* 347–368, 1966.

Davies, D., and D. P. McKenzie, Seismic travel-time residuals and plates, *Geophys. J. Roy. Astron. Soc., 18,* 51–63, 1969.

Davies, G. F., and J. N. Brune, Global and regional fault activity from seismic moments of large shallow earthquakes, *Nature*, in press, 1971.

Denham, D., Distribution of earthquakes in the New Guinea, Solomon Islands region, *J. Geophys. Res., 74*, 4290–4299, 1969.

Duda, S. J., Secular seismic energy release in the circum-Pacific belt, *Tectonophysics, 2*, 409–452, 1965.

Elsasser, W. M., Convection and stress propagation in the upper mantle, in *The Application of Modern Physics to the Earth and Planetary Interiors*, edited by K. Runcorn, pp. 223–246, Wiley-Interscience, 1969.

Engdahl, E. R., and E. A. Flinn, Seismic waves reflected from discontinuities within earth's upper mantle, *Science, 163*, 177–179, 1969.

Engdahl, E. R., S. T. Algermissen, and S. T. Harding, Global patterns of earthquake focal mechanisms, oral presentation, General Scientific Assemblies, IASPEI/IAGA, Madrid, 1969.

Fedotov, S. A., Upper mantle properties of the southern part of the Kurile island arc according to detailed seismological investigation data, *Tectonophysics, 2*, 219–225, 1965.

Fedotov, S. A., On deep structure, properties of the upper mantle, and volcanism of the Kurile-Kamchatka island arc according to seismic data, in *The Crust and Mantle of the Pacific Area, Geophys. Monograph 12*, edited by L. Knopoff, C. L. Drake, and P. J. Hart, pp. 131–139, AGU, Washington, D. C., 1968.

Fitch, T. J., Earthquake mechanisms and island arc tectonics in the Indonesian-Philippine region, *Bull. Seismol. Soc. Amer., 60*, 565–591, 1970*a*.

Fitch, T. J., Earthquake mechanisms in the Himalayan, Burmese, and Andaman regions and continental tectonics in central Asia, *J. Geophys. Res., 75*, 2699–2709, 1970*b*.

Fitch, T. J., and P. Molnar, Focal mechanisms along inclined earthquake zones in the Indonesian-Philippine region, *J. Geophys. Res., 75*, 1431–1444, 1970.

Frank, F. C., Curvature of island arcs, *Nature, 220*, 363, 1968.

Gordon, R. B., Diffusion creep in the earth's mantle, *J. Geophys. Res., 70*, 2413–2418, 1965.

Griggs, D. T., The sinking lithosphere and the focal mechanism of deep earthquakes, in *Symposium in Honor of F. Birch*, edited by E. Robertson, McGraw-Hill, New York, in press, 1971.

Griggs, D. T., and D. W. Baker, The origin of deep-focus earthquakes, in *Properties of Matter under Unusual Conditions*, edited by H. Mark and S. Fernback, 389 pp., John Wiley, New York, 1969.

Griggs, D., and J. Handin, Observations on fracture and a hypothesis of earthquakes, in *Rock Deformation*, edited by D. Griggs and J. Handin, *Geol. Soc. Amer. Memoir 79*, 347–373, 1960.

Gutenberg, B., and C. F. Richter, *Seismicity of the Earth and Associated Phenomena*, 310 pp., Princeton University Press, Princeton, N. J., 1954.

Hamilton, R. M., and A. W. Gale, Seismicity and structure of the North Island, New Zealand, *J. Geophys. Res., 73*, 3859–3876, 1968.

Hamilton, R. M., and A. W. Gale, Thickness of the mantle seismic zone beneath the North Island of New Zealand, *J. Geophys. Res., 74*, 1608–1613, 1969.

Harrington, H. J., Deep focus earthquakes in South America and their possible relation to continental drift, in *Polar Wandering and Continental Drift*, edited by R. C. Munyan, pp. 55–73, American Association of Petroleum Geologists, Tulsa, Okla., 1963.

Hatherton, T., Gravity and seismicity of asymmetric active regions, *Nature, 221*, 353, 1969.

Hatherton, T., Upper mantle inhomogeneities beneath New Zealand: Surface manifestations, *J. Geophys. Res., 75*, 269–284, 1970.

Hatherton, T., and W. R. Dickinson, The relationship between andesitic volcanism and seismicity in Indonesia, the Lesser Antilles, and other island arcs, *J. Geophys. Res., 74*, 5301–5310, 1969.

Hayes, D. E., and W. J. Ludwig, The Manila trench and West Luzon trough—2. Gravity and magnetic measurements, *Deep Sea Res., 14*, 545–560, 1967.

Hedayati, A., and T. Hirasawa, Mechanism of the Hindu Kush earthquake of Jan. 28, 1964,

derived from S wave data: The use of pP phase for the focal mechanism determination, *Bull. Earthquake Res. Inst. Tokyo Univ., 44,* 1419–1434, 1966.

Hirasawa, T., A least squares method for the focal mechanism determinations from S wave data (2), *Bull. Earthquake Res. Inst. Tokyo Univ., 44,* 919–938, 1966.

Hodgson, J. H., and J. I. Cock, Direction of faulting in the deep focus Spanish earthquake of March 29, 1954, *Tellus, 8,* 321–328, 1956.

Holmes, A., *Principles of Physical Geology,* 1288 pp., Ronald, New York, 1965.

Honda, H., Earthquake mechanisms and seismic waves, *J. Phys. Earth, 10,* 1–97, 1962.

Honda, H., and A. Masatsuka, On the mechanisms of earthquakes and the stresses producing them in Japan and its vicinity, *Sci. Rep., Tohoku Univ., Ser. 5, Geophys., 4,* 42–60, 1952.

Honda, H., A. Masatsuka, and K. Emura, On the mechanism of the earthquakes and the stresses producing them in Japan and its vicinity, 2, *Sci. Rep., Tohoku Univ., Ser. 5, Geophys., 8,* 186–205, 1956.

Honda, H., A. Masatsuka, and M. Ichikawa, On the mechanism of earthquakes and stresses producing them in Japan and its vicinity, 3, *Geophys. Mag., 33,* 271–279, 1967.

Ichikawa, M., On the mechanism of the earthquake in and near Japan during the period from 1950 to 1957, *Geophys. Mag., 30,* 355–403, 1961.

Ichikawa, M., Mechanism of earthquakes in and near Japan, 1950–1962, *Pap. Meteorol. Geophys.* (Tokyo), *16,* 201–229, 1966.

Isacks, B., Focal mechanisms of earthquakes in western South America (abstract), *EOS, Trans. AGU, 51,* 355, 1970.

Isacks, B., and P. Molnar, Mantle earthquake mechanisms and the sinking of the lithosphere, *Nature, 223,* 1121–1124, 1969.

Isacks, B., J. Oliver, and L. R. Sykes, Seismology and the new global tectonics, *J. Geophys. Res., 73,* 5855–5899, 1968.

Isacks, B., L. R. Sykes, and J. Oliver, Focal mechanisms of deep and shallow earthquakes in the Tonga-Kermadec region and the tectonics of island arcs, *Bull. Geol. Soc. Amer., 80,* 1443–1470, 1969.

Jacoby, W., Instability in the upper mantle and global plate movements, *J. Geophys. Res., 75,* 5671–5680, 1970.

Karnik, V., *Seismicity of the European Area, Part 1,* 364 pp., D. Reidel, Dordrecht, Holland, 1969.

Katsumata, M., Seismic activities in and near Japan (1)—Distribution of epicenters of earthquakes in and near Japan (in Japanese), *J. Seismol. Soc. Japan (Zisin), 19,* 237–245, 1966.

Katsumata, M., Seismic activities in and near Japan (2)—Vertical distribution of foci of earthquakes in and near the Japanese islands (in Japanese), *J. Seismol. Soc. Japan (Zisin), 20,* 1–11, 1967*a*.

Katsumata, M., Seismic activities in and near Japan (3)—Seismic activities versus depth (in Japanese), *J. Seismol. Soc. Japan (Zisin), 20,* 75–84, 1967*b*.

Katsumata, M., and L. R. Sykes, Seismicity and tectonics of the western Pacific: Izu-Mariana-Caroline and Ryukyu-Taiwan regions, *J. Geophys. Res., 74,* 5923–5948, 1969.

Le Pichon, X., Sea-floor spreading and continental drift, *J. Geophys. Res., 73,* 3661–3697, 1968.

Lliboutry, L., Sea-floor spreading, continental drift and lithosphere sinking with an asthenosphere at melting point, *J. Geophys. Res., 74,* 6525–6540, 1969.

Ludwig, W. J., D. E. Hayes, and J. I. Ewing, The Manila trench and West Luzon trough—1. Bathymetry and sediment distribution, *Deep-Sea Res., 14,* 533–544, 1967.

McConnell, R. K., Viscosity of the mantle from relaxation time spectra of isostatic adjustment, *J. Geophys. Res., 73,* 7089–7105, 1968.

McKenzie, D. P., The relation between fault plane solutions for earthquakes and the directions of the principal stresses, *Bull. Seismol. Soc. Amer., 59,* 591–601, 1969*a*.

McKenzie, D. P., Speculations on the consequences and causes of plate motions, *Geophys. J., 18,* 1–32, 1969*b*.

McKenzie, D. P., Plate tectonics of the Mediterranean region, *Nature, 226,* 239–243, 1970.

McKenzie, D. P., and W. J. Morgan, Evolution of triple junctions, *Nature, 224,* 125–133, 1969.

McKenzie, D. P., and R. L. Parker, The North Pacific: An example of tectonics on a sphere, *Nature, 216,* 1276–1280, 1967.

Mendiguren, J., Study of focal mechanisms of deep earthquakes in Argentina using nonlinear particle motion of S waves, *Bull. Seismol. Soc. Amer., 59,* 1449–1473, 1969.

Mikumo, T., Long period P wave forms and the source mechanism of intermediate earthquakes, *J. Phys. Earth, 17,* 169–192, 1969.

Mitronovas, W., Seismic velocity anomalies in the upper mantle beneath the Tonga-Kermadec island arc, Ph.D. thesis, Columbia University, 1969.

Mitronovas, W., B. Isacks, and L. Seeber, Earthquake locations and seismic wave propagation in the upper 250 km of the Tonga island arc, *Bull. Seismol. Soc. Amer., 59,* 1115–1135, 1969.

Molnar, P., and J. Oliver, Lateral variations of attenuation in the upper mantle and discontinuities in the lithosphere, *J. Geophys. Res., 74,* 2648–2682, 1969.

Molnar, P., and L. R. Sykes, Tectonics of the Caribbean and Middle America regions from focal mechanisms and seismicity, *Bull. Geol. Soc. Amer., 80,* 1639–1684, 1969.

Mooney, H. M., Upper mantle inhomogeneity beneath New Zealand: Seismic evidence, *J. Geophys., Res., 75,* 285–309, 1970.

Morgan, W. J., Rises, trenches, great faults and crustal blocks, *J. Geophys. Res., 73,* 1959–1982, 1968.

Murdock, J. N., Crust mantle system in the central Aleutian region—A hypothesis, *Bull. Seismol. Soc. Amer., 59,* 1543–1558, 1969.

Nowroozi, A., Seismotectonics of the Persian plateau and vicinity, *Bull. Seismol. Soc. Amer.,* in press, 1971.

Ocala, L., Earthquake activity of Peru, in *The Earth beneath the Continents,* edited by J. S. Steinhart and T. J. Smith, pp. 509–528, AGU, Washington, D. C., 1966.

Oliver, J., and B. Isacks, Deep earthquake zones, anomalous structure in the upper mantle, and the lithosphere, *J. Geophys. Res., 72,* 4259–4275, 1967.

Oliver, J., and B. Isacks, Structure and mobility of the crust and mantle in the vicinity of island arcs, *Can. J. Earth Sci., 5,* 985–991, 1968.

Orowan, E., Mechanism of seismic faulting, in *Rock Deformation,* edited by D. Griggs and J. Handin, *Geol. Soc. Amer. Memoir 79,* 323–345, 1960.

Peterschmitt, E., Quelques données nouvelles sur les séismes profonds de la Mer Tyrrhènienne, *Ann. Geofis.* (Rome), *9,* 305–334, 1956.

Press, F., The suboceanic mantle, *Science, 165,* 174–176, 1969.

Radu, C., Le régime séismique de la région de Vrancea, *Rev. Roumaine Géol. Géophys. Géogr., 9,* 49–64, 1965.

Raleigh, C. B., and M. S. Paterson, Experimental deformation of serpentinite and its tectonic implications, *J. Geophys. Res., 70,* 3965–3985, 1965.

Randall, M. J., Relative sizes of multipolar components in deep earthquakes, *J. Geophys. Res., 73,* 6140–6142, 1968.

Ritsema, A. R., Some reliable fault-plane solutions, *Pure Appl. Geophys., 59,* 58–74, 1964.

Ritsema, A. R., The mechanism of some deep and intermediate earthquakes in the region of Japan, *Bull. Earthquake Res. Inst. Tokyo Univ., 43,* 39–52, 1965.

Ritsema, A. R., The fault-plane solutions of earthquakes of the Hindu Kush centre, *Tectonophysics, 3,* 147–163, 1966.

Ritsema, A. R., Seismic data of the West Mediterranean and the problem of oceanization, *Trans. Kon. Ned. Geol. Mynbk., Gen. 26,* 105–120, 1969.

Ritsema, A. R., The mechanism of mantle earthquakes in relation to phase transformation processes, *Phys. Earth Planetary Interiors, 3,* 503–510, 1970.

Ryan, W. B. F., D. J. Stanley, J. B. Hersey, D. A. Fahlquist, and T. D. Allan, The tectonics and geology of the Mediterranean Sea, in *The Seas,* vol. 4, edited by A. E. Maxwell, John Wiley, New York, in press, 1970.

Sacks, I. S., Distribution of absorption of shear waves in South America and its tectonic significance, *Carnegie Inst. Wash. Yearb. 67,* 339–344, 1969.

Santo, T., Characteristics of seismicity in South America, *Bull. Earthquake Res. Inst. Tokyo Univ., 47,* 635–672, 1969*a*.

Santo, T., Regional study on the characteristic seismicity of the world, Part 2, from Burma down to Java, *Bull. Earthquake Res. Inst. Tokyo Univ., 47,* 1049–1061, 1969*b*.

Savage, J. C., The mechanics of deep-focus faulting, *Tectonophysics, 8,* 115–127, 1969.

Savarensky, E. F., and N. V. Golubeva, Seismicity of continental Asia and the region of the Sea of Okhotsk, 1953–1965, in *The Earth's Crust and Upper Mantle, Geophys. Monograph 13,* edited by P. J. Hart, pp. 134–139, AGU, Washington, D. C., 1969.

Shirokova, E. I., General features in the orientation of principal stresses in earthquake foci in the Mediterranean-Asian seismic belt, *Izv. Acad. Sci., USSR, Phys. Solid Earth,* Engl. transl., no. 1, pp. 12–21, 1967.

Silver, E. A., Late Cenozoic underthrusting of the continental margin off northernmost California, *Science, 166,* 1265–1266, 1969.

Soboleva, O. V., The stresses in the foci of the Hindukush earthquakes of July 6, 1962 and of March 14, 1965, *Izv. Acad. Sci., USSR, Phys. Solid Earth,* Engl. transl., no. 2, pp. 126–128, 1967.

Soboleva, O. V., Special features of the directions of the principal stress axes in the foci of Hindu-Kush earthquake, *Izv. Acad. Sci., USSR, Phys. Solid Earth,* Engl. transl., no. 1, pp. 36–40, 1968.

Stauder, W., Mechanisms of the Rat Island earthquake sequence of February 4, 1965, with relation to island arcs and sea-floor spreading, *J. Geophys. Res., 73,* 3847–3858, 1968*a*.

Stauder, W., Tensional character of earthquake foci beneath the Aleutian trench with relation to sea-floor spreading, *J. Geophys. Res., 73,* 7693–7701, 1968*b*.

Stauder, W., The mechanism of South American earthquakes: 18°S to 34°S (abstract), *Earthquake Notes, 40,* 19, 1969.

Stauder, W., and G. A. Bollinger, The S wave project for focal mechanism studies, Earthquakes of 1962, 93 pp., *Sci. Rep. Grant AF-AFOSR-62-458, Project VELA-UNIFORM,* St. Louis University, St. Louis, Mo., 1964.

Stauder, W., and G. A. Bollinger, The S wave project for focal mechanism studies, Earthquakes of 1963, 91 pp., *Sci. Rep. Grant AF-AFOSR-62-458, Project VELA-UNIFORM,* St. Louis University, St. Louis, Mo., 1965.

Stevens, A. E., S-wave focal mechanism studies of the Hindu Kush earthquake of July 6, 1962, *Can. J. Earth Sci., 3,* 367–384, 1966.

Stevens, A. E., and J. H. Hodgson, A study of P nodal solutions (1922–1962) in the Wickens-Hodgson Catalogue, *Bull. Seismol. Soc. Amer., 58,* 1071, 1968.

Sugimura, A., Distribution of volcanoes and seismicity of the mantle in Japan, *Bull. Volcan. Soc. Japan, 2nd Ser., 10,* 37–58, 1965.

Sugimura, A., and S. Uyeda, A possible anistropy in the upper mantle accounting for deep earthquake faulting, *Tectonophysics, 5,* 25–33, 1967.

Sykes, L. R., Deep-focus earthquakes in the New Hebrides region, *J. Geophys. Res., 69,* 5353–5355, 1964.

Sykes, L. R., The seismicity and deep structure of island arcs, *J. Geophys. Res., 71,* 2981–3006, 1966.

Sykes, L. R., and M. Ewing, The seismicity of the Caribbean region, *J. Geophys. Res., 70,* 5065–5074, 1965.

Sykes, L. R., B. Isacks, and J. Oliver, Spatial distribution of deep and shallow earthquakes of small magnitude in the Fiji-Tonga region, *Bull. Seismol. Soc. Amer., 59,* 1093–1113, 1969.

Teng, T., and A. Ben-Menahem, Mechanism of deep earthquakes from spectrums of isolated body wave signals, *J. Geophys. Res., 70,* 5157–5170, 1965.

Tobin, D. G., and L. R. Sykes, Seismicity and tectonics of the Northeast Pacific Ocean, *J. Geophys. Res., 73,* 3821–3845, 1968.

Tryggvason, E., and J. E. Lawson, Jr., The intermediate earthquake source near Bucaramanga, Colombia, *Bull. Seismol. Soc. Amer., 60,* 269–276, 1970.

Utsu, T., Anomalies in seismic wave velocity and attenuation associated with a deep earthquake zone (1), *J. Fac. Sci., Hokkaido Univ., Ser. 7 (Geophys.), 3,* 1-25, 1967.

Vvedenskaya, A. V., and L. Ruprechtova, Characteristic features of stress distribution in the foci of earthquakes at the bend of the Carpathian arc (in Russian), *Izv. Akad. Nauk SSSR, Ser., Geofiz.*, no. 7, 953–965, 1961.

Weertman, J., The creep strength of the earth's mantle, *Rev. Geophys., 8*, 145–168, 1970.

Wyss, M., Stress estimates for South American shallow and deep earthquakes, *J. Geophys. Res., 75*, 1529–1544, 1970.

(Received July 31, 1970.)